Universität Hamburg
DER FORSCHUNG | DER LEHRE | DER BILDUNG

Molecular basis of hypoxia tolerance in the whale brain

Dissertation

submitted by
Alena Krüger

to the

University of Hamburg

with the aim of achieving a
doctoral degree (Dr. rer. nat.)

at the

Faculty of Mathematics,
Informatics and Natural Sciences
Department of Biology

- Hamburg, 2019 -

1st Evaluator: Prof. Dr. Susanne Dobler

2nd Evaluator: Dr. Andrej Fabrizius

Oral defense on the 7th February, 2020

Bestätigung der sprachlichen Korrektheit durch native Speaker:

To Prof. Dr.Streit,

As a native English speaker and an Aquaculture and Sea Ranching M.Sc., I hereby approve the written English in the introduction, manuscripts, discussion and summary of the PhD thesis prepared by Alena Krüger.

Sincerely,

Maria Pierce

Maria E. Pierce Rostock, 09.12.2019

1 Summary

Marine mammals are routinely exposed to low oxygen conditions when submerged. While physiological adaptations that reduce oxygen consumption and improve oxygen storage are well studied, the molecular mechanisms of the cerebral hypoxia tolerance in diving mammals are still widely unknown. Enhanced anaerobic energy production and general energy saving mechanisms via hypometabolism could help the diving brain to survive hypoxic periods. Analyses of the transcriptome of the visual cortex of hooded seal (*Cystophora cristata*) supported this hypothesis and showed less aerobic capacity in the seal brain compared to a terrestrial relative. In addition, an increase in anaerobic metabolism under hypoxic conditions in the seal brain was suspected and verified by transcriptomes of hypoxic brain slices. However, it is believed that seals and whales, which seperated approximately 81 million years ago, have evolved divergent strategies for cerebral hypoxia tolerance.

The aim of this work was to reveal basic molecular differences in the brain of whales and their closest terrestrial relative, the cattle. By using transcriptome analysis, gene expression differences were examined, and based on these results further molecular adaptations to diving were investigated. Transcriptomes of the visual cortex of the killer whale (*Orcinus orca*), the long-finned pilot whale (*Globicephala melas*), as well as the cerebellum of the long-finned pilot whale and the visual cortex of the cow (*Bos taurus*) were sequenced. In order to increase the number of replicates, additional brain transcriptomes of cattle brain, as well as minke whale (*Balaenoptera acutorostrata*) brain and bowhead whale (*Balaena mysticetus*) brain from the NCBI public SRA database were included in the analyses. Comparison of the brain transcriptomes of whales and cattle revealed an increased aerobic capacity in the whale brain (Chapter I). This was suggested based on a significantly higher expression of an above-average number of transcripts involved in oxidative phosphorylation and the electron transport chain in the whale brain. In contrast to seals, whales seem to have developed a more efficient use of oxygen to sustain brain activity instead of a reduced metabolism to save energy. Additionally, the high aerobic capacity might represent an adaptation for the rapid regeneration of ATP production immediately after resurfacing. However, enhanced aerobic metabolism also increases the formation of toxic reactive oxygen species (ROS). Significantly higher expression levels of transcripts involved in the detoxification of ROS seem to protect the whale brain from neuronal damage.

To investigate the role of high expression of specific antioxidant genes, the effects of overexpression of superoxide dismutase 1 (SOD1) in cell culture were investigated (Chapter II). The SOD1 gene of the killer whale was overexpressed in neuronal mouse cells (HN33) and cell viability was analyzed after 24 hours of normoxia, hypoxia and oxidative stress. Increased expression of SOD1 resulted in improved cell viability in both hypoxia and oxidative stress and less production of ROS under hypoxia than in control cells. In addition, whale-specific amino acid changes were found in the sequence of SOD1, which were suggested to reduce the formation of harmful aggregations of the protein. Another important factor in the hypoxia tolerance of the whale brain seems to be the suppression of certain apoptotic signaling pathways. Among the transcripts that were significantly more abundant in the whale brain than in the cow brain, COMM

Domain Containing 6 (COMMD6) was among the transcripts with the highest fold difference. COMMD6 is known to inhibit the pro-apoptotic transcription factor NF-κB. To test the effects of high expression of COMMD6 on neurons under hypoxia and oxidative stress, the COMMD6 gene of the killer whale was overexpressed in HN33 cells (Chapter II). The high expression of COMMD6 led to higher survival rates of the transfected cells under hypoxia and oxidative stress compared to control cells. This may indicate that a high expression of COMMD6 suppresses programmed cell death controlled by NF-κB.

Furthermore, indicators of a switch to anaerobic metabolism in the whale brain under hypoxic conditions were investigated. Several parameters of lactate dehydrogenase (LDH) were analyzed in the brain of whale and cattle (Chapter III). Here, a peculiarity in the composition of LDH isoenzymes was shown. The whale brain has a higher proportion of LDHA / LDHB hybrid isoenzymes, indicating a flexible switch between aerobic and anaerobic energy production. Similar results were also found in the brain of the hooded seal. This might indicate a convergent evolution of a flexible transition between aerobic and anaerobic metabolism in the brain of diving mammals. In addition, it has been shown that LDH in the whale brain has enhanced activity in high concentrations of lactate, which could rapidly break down anaerobically produced lactate after the dive. The results of this work provide initial insights into the molecular adaptations to hypoxia in the whale brain and provide the basis for more extensive studies of brain metabolism in the whale.

2 Zusammenfassung

Tauchende Säuger wie etwa Wale und Robben haben sich perfekt an ihren besonderen Lebensraum angepasst. Die meiste Zeit ihres Lebens verbringen sie unter Wasser, ohne Zugang zu atmosphärischem Sauerstoff und setzen sich dadurch Bedingungen aus, in denen ihre Organe und Gewebe nicht ausreichend Sauerstoff zur Verfügung haben (Hypoxie). Die physiologischen Anpassungen, die Wale nutzen, um den Sauerstoffverbrauch zu reduzieren und ihre Sauerstoffspeicherkapazität zu erhöhen sind sehr gut untersucht. Weitestgehend unklar ist bisher jedoch, welche molekularen Mechanismen für die Hypoxietoleranz des Gehirns tauchender Säuger verantwortlich sind. Eine verstärkte anaerobe Energiegewinnung könnte dem Gehirn tauchender Säuger helfen, auch unter hypoxischen Bedingungen Energie zu produzieren während gleichzeitig Energie eingespart wird indem der Metabolismus heruntergefahren wird. Transkriptomanalysen des Robbengehirns unterstützten diese Hypothese und zeigten eine geringere aerobe Kapazität im Robbengehirn, verglichen mit einem terrestrischen Verwandten. Zusätzlich wurde eine Erhöhung des anaeroben Metabolismus unter hypoxischen Bedingungen in Gehirnschnitten der Klappmützenrobbe (*Cystophora cristata*) gefunden. Es wird jedoch vermutet, dass Robben und Wale unterschiedliche Strategien der zerebralen Hypoxietoleranz entwickelt haben, da sie sich evolutionär bereits vor etwa 81 Millionen Jahren getrennt haben.
Im Rahmen dieser Arbeit sollten grundsätzliche molekulare Unterschiede im Gehirn von Walen und ihren nächsten terrestrischen Verwandten, den Rindern, aufgedeckt werden. Mithilfe von Transkriptomanalysen sollten Genexpressionsunterschiede gefunden werden, auf deren Basis weitere Besonderheiten im Gehirn der Wale untersucht werden. Hierfür wurden Transkriptome des visuellen Cortex des Orcas (*Orcinus orca*), des Grindwals (*Globicephala melas*), sowie des Cerebellums des Grindwals und, zum Vergleich, des visuellen Cortex der Kuh (*Bos taurus*) erstellt. Um die Anzahl der Replikate zu vergrößern wurden außerdem weitere Gehirntranskriptome der Kuh, sowie des Zwergwals (*Balaenoptera acutorostrata*) und des Grönlandwals (*Balaena mysticetus*) aus der öffentlichen SRA Datenbank von NCBI in die Analysen eingeschlossen. Beim Vergleich der Transkriptome von Walen und Rindern zeigte sich eine erhöhte aerobe Kapazität im Walgehirn (Kapitel I). Diese äußerte sich durch eine signifikant stärkere Expression von einer überdurchschnittlich hohen Zahl an Transkripten, die an der oxidativen Phosphorylierung und der Elektronentransportkette beteiligt sind. Dies deutet darauf hin, dass Wale im Gegensatz zu Robben keine Reduktion des Gehirnmetabolismus nutzen, um Energie einzusparen, sondern stattdessen eine effizientere Nutzung des Sauerstoffs entwickelt haben, um die Gehirnaktivität dauerhaft aufrecht zu erhalten. Außerdem scheint das Gehirn der Wale durch eine erhöhte aerobe Kapazität auf eine schnelle Regeneration der ATP Produktion direkt nach dem Auftauchen ausgelegt zu sein. Ein ausgeprägter aerober Metabolismus verstärkt jedoch auch die Bildung von reaktiven Sauerstoffspezies (ROS), die zellschädigend wirken. Eine signifikant höhere Expression von Transkripten, die an der Detoxifizierung der ROS beteiligt sind, scheint das Walgehirn jedoch vor neuronalen Schäden zu schützen.
Um die Rolle der einzelnen stärker exprimierten Transkripte zu untersuchen, wurden beispielhaft die Auswirkungen einer Überexpression der Superoxid-Dismutase 1 (SOD1) in Zellkultur unter-

sucht (Kapitel II). Die SOD1 Gensequenz des Orcas wurde in neuronalen Mauszellen (HN33) überexprimiert und die Zellviabilität wurde nach 24 Stunden Normoxie, Hypoxie und oxidativem Stress untersucht. Die verstärkte Expression von SOD1 führte zu einer verbesserten Zellviabilität sowohl unter Hypoxie als auch unter oxidativem Stress und unter Hypoxie wurde weniger ROS produziert als in Kontrollzellen. Außerdem konnten walspezifische Aminosäureaustausche in der Sequenz von SOD1 gefunden werden, die darauf hindeuten, dass eine schädliche Akkumulation bei hohen Konzentrationen der SOD1 Proteine in der Zelle vermindert wird. Eine weitere wichtige Rolle in der Hypoxietoleranz des Walgehirns scheint die Unterdrückung bestimmter Apoptose Signalwege zu spielen. Unter den Transkripten, die im Walgehirn höher exprimiert waren als im Kuhgehirn zeigte COMM Domain Containing 6 (COMMD6) mit die stärksten Expressionsunterschiede. COMMD6 ist in der Lage den pro-apoptotischen Transkriptionsfaktor NF-κB zu inhibieren. Um die Auswirkungen einer starken Expression auf Neurone unter Hypoxie und oxidativem Stress zu testen, wurde auch dieses Gen des Orcas in HN33 Zellen überexprimiert. Es zeigte sich, dass die starke Expression von COMMD6 dazu führte, dass HN33 Zellen eine signifikant höhere Überlebensrate unter Hypoxie und unter oxidativem Stress aufwiesen als Kontrollzellen. Dies könnte darauf hinweisen, dass die starke Expression von COMMD6 den programmierten Zelltod, gesteuert durch NF-κB unterdrückt.
Weiterhin sollte in dieser Arbeit untersucht werden, ob es Hinweise auf anaeroben Metabolismus im Walgehirn unter hypoxischen Bedingungen gibt. Hierfür wurden verschiedene Parameter der Laktatdehydrogenase (LDH) im Wal- und Kuhgehirn verglichen (Kapitel III). Hier zeigte sich eine Besonderheit in der Zusammensetzung der LDH-Isoenzyme. Das Walgehirn weist einen höheren Anteil an LDHA/LDHB Hybrid-Isoenzymen auf, was auf einen flexiblen Wechsel zwischen aerober und anaerober Energiegewinnung hindeutet. Ähnliche Ergebnisse wurden auch im Gehirn der Klappmützenrobbe gefunden. Dies könnte bedeuten, dass zumindest die Anpassung an eine flexible Umstellung zwischen aerober und anaerober Energiegewinnung im Gehirn tauchender Säuger konvergent ist. Außerdem konnte gezeigt werden, dass LDH im Walgehirn verstärkte Aktivität bei hohen Laktatkonzentrationen aufweist, was dabei helfen könnte, anaerob produziertes Laktat nach dem Tauchgang schnell abzubauen. Die Ergebnisse dieser Arbeit geben erste Einblicke in die molekularen Anpassungen des Walgehirns an Hypoxie und bieten die Grundlage für weiterreichende Untersuchungen des Gehirnmetabolismus im Wal.

Contents

3 List of abbreviations

ADL: aerobic diving limit

ANLS: astrocyte-neuron lactate shuttle

ANOVA: Analysis of Variance

ATP: adenosine triphosphate

cADL: calculated aerobic diving limit

BSA: bovine serum albumin

CAT: catalase

CE: cerebellum

CLU: clusterin

CO_2: carbon dioxide

COMMD6: COMM domain containing 6

COX: cytochrome c oxidase

CYCS: cytochrome c

DNA: deoxyribonucleic acid

EQ: encephalization quotient

$FADH_2$: flavin adenine dinucleotide (hydroquinone form)

FL: frontal lobe

GFAP: glial fibrillary acidic protein

GLUT1/3: glucose transporter 1/3

GO: gene ontology

GPX(2): glutathione peroxidase (2)

GSH: reduced glutathione

GST(P1): glutathione S-transferase (P)

H_2O_2: hydrogen peroxide

HIF-1 (α): hypoxia-inducible factor 1 (α)

HK: hexokinase

HN33: murine hippocampal neurons x neuroblastoma

LDH(1-5): lactate dehydrogenase (isoenzymes 1-5)

LDHA: lactate dehydrogenase isoenzyme A

LDHB: lactate dehydrogenase isoenzyme B

MCT1/2/4: monocarboxylate transporters 1/2/4

mRNA: messenger ribonucleic acid

NaCN: sodium cyanide

NAD^+: nicotinamide adenine dinucleotide

NADH: nicotinamide adenine dinucleotide (reduced form)

NADPH: nicotinamide adenine dinucleotide phosphate

NCF2: neutrophil cytosol factor 2

NF-κB: nuclear factor-κB

NGB: neuroglobin

NMDA: N-methyl-D-aspartate

NOX: nicotinamide adenine dinucleotide phosphate (NADPH) oxidase

NRF-1: nuclear respiratory factor-1

O_2: oxygen

O_2^-: superoxide anion

·OH: hydroxyl radicals

PCA: principal component analysis

PFK: phosphofructokinase

PK: pyruvate kinase

PO_2: partial oxygen pressure

PON2: paraoxonase 2

PRDX (6): periredoxin (6)

RNA: ribonucleic acid

RNA-Seq: RNA Sequencing

ROS: reactive oxygen species

RPKM: Reads Per Kilobase per Million mapped reads

SOD(1/2/3): superoxide dismutase (1/2/3)

TCA: tricarboxylic acid circle

TRX (2): thioredoxin (2)

VC: visual cortex

4 Introduction

4.1 Energy metabolism and oxygen in the mammalian brain

The mammalian brain is the control center of somatic functions and sensory processing, complex procedures that require high amounts of energy. Although the brain represents only a small proportion of the total body mass, for example in the human body it is 2-3 %, it consumes up to 20 % of the available oxygen (O_2) (Rolfe et al. 1997) and accounts for approximately 20 % of the total body glucose utilization (Erbsloh et al. 1958). Glucose is the main energy substrate in the brain. In neurons, most of the energy is produced by the aerobic metabolism of glucose, which is processed through glycolysis, the tricarboxylic acid (TCA) circle and oxidative phosphorylation (for review see: Falkowska et al. 2015; Magistretti et al. 2015). Astrocytes utilize glucose predominantly via glycolysis with the production of lactate and a low percentage of mitochondrial oxidation (Itoh et al. 2003). The ATP produced in the brain is mainly used to fuel the maintenance of ionic gradients across the plasma membrane to sustain excitability. Ion pumps that maintain resting and action potentials in neurons and glia cells account for up to 44 % of the ATP consumption. Other energy consuming housekeeping tasks in the brain, such as synthesis of neurotransmitters and structural proteins or the mitochondrial proton leak require 25 – 50 % of the total energy use (Howarth et al. 2012).

During the last few decades, it has become evident that neurons rely not only on glucose supply but also utilize lactate produced by astrocytes leading to the astrocyte-neuron lactate shuttle hypothesis (ANLS) (Fig. 1; Pellerin 2005). The contribution of lactate to the energy consumption of the brain varies depending on substrate availability (van Hall et al. 2009). Furthermore, the brain uses ketone bodies derived from fatty acid metabolism in the liver (for review see: Camandola et al. 2017) and is able to use non-glucose substrates such as pyruvate, glutamine or α-ketoglutarate in case of the absence of glucose (hypoglycemia) (Suh et al. 2005; Zielke et al. 2009).

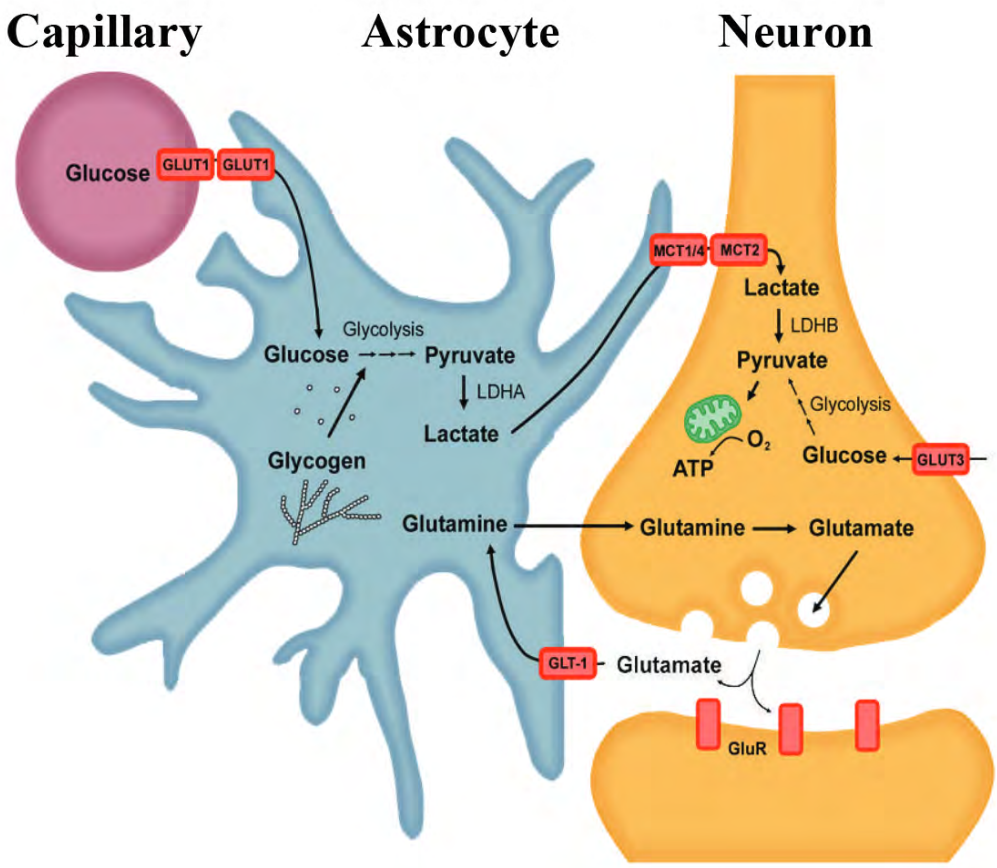

Figure 1 Energy metabolism in the mammalian brain according to the astrocyte-neuron lactate shuttle hypothesis. Glucose enters astrocytes via glucose transporters (GLUT1) from surrounding capillaries or can be released from the breakdown of intracellular glycogen stores. Following glycolysis pyruvate is converted to lactate by lactate dehydrogenase isoenzyme A (LDHA). Lactate is exported from the astrocytes and imported into neurons via monocarboxylate transporters (MCT1/4, MCT2). Within the neurons lactate is converted back to pyruvate by LDHB and is used to fuel ATP production via oxidative phosphorylation. GLUT3 transporters facilitate additional glucose uptake of neurons which is also converted to pyruvate (from Newington et al. 2013).

While neurons can maintain activity during periods of hypoglycemia, a shortage of oxygen in brain tissue (hypoxia) has a devastating impact on neurons. Within five minutes of oxygen shortage, neuronal cell death is triggered in most mammals, compromising the structural and functional integrity of the brain (Acker et al. 2004; Lee et al. 2000; Semenza 2001). The cellular energy supply via oxidative phosphorylation fails in hypoxic conditions leading to a drop in ATP production (Erecinska et al. 2001; Lopez-Barneo et al. 2001). With ATP levels below 35 % of basal levels, ion transport is impaired causing membrane depolarization (Bickler et al. 2002). A loss of membrane potential causes Ca^{2+} influx via voltage gated Ca^{2+} channels and the release of excitatory neurotransmitter like glutamate into the extracellular space. Glutamate triggers the overstimulation of N-methyl-D-aspartate (NMDA) receptors which increase the Ca^{2+} influx.

The excess of Ca^{2+} in the cells promotes free radical production, activation of phospholipases and proteases leading to critical structural damage and apoptotic cell death (Acker et al. 2004; Durukan et al. 2007; Hossmann 2006; Lipton 1999; Michiels 2004; White et al. 2000). Neurons are thought to be more vulnerable to hypoxia than astrocytes (Xu et al. 2001). Astrocytes serve as oxygen sensors and, under hypoxic stress, play a role in the protection of neuronal cells from excitotoxicity and oxidative stress (Angelova et al. 2015; Dugan et al. 1995; Marina et al. 2016). Astrocytes exhibit bigger glycogen stores (Phelps 1972; Swanson et al. 1993), higher levels of the antioxidant glutathion (GSH) (Chen et al. 2003; Makar et al. 1994) and lower energy demands than neurons (Silver et al. 1997). The function of astrocytes during hypoxia has attracted attention in recent years, but seems to be a double edged sword involving both protective and pathological functions (Vangeison et al. 2008; Vangeison et al. 2009; Xu et al. 2011). However, there are still gaps in the understanding of the effects of hypoxia on glia cells and the complex mechanisms underlying neuronal cell death under hypoxia.

During hypoxic events and afterwards when oxygen supply is restored (reoxygenation) additional brain injury is caused by an enhanced formation of reactive oxygen species (ROS) like superoxide anion (O_2^-), hydrogen peroxide (H_2O_2), and hydroxyl radicals ($\cdot OH$). ROS are formed as a byproduct of normal oxidative mitochondrial metabolism and play a role as signaling molecules in regular physiological conditions (Devasagayam et al. 2004). Non-enzymatic and enzymatic endogenous antioxidant defenses control the harmful effects of the highly reactive ROS to prevent damage of RNA, DNA, proteins and lipids (Beckman et al. 1997; de Zwart et al. 1999; Stadtman et al. 2000). The enzymatic cascade reaction in mammals to detoxify ROS relies mainly on three enzymes: Superoxide dismutase (SOD) which is divided into three distinct enzymes, located in the cytoplasm (SOD1), in the mitochondria (SOD2) and in the extracellular space (SOD3) is responsible for the catalysis of superoxide into oxygen and hydrogen peroxide (Mann et al. 2007a). Hydrogen peroxide is transformed into oxygen and water by glutathione peroxidase (GPX) and catalase (CAT) (Mann et al. 2007a; Mann et al. 2007b). Other antioxidants like thioredoxins (TRXs), periredoxins (PRDXs) or heme oxygenase-1 also play a role in the defense mechanisms of cells (Schieber et al. 2014). Non-enzymatic antioxidants like vitamin C or vitamin E serve as electron donor (Burton et al. 1990; Padayatty et al. 2003) and metabolomics, which is defined as measurement of metabolite concentration in a cell or tissue, have extended the knowledge about non-enzymatic defense mechanisms in recent years (Andrisic et al. 2018). Hypoxia and reoxygenation increase oxidative stress by enhancing the levels of oxygen radicals

in mitochondria (Halliwell et al. 2015; Lluis et al. 2005). An excess amount of ROS overwhelming the cellular antioxidant defense causes lipid peroxidation, damage of membranes, enzymes and receptors, and DNA mutations leading to cell damage or cell death (Murphy 2009). In humans, a variety of pathological conditions are associated with hypoxia or oxidative stress for example stroke, chronic bronchitis, reperfusion injury after cardiac arrest or cancer (McGuire 2007; Ramirez et al. 2007). Investigating the adaptive mechanisms of hypoxia tolerant animals improves the understanding of defense mechanisms against hypoxia and oxidative stress and is of clinical significance.

4.2 Adaptations to hypoxia in diving and non-diving mammals

Many mammals live in extreme environments with a limited supply of oxygen. Animals inhabiting burrows or high altitudes experience chronic hypoxia due to a low oxygen partial pressure. Diving or hibernating mammals are exposed to acute intermitted hypoxia, occurring when diving mammals are submerged or hibernating mammals reduce their cerebral blood flow (Ramirez et al. 2007). The physiological adaptations to deal with chronic or acute hypoxia are diverse. However, mammals living in a low oxygen habitat display partly convergend physiological adaptations to assure oxygen supply. Burrowing animals, like the blind subterranean mole rat (*Spalax ehrenbergi*) or animals living at high altitude like the llama (*Lama glama*) have increased capillarization and enhanced levels of respiratory proteins as well as hypoxia-induced pulmonary vasoconstrictor response, indicating convergent evolution of maximizing oxygen supply (Groves et al. 1993; Monge et al. 1991; Ramirez et al. 2007; Widmer et al. 1997). However, beside these general adaptations, the physiological basis of hypoxia tolerance is highly dependent on the environment of the particular species. For example, while animals at high altitudes maximize their oxygen uptake with a high respiration rate (Banchero et al. 1971; Bickler et al. 2002; Monge et al. 1991), burrowing animals mostly maintain hypometabolism to reduce energy demands (Widmer et al. 1997; Nathaniel et al. 2013).

Marine species are most impressively adapted to their special lifestyle, with periods of entire isolation from atmospheric oxygen when submerged. In contrast to terrestrial mammals, like humans, who die within 3-4 minutes without breathing (Lutz et al. 2003), some marine mammals like the sperm whale (*Physeter macrocephalus*) or the elephant seal (*Mirounga leonine*)

execute dives to depth more than 1000 m and remain submerged for up to 2 h (Hindell et al. 1991; Watkins 1985). To survive these extreme conditions, marine mammals have developed extensive physiological adaptations (for review see: Allen et al. 2019; Butler 2004; Butler et al. 1997; Ponganis 2011; Ramirez et al. 2007). The diving response exists in almost all mammals, but is particularly pronounced in marine mammals to conserve O_2 during the dive. It consists of breathing cessation (apnea), decreasing heart rate (bradycardia) and selective vasoconstriction (Allen et al. 2019; Butler et al. 1997; Ramirez et al. 2007). The reduction of heart rate (bradycardia) is an efficient way to reduce the overall energy consumption of the body and can be decelerated to 5 beats per minute in extreme divers like northern elephant seals (*Mirounga angustirostris*) (Andrews et al. 1997). Bradycardia is also important to compensate for the enhanced blood pressure vasoconstriction would cause. Marine mammals constrict their arteries favoring blood flow to central organs like heart and brain, while peripheral tissues must rely on local oxygen stores provided by e.g. myoglobin as a local oxygen reservoir in muscle or on anaerobic metabolism (Blix et al. 1983; Butler et al. 1997; Kooyman et al. 1998; Scholander 1940). An increase of blood lactate levels in diving mammals, indicating energy production via anaerobic glycolysis, was observed only after long dives, resulting in the definition of the aerobic diving limit (ADL). The ADL is characterized as the diving duration at which the post-dive level of lactate in the blood rises above the pre-dive level (Kooyman et al. 1983; Scholander 1940; Shaffer et al. 1997; Williams et al. 1999). Downregulation of the body temperature is part of the diving response and is at least in some marine mammals expanded to the brain. Using a counter-current heat exchanger in the fore-flippers, harp seals and hooded seals are able to cool their brain as much as 3°C during diving (Blix et al. 2010; Odden et al. 1999). The reduction of brain temperature is thought to reduce the energy demand by up to 25 % and might extend the aerobic diving duration (Blix et al. 2010).

An increased oxygen storage capacity helps marine mammals to maintain oxidative metabolism during the dive. Since the lungs of marine mammals collapse during the dive (Falke et al. 1985; Kooyman et al. 1970; Moore et al. 2011), O_2 storage is depending on the storage capacity of blood and muscle. Because of this marine mammals have evolved elevated levels of the respiratory blood protein hemoglobin together with a larger blood volume compared to terrestrial mammals and high concentrations of oxygen storing myoglobin in muscles (Lenfant et al. 1970; Polasek et al. 2001; Ponganis 2011; Scholander 1940; Snyder 1983). Hematocrit and hemoglobin concentrations correlate positively with diving capacity (Hochachka 2000) implicating the ne-

cessity of an increased blood volume to prevent increased blood viscosity (Lenfant et al. 1970). A low O_2 affinity and a high Bohr coefficient of hemoglobin are also beneficial for deep diving mammals to facilitate O_2 unloading during the dive when acidosis rises (Snyder 1983; Willford et al. 1990). As for hemoglobin, the concentration of myoglobin in the muscles of diving mammals is positively correlated with their diving capacity (Lenfant et al. 1970; Polasek et al. 2001; Somero et al. 1990). On the basis of the O_2 storage capacity, body mass and oxygen consumption a theoretically calculated aerobic dive limit (cADL) can be determined for diving mammals (reviewed by Butler 2006). Diving within the cADL allows marine mammals to dive repeatedly without long recovery periods at the surface to remove accumulated lactate from the body (Butler 2006). However, in nature several species perform dives beyond their aerobic capacity, signifying the necessity for additional O_2- and energy saving adaptations (Butler 2006; Kooyman et al. 1980; Ponganis 2011; Tyack et al. 2006).

Recently, adaptations of marine mammals to diving on the molecular and genetic levels have attracted attention. Positive selection was found in whales in the hemoglobin genes and in myoglobin as well as in genes involved in the regulation of vasoconstriction (Mirceta et al. 2013; Nery et al. 2013; Tian et al. 2016). Mutations in the hemoglobin genes of whales are thought to play a role in their ability to cope with limited oxygen availability by modulating the physiochemical properties of the protein (Nery et al. 2013; Tian et al. 2016). While the oxygen affinity of myoglobin does not differ between terrestrial and diving mammals (Antonini 1965 1965; Jensen et al. 2004; Schenkman et al. 1997; Suzuki et al. 1998), mutations in the cetacean myoglobin contribute to protein stabilization correlating with higher expression (Dasmeh et al. 2013). An elevated myoglobin net surface charge in diving mammals is suggested to inhibit self-association at high concentrations (Mirceta et al. 2013). Genetic analyses revealed a strong positive selection in the citrate cycle pathway and the gluconeogenesis pathway in cetaceans, suggesting an enhanced aerobic metabolism as well as an improved removal of lactate after the dive (Tian et al. 2017). In genome wide scans for amino acid changes in whales and other hypoxia-tolerant mammals, positive selection was found in key-hypoxia related genes, for example in hypoxia-inducible factor 1 (HIF-1) (Tsagkogeorga et al. 2015; Zhu et al. 2018). HIF-1 is composed of two subunits HIF-1α and HIF-1β. Under normoxic conditions, HIF1-α is continuously degraded, while hypoxa causes the dimerization of HIF-1α and HIF-1β. The dimer translocates into the nucleus and ragultaes the transcription of genes involved in the hypoxia response (Lee et al. 2004; Wang et al. 1995). Seals exibit amino acid changes in the oxygen-dependent degradation

domain of the HIF-1α gene (Johnson et al. 2005) and amino acid changes in the HIF-1α gene are suggested to affect sensitivity and responsiveness to changing oxygen conditions (Bi et al. 2015), signifying its role as master regulator of the molecular response to hypoxia.

Sequencing of the minke whale (*Balaenoptera acutorostrata*) genome has revealed an expansion of gene families associated with stress response and anaerobic metabolism as well as whale specific mutations of genes involved in controlling blood pressure and in antioxidant genes (Yim et al. 2014).

Antioxidant systems in marine mammals have been investigated on the enzymatic and genetic levels. Higher concentrations and activities of antioxidant enzymes were found in tissues of diving mammals when compared to terrestrial mammals (Vazquez-Medina et al. 2006; Vazquez-Medina et al. 2012; Wilhelm Filho et al. 2002; Zenteno-Savin et al. 2002). For example, high gluthatione levels and acitivity of enzymes involved in its recycling were found in tissue of ringed seals but not in pig (*Sus scrofa*) (Vázquez-Medina et al. 2007). Comparing shallow-diving and deep-diving whales, Cantú-Medellín et al. (2011) found higher levels of antioxidant enzymes in tissues of deep-diving whales. In phylogenetic studies of cetaceans, several genes in the glutathione system and of the peroxiredoxin family were found to be expanded or under positive selection, indicating an enhanced capacity for antioxidant protection (Yim et al. 2014; Zhu et al. 2018).

4.3 Intrinsic mechanisms of cerebral hypoxia tolerance in diving and non-diving mammals

As described above, hypoxia tolerance of mammals is achieved through a complex synergy of mechanisms occurring on many levels. While the physiological adaptations are mostly understood the hypoxia tolerance of the diving brain still poses puzzles. The mammalian central nervous system must maintain persistent activity and cannot shut down to reduce oxygen consumption. The challenges for the brain during oxygen deprivation include managing metabolic costs, maintaining functional integrity and neuroprotection (Ramirez et al. 2007).

Small rodents display an excellent model organism to study cerebral hypoxia tolerance, since they are easy to obtain, and they can be exposed to hypoxia under laboratory conditions. The wide range of experimental procedures realizable with small model organisms has led to a high

number of studies examining the cerebral response to hypoxia and mechanisms of hypoxia tolerance in the brain of rodents. Several studies were performed on the hypoxia sensitive brain of mouse and rat to elucidate the protective mechanisms of preconditioning the brain with short insults of hypoxia (e.g. Bernaudin et al. 2002; Feng et al. 2007; Stenzel-Poore et al. 2007; Tang et al. 2006). The consistent finding of these experiments was an involvement of the anti-apoptotic ERK1/2 pathway in the neuroprotective mechanism of preconditioning (for review see: Cox-Limpens et al. 2014).

While these studies aim to examine short term adaptations of hypoxia sensitive mammals, the brain of hypoxia tolerant animals can reveal distinct adaptive molecular mechanisms of the brain under chronic and acute hypoxia. Subterranean rodents experience chronic hypoxia, as well as acute hypoxia-reoxygenation cycles and are an important model to study natural hypoxia tolerance (Shams et al. 2005). Comparative transcriptomics between blind mole rat (*Spalax sp.*) and rat (*Rattus norvegicus*) whole brain samples revealed a high expression of genes involved in DNA repair and response to oxidative DNA damage in the mole rat. Genes related to redox metabolism and oxidative phosphorylation were lower expressed in Spalax brain compared to rat, indicating differences in the regulation of energy production and ROS levels (Malik et al. 2016). Antioxidant enzymes showed a constitutively enhanced expression in Spalax brain compared to the rat and were higher in Spalax living at high altitude than in those living at lower altitudes, suggesting an increased antioxidant defense (Schülke et al. 2012; Cai et al. 2018). High expression of the respiratory genes neuroglobin (NGB) and cytoglobin (Cygb) in the brain of the mole rat indicate a function of both genes in hypoxia adaptation (Avivi et al. 2010). Under natural conditions, Spalax routinely experiences oxygen levels of 6 % and CO_2 levels of up to 7 %. In the laboratory, Spalax survived oxygen levels of 3 % for up to 14 h while rats died within 4 h (Shams et al. 2005). A regulatory response of the Spalax brain to these severe hypoxic conditions included upregulation of angiogenesis genes (the process of forming new blood vessels), genes suppressing apoptotic pathways and transcription factors which are activated by oxidative stress (Malik et al. 2012). Similar results were obtained in a transcriptomic approach examining the brain of the subterranean mandarin vole (*Lasiopodomys mandarinus*) under normoxia and hypoxia. The high altitude adapted mandarin vole upregulated genes associated with angiogenesis and oxygen transport capacity and downregulated genes involved in aerobic metabolism and immune response under hypoxia (Dong et al. 2018). While transcriptomic analyses of rodent brain under hypoxia provide valuable insights into the molecular mechanisms of cerebral hypoxia

tolerance in these species, the applicability to marine mammals is not assured. In contrast to burrowing rodents, marine mammals are exposed only to repeated acute hypoxia and not to chronic hypoxia and therefore, gene expression analyses of the brain of marine mammals might provide insights into hypoxia tolerance from a distinct perspective.

To date, it remains unclear to which extend the brain of seals and whales is exposed to hypoxia during natural dives. However, seals and porpoises have been found to maintain cerebral integrity at extremely low arterial partial oxygen pressure (PO_2) of 10 mmHg (Ponganis et al. 1993; Qvist et al. 1986; Stockard et al. 2007; Meir et al. 2009; Elsner et al. 1970; Ridgway et al. 1969), which is considerably lower than the human threshold for black-out of about 25 mmHg (Ferretti et al. 1991; Grocott et al. 2009), indicating a high cerebral hypoxia tolerance. Electrophysiological experiments of cerebral cortex slices of the hooded seal (*Cystophora cristata*) showed indeed a remarkable intrinsic neuronal hypoxia tolerance. Synaptic transmission in hooded seal neurons was maintained in extreme hypoxia with less than 1 % O_2 for up to an hour and in chemical anoxia (2 mN NaCN) for 15 minutes and recovered after 3 h of severe hypoxia while neurons of adult mice (*Mus musculus*) died within minutes (Fig. 2; Folkow et al. 2008; Larson et al. 2014; Ramirez et al. 2011; Geiseler et al. 2016).

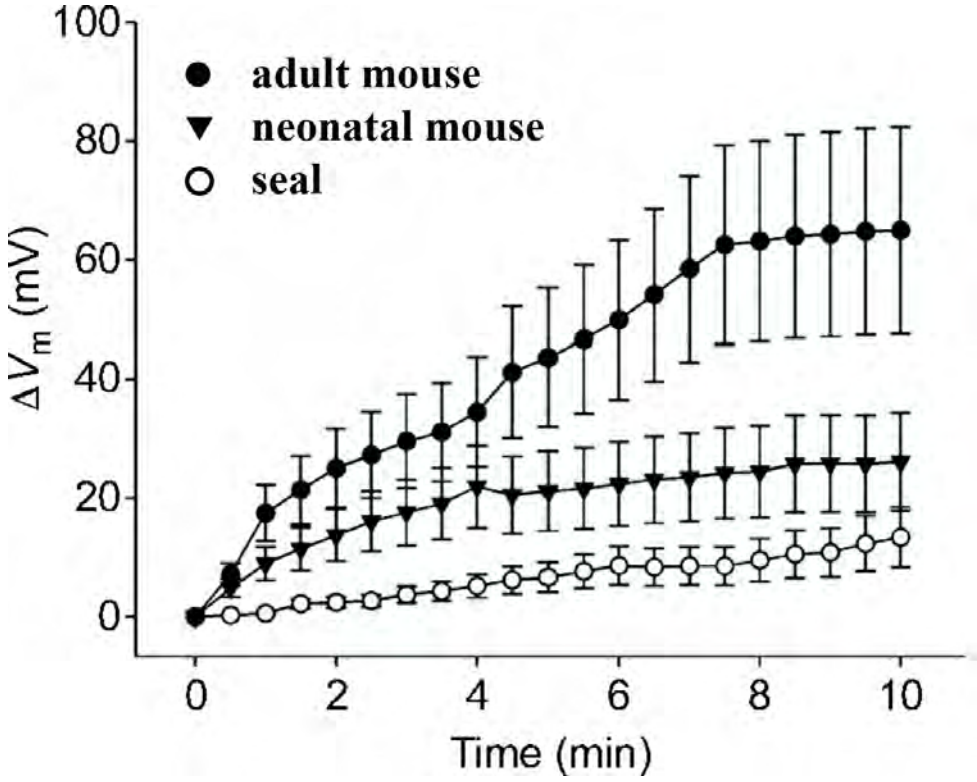

Figure 2 Changes in membrane potential (Δ Vm) in neurons during 10 minutes of severe hypoxia (>1 % O_2) in cortical neurons of hooded seal and mice (from Folkow et al. 2008)

The cellular and molecular mechanisms underlying the neuronal hypoxia tolerance are still poorly known. A higher capillary density in the diving brain may increase blood flow and decrease the diffusion distance for oxygen (Folkow et al. 2008; Kerem et al. 1973a; Kerem et al. 1973b; Odden et al. 1999; Ramirez et al. 2007; Williams et al. 2008). The respiratory protein neuroglobin, located in neurons, is thought to facilitate oxygen storage and transport in the brain (Burmester et al. 2000; Burmester et al. 2014). Enhanced levels of NGB were observed in the brains of the harbor porpoise (*Phocoena phocoena*) and the minke whale when compared to the cattle brain (Schneuer et al. 2012). NGB is also thought to play a role in ROS detoxification (Fordel et al. 2007; Li et al. 2010). Higher NGB levels in the diving brain might, therefore, contribute to the diving adaptation of the whale brain by ensuring oxygen supply during the dives or protect from ROS, which are generated during hypoxia or after reoxygenation. In seal brains however, protein levels of NGB did not differ from those of terrestrial mammals, but were located in astrocytes instead of neurons (Fig. 3; Mitz et al. 2009; Schneuer et al. 2012). Since NGB is a marker for aerobic metabolism (Bentmann et al. 2005. 2005; Schmidt et al. 2003), which co-localizes with cytochrome c (CYCS), a component of the respiratory chain, a divergent strategy in whales and seals was hypothesized (Mitz et al. 2009; Schneuer et al. 2012). NGB in the seal brain, present in astrocytes, lead to the suggestion of a reverse astrocyte-lactate shuttle in the seal brain. In terrestrial mammals as well as in whales, aerobic metabolism takes place mainly in neurons and is, at least partly, fueled by lactate which is produced by astrocytes via glycolysis (Pellerin 2005; Schneuer et al. 2012). The shift of the oxidative metabolism from neurons to astrocytes in the seal brain might enhance neuroprotection from oxidative stress and lower neuronal dependence on O_2 and on aerobic metabolism.

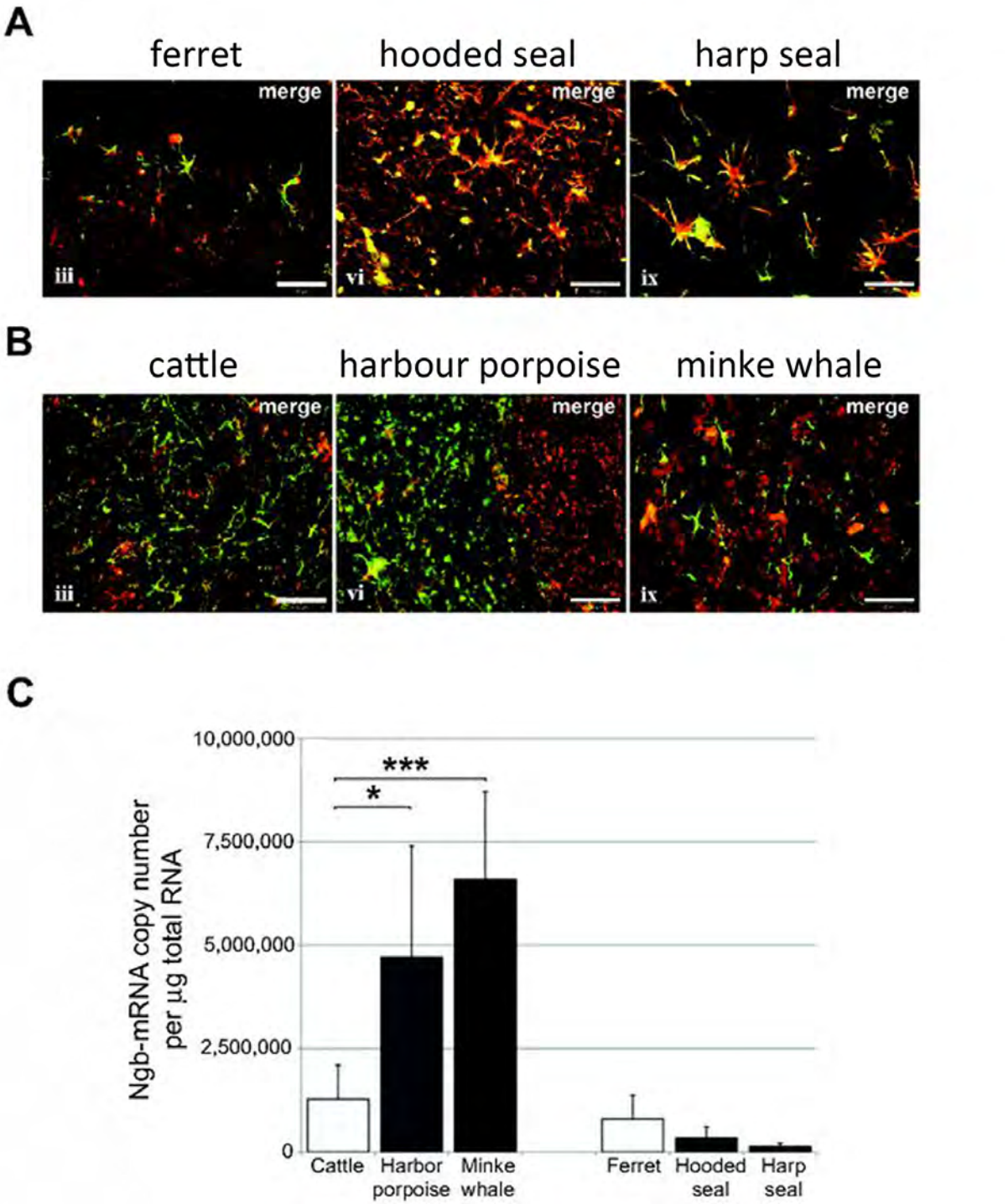

Figure 3 Distribution of neuroglobin in terrestrial and marine mammals. Merged immunofluorescence (yellow) of the glial marker glial fibrillary acidic protein (GFAP; green) and neuroglobin (NGB; red) in the cerebrum of A) ferret, (*Mustela putorius furo*), hooded seal, (*Cystophora cristata*) and harp seal, (*Pagophilus groenlandicus*), showing colocalization of GFAP and NGB and B) in the cerebrum of cattle, (*Bos taurus*), the harbor porpoise, (*Phocoena phocoena*) and the minke whale, (*Balaenoptera acutorostrata*), showing NGB immunoreactivity in neurons of the cerebral cortex in all species and only marginal colocalization of GFAP and NGB. C) Quantification of *Ngb* mRNA expression in the cerebral cortex of whales and seals compared with cattle and ferret (***p$\leq$ 0.001, *p$\leq$ 0.05). Scale bars: 50 μm (modified from Larson et al. 2014; Schneuer et al. 2012).

To increase anaerobic metabolism under hypoxic conditions is a possibility to avoid the detrimental effects associated with energy depletion (Hong et al. 2004; Larson et al. 2014). Anaerobic metabolism generates energy through the combustion of carbohydrates in the absence of oxygen and is, therefore, an alternative to oxidative phosphorylation under low oxygen conditions. The ATP yield of anaerobic energy metabolism is lower than that of a complete glucose oxidation. While glycolysis followed by oxidative phosphorylation produces 30 to 32 ATP per molecule glucose, anaerobic glycolysis yields only 2 ATP per molecule glucose (Berg et al. 2002). During long dives lactate accumulation in the blood plasma occurs, derived from anaerobic glycolysis in muscles and peripheral organs without sufficient oxygen supply, and may reach up to 14 mM (Davis 1983; Elsner et al. 1989; Hochachka 1981; Hochachka et al. 1977; Kerem et al. 1973a; Ponganis 2011). While acidosis caused by high concentrations of lactate damages neurons of terrestrial mammals (Giffard et al. 1990; Siesjo et al. 1996), the brain of the hooded seal tolerates high levels of lactate under normoxia and hypoxia (Czech-Damal et al. 2014). The low ATP yield of anaerobic glycolysis is insufficient for normal brain function and can only be compensated by high glycolytic rates and high substrate supply, such as intracellular glycogen stores. This lead to the suggestion that a high anaerobic capacity together with increased glycogen stores is fundamental for the hypoxia tolerance of the brains of diving mammals (Czech-Damal et al. 2014; Larson et al. 2014). Studies have investigated the anaerobic capacity of the brain of diving mammals with conflicting results. The glycogen content in the brain of adult weddel seal (*Leptonychotes weddellii*) and hooded seal was up to three-fold higher than in terrestrial mammals (Czech-Damal et al. 2014; Hoff et al. 2017; Kerem et al. 1973b), indicating indeed a higher anaerobic capacity in the diving brain. Lactate dehydrogenase (LDH), a key enzyme in the anaerobic metabolism, responsible for the interconversion of lactate and pyruvate, is an indicator for glycolytic metabolism (Holbrook et al. 1975). High activity of LDH as well as high activities of other glycolytic enzymes like hexokinase (HK), phosphofructokinase (PFK) and pyruvate kinase (PK), indicated a high anaerobic capacity in the brain of the weddel seal (Messelt et al. 1976; Murphy et al. 1980). In contrast to earlier studies, Castellini et al. (1981) found no evidence for higher anaerobic capacity when measuring activities of LDH and PK in brains of various species of diving and terrestrial animals. However, this study only used several species of seal and shallow diving porpoise (*Stenella attenuate*). Therefore, the anaerobic capacity of most species of whales and especially deep-diving whales remains unknown.

4.4 Animals used in this study

4.4.1 Whales

Whales are fully aquatic marine mammals and include the largest animals on earth. They are divided into baleen whales (Mysticeti) and toothed whales (Odontoceti) and belong to the order of even-toed ungulates (Cetartiodactyla). Among the toothed whales several record-breaking divers are found. The sperm whale is known to dive for more than one hour to a depth of up to 2000 meters (Amano et al. 2003; Watkins 1985). Recently, the Cuvier's beaked whale (*Ziphius cavirostris*) was found to dive even deeper than the sperm whale. With a diving duration of 2 hours and 17 minutes to a depth of 2992 meters, the Cuvier's beaked whale is the longest and deepest diving mammal on record (Schorr et al. 2014). However, brain samples of whales have to be obtained opportunistically and originate mostly from stranding events followed by prompt dissection.

In this study, no brain samples of the above mentioned deep-diving whales were available. Instead, several brain samples of different species of toothed whales were obtained and analyzed. One sample of the visual cortex of a stranded killer whale (*Orcinus orca*), one undefined brain sample of a bottlenose dolphin (*Tursiops truncatus*) that died in a German zoo and several samples of visual cortex and cerebellum of long-finned pilot whales (*Globicephala melas*) that were harvested in traditional whaling on Faroe Islands were used to unravel molecular mechanisms of cerebral hypoxia tolerance in whales. All three species belong to the superfamily of dolphins (Delphinoidea) which is the largest family within the toothed whales (Berta et al. 2005; Hoelzel 2009).

The killer whale (*Orcinus orca*)

The killer whale (Fig. 4) can reach 5.5 – 9.7 meter and up to 6 tons and is the largest dolphin and one of the marine apex predators (Baird 2000). The diet of killer whales consists of fish, cephalopods, marine mammals, sea birds and sea turtles (Baird 2000). Usually, killer whales perform shallow dives (<300 m) for under 4 minutes (Baird et al. 2005; Miller et al. 2010; Wright et al. 2017), but can descend to a depth of over 1000 m and stay submerged for up to 16 minutes (Reisinger et al. 2015; Towers et al. 2018). The brain of the killer whale is the second largest of all animals (5.4 – 6.8 kg) (Marino 2004; Pilleri et al. 1970) with only the sperm whale having a larger brain (~7 kg) (Kojima 1951; Pilleri et al. 1970; Ridgway et al. 1984). Showing cortical folding and development of spindle cells similar to humans and chimpanzees, the brain structure of the killer whale points to high intelligence (Marino et al. 2004) which is supported by self-awareness in the "mirror self-recognition paradigm" (Delfour et al. 2001).

Figure 4 Male killer whale (*Orcinus orca*) (Picture by www.pixabay.com)

The long-finned pilot whale (*Globicephala melas*)

The long-finned pilot whale (Fig. 5) is one of the largest dolphins reaching a length of 6.3 m and a weight of 2.5 tons (Desportes et al. 1993). The main diet of long-finned pilot whales consists of squid, including large-bodied species, and bony fish (de Stephanis et al. 2008; Gannon et al. 1997; Santos et al. 2014; Baird et al. 2002). The dives of long-finned pilot whales can last for up to 18 minutes. While most dives are shallow, a depth of over 800 m can be reached (Heide-Jørgensen et al. 2002). The cognitive capabilities of the long-finned pilot whale are not known, but a high number of neocortical neurons relative to body weight have been found, which might be related to advanced cognitive performance. In fact, long-finned pilot whales have more neocortical neurons than any other mammal studied so far (Mortensen et al. 2014).

Figure 5 Long-finned pilot whales (*Globicephala melas*) (Picture by https://www.flickr.com)

The common bottlenose dolphin (*Tursiops truncatus*)

Adult bottlenose dolphins (Fig.6) can reach up to 4 m in length with a weight of up to 500 kg. Pursuing the topic of cetacean intelligence, bottlenose dolphins in captivity and in the wild have been studied extensively. Those studies demonstrated for example tool usage, acoustic and behavioral mimicry, social learning, understanding of Numerical values and self-awareness for bottlenose dolphins, indicating a high cognitive ability (Kilian et al. 2003; Krutzen et al. 2005; Premack et al. 2001; Reiss et al. 1993; Rendell et al. 2001). Like most other toothed whales, bottlenose dolphins have a high encephalization quotient (EQ) (ratio between observed to predicted brain mass for an animal of a given size) of 4.4 (Marino 2004) and have been shown to possess spindle cells, like killer whales, which are thought to play a role in the development of intelligence (Butti et al. 2009).

Figure 6 Common bottlenose dolphins (*Tursiops truncatus*) (Picture by https://www.needpix.com)

4.4.2 The cattle (*Bos taurus*)

The cattle, or commonly known as the cow, is a member of ungulates (Fig. 7). Belonging to the taxon cetartiodactyla, cattle are the closest exclusively terrestrial relatives of cetaceans. Artiodactyla (the even-toed ungulates) and cetaceans separated approximately 56 million years ago, when the artiodactyl ancestor of cetaceans returned to the aquatic environment (Thewissen et al. 2007). The brain of cattle is slightly smaller than expected for an animal of its size with an EQ of 0.57 – 0.59, similar to other large terrestrial Cetartiodactyla. Compared to the EQ of whales, the cattle brain is similar to baleen whales, but not to toothed whales, indicating separate evolutionary pathways depending on feeding style (Ballarin et al. 2016. 2016). The cattle genome was the first fully mapped genome of livestock and contains approximately 22,000 genes of which 14,000 are found in all mammals (Elsik et al. 2009).

Figure 7 Female cattle (*Bos taurus*) with calf (Picture by: www.pxhere.com)

4.5 Aims of this study

The molecular mechanisms underlying the neuronal hypoxia tolerance of marine mammals are still mostly unknown. Modern experimental set-ups like genome or transcriptome sequencing begin to unravel genetic and molecular adaptations of marine mammals and allow more in-depth analyses of the molecular mechanisms behind the hypoxia tolerance of the diving brain. To increase the anaerobic energy production is one way to avoid damaging effects of hypoxic conditions and therefore, a high anaerobic capacity in the brain of marine mammals was proposed (Hong et al. 2004; Larson et al. 2014). Recent work by Fabrizius et al. (2016) found no evidence for a higher anaerobic capacity, but indications for a reduced aerobic energy metabolism in the seal. However, when measuring RNA levels of brain slices of the hooded seal under normoxia, hypoxia and reoxygenation, an upregulation of glycolytic genes was observed in hypoxic conditions. Additionally, an upregulation of typical stress genes involved in inflammation was found under hypoxia and reoxygenation, suggesting an at least partly conserved mammalian response (Hoff et al. 2017). Together, these findings indicate that the seal brain has no general high anaerobic capacity, but responds to hypoxic conditions with an increase in the anaerobic metabolism supported by high intrinsic glycogen stores (Czech-Damal et al. 2014; Larson et al. 2014).

So far, most of the physiological, molecular and electrophysiological studies unraveling the mechanisms of diving adaptation have been performed on pinnipeds and not on whales. This can be explained by the higher conservation status of whales and the reliance on opportunistically obtained samples. The preparation of brain slices of whales is nearly impossible to realize. Therefore, the RNA-Seq analysis of brain slices of the hooded seal under hypoxia is the only study so far examining the transcriptome of a marine mammal "brain" in hypoxic conditions. The estimated divergence time of seals and whales was 81 million years ago (Fig. 8; Kitazoe et al. 2007; Soares et al. 2013). While seals evolved from a caniform ancestor and are related to bears and musteloids (e.g. weasels) (Higdon et al. 2007; Lento et al. 1995), whales originate from even-toed ungulates (Vislobokova 2013).

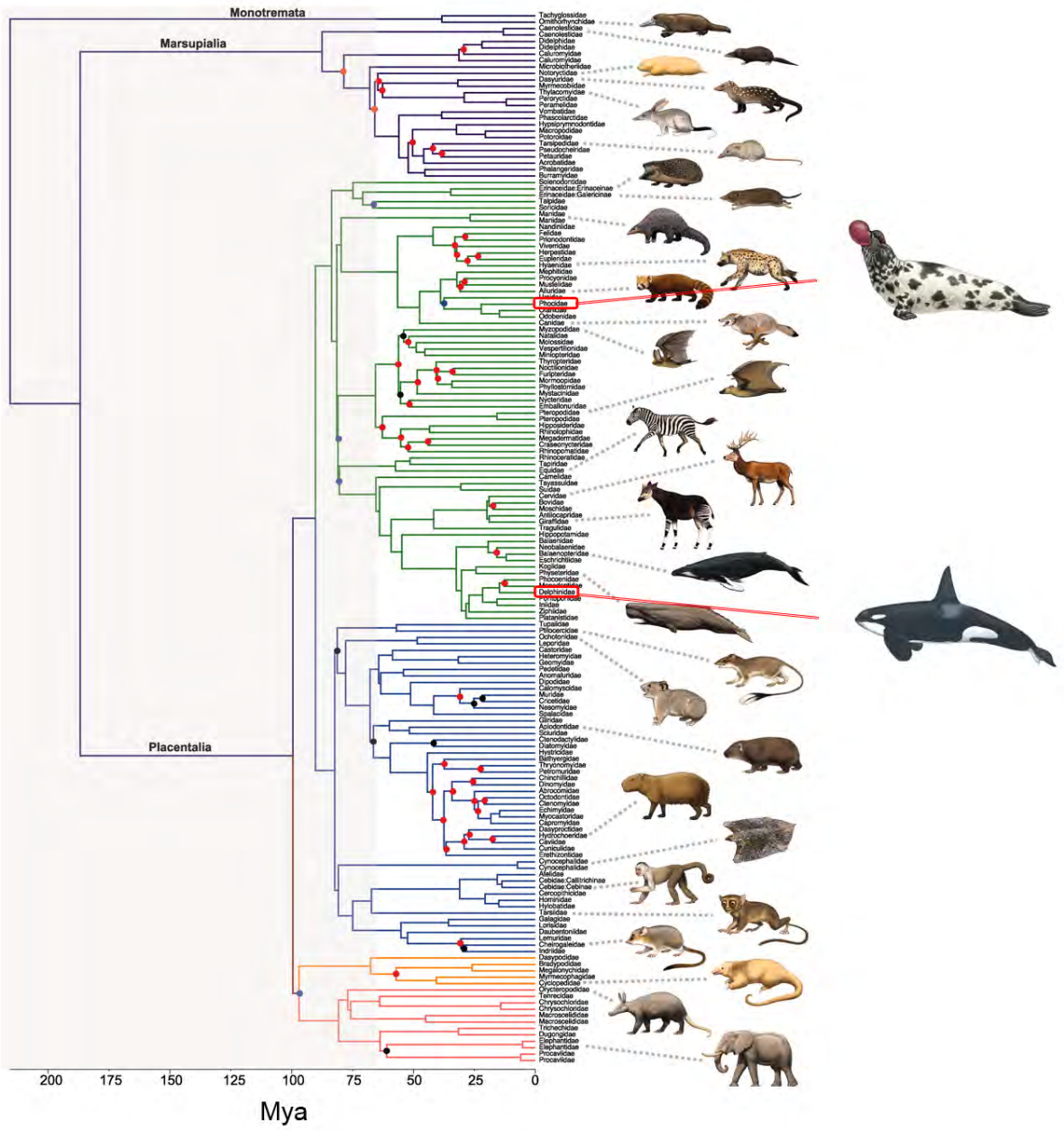

Figure 8 Phylogenetic timetree of mammalian families. Hooded seal and killer whale as representatives of phocid seals and toothed whales respectively, are highlighted (modified from Meredith et al. 2011).

The secondary aquatic transition of seals and whales has occurred independently and while convergent evolution of adaptations to the aquatic lifestyle has been found (e.g. formation of flippers), molecular strategies to cope with hypoxia might be very distinct. For example, the reverse ANLS found in seal brain but not in whale brain and the high expression of NGB only found in the whale brain suggest divergent strategies of cerebral hypoxia tolerance in seals and whales (Mitz et al. 2009; Schneuer et al. 2012). Therefore, specific investigations of the

adaptations in the whale brain are necessary to elucidate the basis of cerebral hypoxia tolerance in cetacean and to compare it with the molecular mechanisms in the seal brain.

To date, the only possibility to examine the molecular mechanisms underlying the cerebral hypoxia tolerance in whales is a comparative analysis of baseline levels and activities of enzymes. One can hypothesize that fundamental differences in the steady-state composition of energy metabolism pathways between whales and terrestrial relatives permit conclusions about cerebral adaptations to diving on the molecular level.

This study aimed to investigate the fundamental adaptations of the whale brain on the molecular level, focusing on gene expression and the consequences for brain function under hypoxia. A comparative approach was performed to find interspecific differences between brain samples of several species of whales and their closest terrestrial relative, the cattle. Here another difficulty becomes obvious. Whales and cattle separated approximately 56 million years ago and their lifestyles are very distinct (Thewissen et al. 2007). However, the only extant relative closer to whales than cattle is the hippo. Samples of hippo brain were not available for this study and no reference genome is published. In contrast, a well annotated genome of the cattle is available (Elsik et al. 2009). Therefore, comparison of whale brain samples to the cattle provides the most reliable results.

The fundament of the study was laid in Chapter I where transcriptomes of the cerebellum and the visual cortex of the long-finned pilot whale, of the visual cortex of the killer whale and the visual cortex of the cattle, were sequenced. In an RNA-Seq approach differences in gene expression in the brains of whales and cattle were analyzed to reveal possible adaptations to hypoxia in the whale brain on the molecular level. Additional transcriptomes from the NCBI SRA dataset of the brain of the bowhead whale (*Balaena mysticetus*) and the minke whale as well as four brain transcriptomes of cattle were included, and global gene expression levels between cattle and whale brain samples were compared. Furthermore, brain region specific differences in gene expression in the visual cortex and the cerebellum of the long-finned pilot whale were examined. A comparison of the transcriptomes of solely the visual cortex of whale and cattle was performed to elude brain region specific differences in gene expression and reveal possible gene expression involved in the diving adaptation of the whale brain.

Specific candidate genes for hypoxia tolerance with high expression differences in whale and cattle brains were further investigated in Chapter II. One candidate gene, superoxide dismutase 1 (SOD1), is involved in the antioxidant defense cascade and is thought have neuroprotective

functions (Sea et al. 2015). The second candidate gene COMM domain containing 6 (COMMD6) is involved in the regulation of the transcription factor NF-κB (de Bie et al. 2006), which functions in the hypoxia response of cells (Crack et al. 2006; Schneider et al. 1999). The effect of overexpression of these genes was analyzed in a neuronal mouse cell line (HN33) exposed to hypoxic and oxidative stress to investigate the role of individual genes in the diving brain.

The hypothesis of increased anaerobic capacity in the whale brain, represented by the analysis of the key enzyme lactate dehydrogenase (LDH) was investigated in Chapter III. Several parameters of LDH including gene expression, gene duplication, activity and isoenzyme distribution were compared between brain samples of killer whale, long-finned pilot whale, bottlenose dolphin and cattle, to reveal adaptations to diving in the lactate metabolism of the whale brain.

5 Statement of contributions

Chapter I

Krüger, A., Fabrizius, A., Mikkelsen, B., Siebert, U., Folkow, L. P. and Burmester, T. (2019). "Transcriptome analysis reveals a high aerobic capacity in the whale brain." Comp. Biochem. Physiol. A Mol. Integr. Physiol. 240: 110593

- Preparation of RNA for Illumina sequencing
- Analysis and interpretation of the Illumina data
- Draft of the manuscript

Chapter II

Krüger, A., Geßner, C., Fabrizius, A., Mikkelsen, B., Siebert, U., Folkow, L. P. and Burmester, T.: "The SOD1 and COMMD6 genes of the killer whale (*Orcinus orca*) protect hippocampal neuronal cells from hypoxia and oxidative stress." (in preparation)

- Contribution to study design
- Experiments: sequence analysis, RNA extraction and cloning, qRT-PCR, cell culture experiments
- Analysis (except statistics in R) and interpretation of data
- Draft of the manuscript

Chapter III

Krüger, A., Dönmez, E., Fabrizius, A., Mikkelsen, B., Siebert, U., Folkow, L. P. and Burmester, T.: "The composition of lactate dehydrogenase isoenzymes in the cetacean brain may reflect adaptation to diving." (submitted to Journal of Comparative Physiology B)

- Study design
- Experiments: expression analysis (RNA-Seq), sequence analysis, protein structure, enzyme activity assays, native protein gel electrophoresis
- Analysis and interpretation of data (except qRT-PCR)
- Draft of the manuscript

6 Chapter I

Transcriptome analysis reveals a high aerobic capacity in the whale brain

Alena Krüger[a], Andrej Fabrizius[a], Bjarni Mikkelsen[b], Ursula Siebert[c], Lars P. Folkow[d], Thorsten Burmester[a]

[a]Institute of Zoology, University of Hamburg, Germany

[b]Natural History Museum, Faeroe Islands

[c]Institute for Terrestrial and Aquatic Wildlife Research, University of Veterinary Medicine Hannover, 25761 Büsum, Germany

[d]University of Tromsø – The Arctic University of Norway, NO-9037 Tromsø, Norway

Published: Oct 30 2019 in Comparative Biochemistry and Physiology, Part A

Krüger, A., Fabrizius, A., Mikkelsen, B., Siebert, U., Folkow, L. P., & Burmester, T. (2019). Transcriptome analysis reveals a high aerobic capacity in the whale brain. Comparative Biochemistry and Physiology Part A: Molecular & Integrative Physiology, 110593

Abstract

The brain of diving mammals is repeatedly exposed to low oxygen conditions (hypoxia) that would have caused severe damage to most terrestrial mammals. Some whales may dive for >2 h with their brain remaining active. Many of the physiological adaptations of whales to diving have been investigated, but little is known about the molecular mechanisms that enable their brain to survive sometimes prolonged periods of hypoxia. Here, we have used an RNA-Seq approach to compare the mRNA levels in the brains of whales with those of cattle, which serves as a terrestrial relative. We sequenced the transcriptomes of the brains from cattle (*Bos taurus*), killer whale (*Orcinus orca*), and long-finned pilot whale (*Globicephala melas*). Further, the brain transcriptomes of cattle, minke whale (*Balaenoptera acutorostrata*) and bowhead whale (*Balaena mysticetus*), which were available in the databases, were included. We found a high expression of genes related to oxidative phosphorylation and the respiratory electron chain in the whale brains. In the visual cortex of whales, transcripts related to the detoxification of reactive oxygen species were more highly expressed than in the visual cortex of cattle. These findings indicate a high oxidative capacity in the whale brain that might help to maintain aerobic metabolism in periods of reduced oxygen availability during dives.

Keywords: Cetacean, Hypoxia tolerance, Aerobic metabolism, Marine mammals, Diving

Introduction

In most mammals, including humans, a shortage in O_2 supply (hypoxia) leads to irreversible damage to the brain and death of neurons within a few minutes (Choi et al. 1990; Dirnagl et al. 1999; Peers et al. 2007; Walton et al. 1999). Without O_2, the oxidative phosphorylation stops and alternative pathways cannot produce sufficient amounts of ATP, which leads to an impairment of highly energy-consuming processes such as ion transport or neurotransmitter uptake. Depolarization and an excessive extracellular release of neuro-transmitters results in overstimulation of receptors and uncontrolled Ca^{2+} influx, which triggers cell damage and, eventually, cell death (Bano et al. 2007; Lipton 1999). For a limited period, ATP production can be sustained by anaerobic glycolysis, which, however, leads to the production of lactate. An excess of lactate decreases the pH, resulting in additional energy consumption and cell damage. When the O_2 supply is re-established, the excess of O_2 causes the generation of reactive oxygen species (ROS), which leads to additional damage (Cherubini et al. 2005; Murphy 2009; Therade-Matharan et al. 2005). In humans, an impaired supply of O_2 to the brain is involved in various diseases that cause millions of casualties. For example, cerebral ischemia (stroke) has a devastating impact on the nerve cells, which is largely impossible to repair (Ding et al. 2014; Horner et al. 2000).
Diving mammals can cope with extended periods of quite severe hypoxia, apparently without damage to their brain (Butler 2004; Butler et al. 1997; Kerem et al. 1973a; Meir et al. 2009; Ramirez et al. 2007). Expert divers may perform dives exceeding 2 h (Schorr et al. 2014), which require multiple behavioral, morphological, physiological and molecular adaptations. For example, since marine mammals cannot breathe during the dives, O_2 must be stored bound to hemoglobin, which is present in very high levels in their blood (Burns et al. 2007; Scholander 1940; Snyder 1983). The high myoglobin content of their muscles provides additional local O_2 stores (Lenfant et al. 1970; Polasek et al. 2001; Scholander 1940; Snyder 1983). During long-duration diving, circulatory mechanisms such as peripheral arterial constriction ensure blood supply to the most O_2-sensitive organs (e.g., the brain) while reducing the O_2-delivery to other organs (e.g., kidney and gut) to a minimum (Blix 2018; Blix et al. 1983; Scholander 1940; Zapol et al. 1979). Under such conditions, these tissues subsist based on a combination of hypometabolic and anaerobic processes (Blix 2018; Butler 2004; Butler et al. 1997; Ramirez et al. 2007; Scholander 1940).
In recent years, the first data on the molecular adaptations of marine mammals have emerged. For example, the genome of the minke whale (*Balaenoptera acutorostrata*) showed amplification of genes involved in stress-response and anaerobic metabolism, and a loss of genes involved in hair formation and sensing (Yim et al. 2014). The return into the water was accompanied by a shift in the molecular evolutionary rate (Chikina et al. 2016), including positive selection in genes involved in hypoxia adaptation (Tian et al. 2016) and energy metabolism (McGowen et al. 2012). The comparative analysis of the genomes of unrelated marine mammals, such as killer whale, walrus (*Odobenus rosmarus*) and the manatee (*Trichechus manatus latirostris*) identified multiple convergent substitutions in distinct genes, suggesting that similar molecular mechanisms and metabolic pathways are involved (Foote et al. 2015). In addition, Mirceta et al.

(2013) revealed that net surface charge characteristics of myoglobin allow elevated myoglobin levels in several species of diving mammals, thus indicating a convergent molecular adaptation. Brain-specific adaptations have been investigated in the hooded seal (*Cystophora cristata*) (Fabrizius et al. 2016; Hoff et al. 2017). Comparative transcriptomics showed, for example, lower levels of enzymes involved in aerobic metabolism in the seal brain compared to the closely related ferret (*Mustela putorius*), which may reflect an energy saving strategy. The mRNA levels of certain stress-related proteins, i.e., clusterin and S100B, were found enhanced in the hooded seal brain, and it may be that these genes contribute to convey hypoxia tolerance to the seal brain (Fabrizius et al. 2016). However, it is still largely unknown how the brain of whales copes with the hypoxic stress during the dive and reperfusion after surfacing. We found that the brains of the harbor porpoise (*Phocoena phocoena*) and the minke whale have higher neuroglobin levels than the brain of cattle (*Bos taurus*), which may contribute to enhanced O_2 supply (Schneuer et al. 2012).

To better understand the molecular adaptations of the whale brain, we have sequenced the brain transcriptomes of the killer whale (*Orcinus orca*), the long-finned pilot whale (*Globicephala melas*), and cattle (*B. taurus*). Although not generally deep divers, foraging killer whales can dive to at least 700 m (Reisinger et al. 2015). The pilot whale reaches >800 m with high speed ("cheetahs of the sea" (de Soto et al. 2008)), suggesting high energy and O_2 consumption. The available brain transcriptomes of the minke whale (*B. acutorostrata*), the bowhead whale (*Balaena mysticetus*) and additional cattle transcriptomes were integrated into the analysis of the gene expression levels by RNA-Seq.

Materials and methods

Animals

The brain samples of all animals used in this study were obtained opportunistically. The brain of a cattle (*B. taurus*) (male, 22 months) was acquired from a German butchery under the exceptional permission of the German law (*Tierische Nebenprodukte-Beseitigungsgesetz*). Dissection of the skull and sampling of the visual cortex was performed by the University of Hamburg taxidermist. The brain of a juvenile killer whale (*O. orca*), which died after stranding alive, was transported to the Institute of Terrestrial and Aquatic Wildlife Research, University of Veterinary Medicine Hannover, Foundation, in Büsum for necropsy. A brain sample of the visual cortex was preserved in RNAlater at -80 °C (Qiagen, Hilden, Germany). Samples of the visual cortex and the cerebellum from a long-finned pilot whale (*G. melas*) (male, body length 569 cm) were obtained from an animal that was harvested during traditional whaling on the Faroe Islands. The visual cortex was chosen because this tissue was used in the first electrophysiological recordings from seal brain slices, demonstrating its remarkable hypoxia tolerance (Folkow et al. 2008), later followed by further studies on potential mechanisms underlying hypoxia tolerance in the seal brain, e.g., by Fabrizius et al. (2016) and Hoff et al. (2017). The cerebellum was used as a reference tissue to address regional differences in gene expression and to detect

potential global adaptations in the brain. This particular region was also largely chosen because of previous studies (e.g. Mitz et al. 2009; Schneuer et al. 2012). *Regulations of the Convention on Biological Diversity* (CBD) and *Convention on International Trade in Endangered Species of Wild Fauna and Flora* (CITES) were followed, and the appropriate permits were obtained (Permit number: E-01456/17).

RNA preparation and sequencing

Total RNA was extracted using peqGOLD Trifast (PEQLAB, Erlangen, Germany) or Crystal RNA Mini Kit (Biolab Products, Bebensee, Germany). The quality and quantity of the RNA were analyzed by spectrophotometry and gel electrophoresis. Total RNA from the visual cortices of the cattle (2 μg), the killer whale (9 μg), and from the visual cortex and cerebellum of the long-finned pilot whale (2.5 μg each) were used for the generation of a cDNA library. Paired-end sequencing (PE 150) was performed on a NextSeq 500 platform (StarSEQ, Mainz, Germany) with an estimated output of 50 million reads per sample. Analysis of the data was performed with the aid of CLC Genomics Workbench, Version 10.0.1 (Qiagen, Venlo, Netherlands). For quality trimming the first 15 nucleotides from the 5′ end were removed. Additionally, all reads with more than two ambiguous nucleotides and reads with a mean Phred quality lower than 15 were discarded. The raw Illumina files of the transcriptomes are available from the NCBI Sequence Read Archive (SRA) from the visual cortex of the cattle (SRR8305676), the visual cortex of the killer whale (SRR8305677), and from the visual cortex (SRR8305674) and cerebellum (SRR8305675) of the long-finned pilot whale and under the Bioproject PRJNA506903.

Differential expression analysis using RNA-Seq

To identify genes differentially expressed between the brains of cattle and whale, the transcriptome datasets of long-finned pilot whale (visual cortex and cerebellum), killer whale (visual cortex), bowhead whale (cerebellum) (*B. mysticetus*) (SRX790347) and minke whale (brain region not specified) (*B. acutorostrata*) (SRX313597) were compared with five transcriptomes of the cattle (3 × visual cortex, 2 × frontal lobe) (SRX211675, SRX211674, SRX196362, SRX196353, SRX196362). Mapping of the quality-trimmed reads was performed using the RNA-Seq algorithm of the CLC Genomics Workbench. Due to a high percentage of mitochondrial reads in some datasets, the mitochondrial transcripts were excluded. Whale reads matching 75 % of the read length and 75 % of the nucleotides of the cattle mitochondrial genome were excluded from further analysis. For the filtering of the cattle mitochondrial reads parameters were adjusted to 85 % read length and 85 % identity. The NCBI cattle genome (assembly ARS-UCD1.2) was used as reference genome. Only reads that matched 85 % of the read length and 85 % of nucleotides of the reference were included in the mapping of the whale reads. For the mapping of the cattle reads, parameters were adjusted to 90 % length match and 90 % similarity. Reads with non-specific matches were ignored in the mapping. The paired read distance was calculated automatically. Differential gene expression analysis was carried out using the CLC Genomics Workbench tool for statistical analysis. The unique gene read number normalized to total reads of each sample was used as count values for the “Exact Test” (Robinson et al. 2007). A cut-off

of 5 reads and a Bonferroni-correction of the p-values were applied. Only genes with a fold change ≥2, a range (difference between the highest and the lowest expression value) ≥5 and a Bonferroni-corrected p-value ≤0.05 were considered significant. Gene expression was calculated as RPKM (Reads Per Kilobase per Million mapped reads) (see Additional File I.1). Differential expression analysis was also conducted with two brain transcriptomes of the beluga whale (*Delphinapterus leucas*) that were available at the Short Read Archive (SRX2585929, SRX2585928) (see Additional File I.2), but these data were not included in the analyses due to large differences in overall gene expression compared to other species of whales.

Gene ontology analysis

Gene Ontology (GO) analyses were performed using the PANTHER Overrepresentation Test (Protein Analysis Through Evolutionary Relationships, http://go.pantherdb.org/) version 13.1 released 2018-02-03 (Mi et al. 2017). Contigs with high expression in whales transcriptomes but annotated as pseudogenes in the cattle genome were considered functional in whales and renamed to their parental genes (Additional File I.3). The annotated cattle genes in the PANTHER DB were used as a reference list, and overrepresentation was tested in the PANTHER GO-Slim terms and Reactome pathways with Fisher's Exact Test with FDR multiple test correction. Only categories with corrected p-values <0.05 were considered significant.

Principal component analysis

Principal component analysis (PCA) was performed by plotting the two principal components of the log10 transformed expression values of all 34,436 transcripts using the CLC Genomics Workbench Principal Component Analysis tool with default settings.

Results

Generation of transcriptomes of the whale brain

We generated ~40 million Illumina reads (150 nt, paired-end) of the transcriptomes from the brains of each, the killer whale (visual cortex), the long-finned pilot whale (visual cortex and cerebellum), and – to allow a comparative approach – of cattle (visual cortex). We included the transcriptomes of four additional cattle brains in the analyses, which were available from the SRA database at NCBI (Table I.1). To trace possible adaptations of the whale brain to diving on the molecular level, we estimated the mRNA levels of the brain transcriptomes by RNA-Seq. Due to the lack of an annotated whale genome, the cattle genome was employed as a reference.

Table I.1 Summary of illumina sequencing.

Sample[a]	SRA accession	Raw reads #	Trimmed	Trimmed without mitochondrial reads	Mapped reads %
Oor	SRR8305677	29,964,586	29,861,576	26,448,179	39.76
Gme VC	SRR8305674	49,465,538	49,462,293	47,712,366	52.95
Gme CE	SRR8305675	41,444,974	41,442,287	42,197,185	50.84
Bac	SRR918699	51,470,260	51,341,266	50,624,402	63.7
Bmy	SRR1685414	21,182,210	17,750,937	20,935,295	49.39
Bta1	SRR8305676	32,089,626	32,086,347	24,615,661	80.37
Bta cowb	SRR594482	56,890,388	56,292,520	51,624,386	91.41
Bta cowc	SRR594491	67,256,226	64,242,921	59,311,464	89.93
Bta br1	SRR636934	53,310,044	53,119,486	48,272,031	92.16
Bta br2	SRR636935	29,597,408	29,429,907	26,871,240	90.85
Dle A[b]	SRX2585928	246,941,740	246,909,289	238,525,305	53.82
Dle Q[b]	SRX2585929	270,336,352	270,299,555	258,319,503	47.46

The number of reads per sample before and after quality trimming is given. The reads used for RNA-Seq after elimination of reads originating from mitochondrial genes and the percentage of reads mapped to the cattle genome is denoted. [a] Oor = *Orcinus orca*; Gme VC = *Globicephala melas* (visual cortex); Gme CE = *Globicephala melas* (cerebellum); Bac = *Balaenoptera acutorostrata*; Bmy = *Balaena mysticetus*; Bta = *Bos taurus*; cowb = *Bos taurus* sample b; cowc = *Bos taurus* sample c; br1 = *Bos taurus* sample br1, br2 = *Bos taurus* sample br2; Dle = *Delphinapterus leucas*. [b] Only used for PCA.

Generation of transcriptomes of the whale brain

We first examined the regional differences of mRNA levels within the whale brain by comparing the transcriptomes of the visual cortex and the cerebellum from the long-finned pilot whale. In the visual cortex, the most highly expressed gene was synaptosomal nerve-associated protein 25 (SNAP25; 2151 RPKM), followed by the glycolytic enzyme glyceraldehyde 3-phosphate dehydrogenase (GAPDH; 1871 RPKM), and the proteolipid-protein 1 (PLP1; 1431 RPKM). In the cerebellum, the highest expression also was found for SNAP25 (1966 RPKM), followed by the glycolytic enzyme aldolase C (ALDOC; 1327 RPKM) and S100 calcium-binding protein B (S100B; 1277 RPKM) (see Additional File I.4 Table S1).

The most highly overrepresented (highest RPKM-fold difference) transcript in the visual cortex relative to the cerebellum was the guanine deaminase (GDA; 8594-fold difference), which plays a role in the guanine degradation (Yuan et al. 1999). The second highest difference was found for neurogranin (NRGN; 4002-fold), a gene that interacts with the calcium regulator calmodulin (Prichard et al. 1999), followed by the mechanosensory transduction mediator homolog STUM (738-fold difference) that is essential for mechanical sensing in proprioceptive neurons in the fruit fly (Desai et al. 2014), and the G protein-coupled receptor 26 (GPR26; 721-fold difference), which is involved in responses to environmental stimuli (Jones et al. 2007) and, at last, the gamma-aminobutyric acid type A receptor alpha 5 subunit (GABRA5; 665-fold difference) that acts as receptor to GABA which is the major inhibitory neurotransmitter in the mammalian

brain (Wingrove et al. 1992) (Table I.2A).
The transcripts that were most highly overrepresented in the cerebellum compared to the visual cortex were: fat atypical cadherin 2 (FAT2; 10,143-fold difference), a cerebellar development protein (Nakayama et al. 2002), another GABA receptor subunit (GABRA6; 2190-fold difference), and a glutamate ionotropic receptor NMDA type subunit 2C (GRIN2C; 1648-fold difference) that is involved in learning, memory, and synaptic development (Ogden et al. 2017). The next two were the rho guanine nucleotide exchange factor 33 (ARHGEF33; 1494-fold difference) and the zic family member 4 transcript (ZIC4; 1195-fold difference), which plays a role in the cerebellar development (Blank et al. 2011) (Table I.2B).

Table I.2 Transcripts overrepresented in different brain regions of the long-finned pilot whale.

Gene	Gene symbol	Function	Visual cortex (RPKM)	Cerebellum (RPKM)	Fold difference
A. Visual cortex					
Guanine deaminase	GDA	Microtubule assembly	69.46	0.01	8594
Neurogranin	NRGN	Protein kinase substrate that binds calmodulin	740.41	0.19	4002
Stum, mechanosensory transduction mediator homolog	STUM	Essential for mechanical sensing in proprioceptive neurons	21.03	0.03	738
G protein-coupled receptor 26	GPR26	Responses to environmental stimuli	8.40	0.01	721
Gamma-aminobutyric acid type a receptor alpha5 subunit	GABRA5	Ligand-gated chloride channel	91.53	0.14	665
B. Cerebellum					
FAT atypical cadherin 2	FAT2	Cerebellar development	0.01	109.15	10,143
Gamma-aminobutyric acid type a receptor alpha6 subunit	GABRA6	Ligand-gated chloride channel	0.18	385.03	2190
Glutamate ionotropic receptor nmda type subunit 2C	GRIN2C	Learning, memory, and synaptic development	0.03	49.48	1648
Rho guanine nucleotide exchange factor 33	ARHGEF33	Rho guanyl-nucleotide exchange	0.01	16.89	1494
Zic family member 4	ZIC4	Transcriptional regulation	0.01	13.14	1195

Transcripts most highly overrepresented in the visual cortex (A) vs. the cerebellum (B) of the long-finned pilot whale.

We conducted a gene ontology (GO) analysis with the PANTHER GO-Slim tool of transcripts overrepresented in either the visual cortex or the cerebellum. Only transcripts with an RPKM-fold difference >2 and RPKM >5 in one sample were considered. We found 1184 transcripts higher expressed in the visual cortex and 1020 transcripts higher expressed in the cerebellum (see Additional File I.5). The 1184 transcripts that were higher expressed in the visual cortex showed enrichment in several GO terms in the category Biological Process (Fig. I.1). The highest enrichment was found for the terms: "skeletal system development (GO:0001501)" (7.1-fold, corrected p-value: 0.0103), "cell growth (GO:0016049)" (4.1-fold, p-value: 0.00001) and "JNK cascade (GO:0007254)" (3.9-fold, p-value: 0.0407). In total, 303 transcripts were found to be statistically enriched in ten GO terms in the category Biological Process (Fig. I.1).

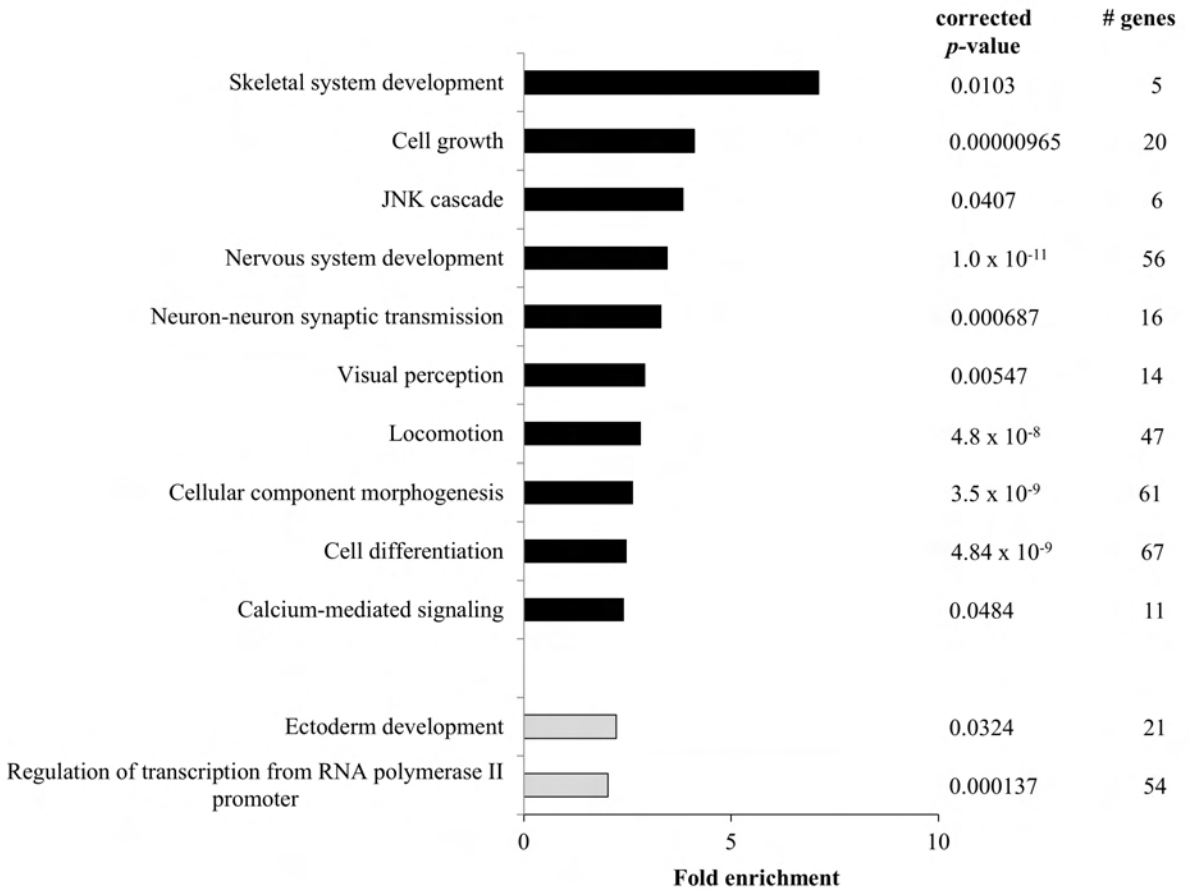

Figure I.1 Enriched GO-Slim terms in the visual cortex vs. cerebellum of the long-finned pilot whale. Significantly enriched GO-Slim terms for the gene set higher expressed in the visual cortex (black) and the cerebellum (grey) of the long-finned pilot whale for the category Biological Process according to their Fold Enrichment, with corrected p-values and the number of genes. (Note: JNK cascade is defined as intracellular protein kinase cascade containing at least a JNK (a MAPK), a JNKK (a MAPKK) and a JUN3K (a MAP3K).)

In the 1020 transcripts that were higher expressed in the cerebellum only the terms "ectoderm development (GO:0007398)" (2.2-fold, p-value: 0.0324) and "regulation of transcription from RNA polymerase II promoter (GO:0006357)" (2-fold, p-value: 0.00014) were found to be enriched in the GO-category Biological Process, totaling 75 transcripts.

Analysis of gene set enrichment in the visual cortex of whales and cattle

As we found significant regional differences in the gene expression profiles in the brain of the long-finned pilot whale, we used for the following comparative analyses only the visual cortex of pilot whale, killer whale, and cattle. Only transcripts that had an RPKM >2 in all samples were included. The transcript most highly overrepresented in the visual cortex of the killer whale and the long-finned pilot whale was tubulin alpha-1C chain-like (LOC100141266; 44.6-fold), which may be important for microtubule cytoskeleton organization, followed by complement C1q C chain (C1QC; 20-fold), which may be involved in immune regulation (Petry 1998), and dehydrogenase/reductase 7 (DHRS7; 17.3-fold), which encodes a member of the short-chain dehydrogenases/reductases family that metabolize many compounds such as steroid hormones, prostaglandins and retinoids (Matsunaga et al. 2008). The ribosomal protein S4 y-linked 1 (RPS4Y1) showed a 16-fold difference and was followed by the solute carrier family 38 member 5 (SLC38A5; 11.2-fold), which functions as a sodium-dependent amino acid transporter (Nakanishi et al. 2001) (Table I.3).

Table I.3 Transcripts most highly overrepresented in the visual cortex of the long-finned pilot whale and the killer whale

Gene	Gene symbol	Function	Whale mean (RPKM)	Cattle mean (RPKM)	Fold difference	p-value (Bonferroni)
Tubulin alpha-1C chain-like	LOC100141266	Microtubule cytoskeleton organization	162	3.6	44.6	4×10^{-16}
Complement C1q C chain	C1QC	Immune response	59.6	3	20	7.5×10^{-5}
Dehydrogenase /reductase 7	DHRS7	Oxidoreductase activity	75	4.3	17.3	2.7×10^{-8}
Ribosomal protein S4 Y-linked 1	RPS4Y1	Translation	364.9	22.8	16	1.6×10^{-5}
Solute carrier family 38 member 5	SLC38A5	Amino acid transport	47.6	4.3	11.2	0.517

Transcripts most highly overrepresented in the visual cortex of the killer whale and the long-finned pilot whale compared to the visual cortex of cattle are shown.

For differential expression analyses, only transcripts with at least a two-fold difference of normalized unique gene reads, a range (difference between the highest and the lowest normalized unique gene reads) >5, and a Bonferroni corrected p-value <0.05, were considered. We found 560 genes that were significantly higher expressed in the visual cortex of cattle compared to the mean value for killer whale and long-finned pilot whale visual cortices. In total 613 genes were

higher expressed in the mean expression values of visual cortices of the pilot whale and the killer whale (Additional File I.6), compared to the visual cortex of cattle. No enrichment was found in the PANTHER Overrepresentation Test for the genes that were more highly expressed in the cattle brain. Annotating the transcripts more highly expressed in the visual cortex of whale, the PANTHER GO-Slim category Biological Process showed several enriched terms (Fig. I.2). The terms "oxidative phosphorylation (GO:0006119)" (7-fold, corrected p-value: 0.00158) with eight genes and "respiratory electron transport chain (GO:0022904)" (4.1-fold, p-value: 0.00406) with ten genes, showed the highest fold enrichment. These oxygen-related GO-Terms were followed by the terms "protein folding (GO:0006457)" (4.1-fold, p-value: 0.006) and "rRNA metabolic process (GO:0016072)" (3.9-fold, p-value: 0.00352), both being related to protein translation. Other significantly enriched terms were "mitochondrion organization (GO:0007005)" (3.7-fold, p-value: 0.0192), "cellular component biogenesis (GO:0044085)" (1.7-fold, p-value: 0.0304) and "biosynthetic process (GO:0009058)" (1.5-fold, p-value: 0.0215), which are related to macromolecular modifications and cell metabolism.

In the transcripts that are more highly expressed in the whale cortex, reactome pathway enrichment analyses revealed the term "detoxification of reactive oxygen species" (11.1-fold, p-value: 0.00471), followed by "L13a-mediated translational silencing of ceruloplasmin expression" (8.6-fold, p-value: 0.00437),"HSP90 chaperone cycle for steroid hormone receptors (SHR)" (6.8-fold, p-value: 0.0266), and "respiratory electron transport" (5.1-fold, p-value: 0.0472) (Fig. I.2).

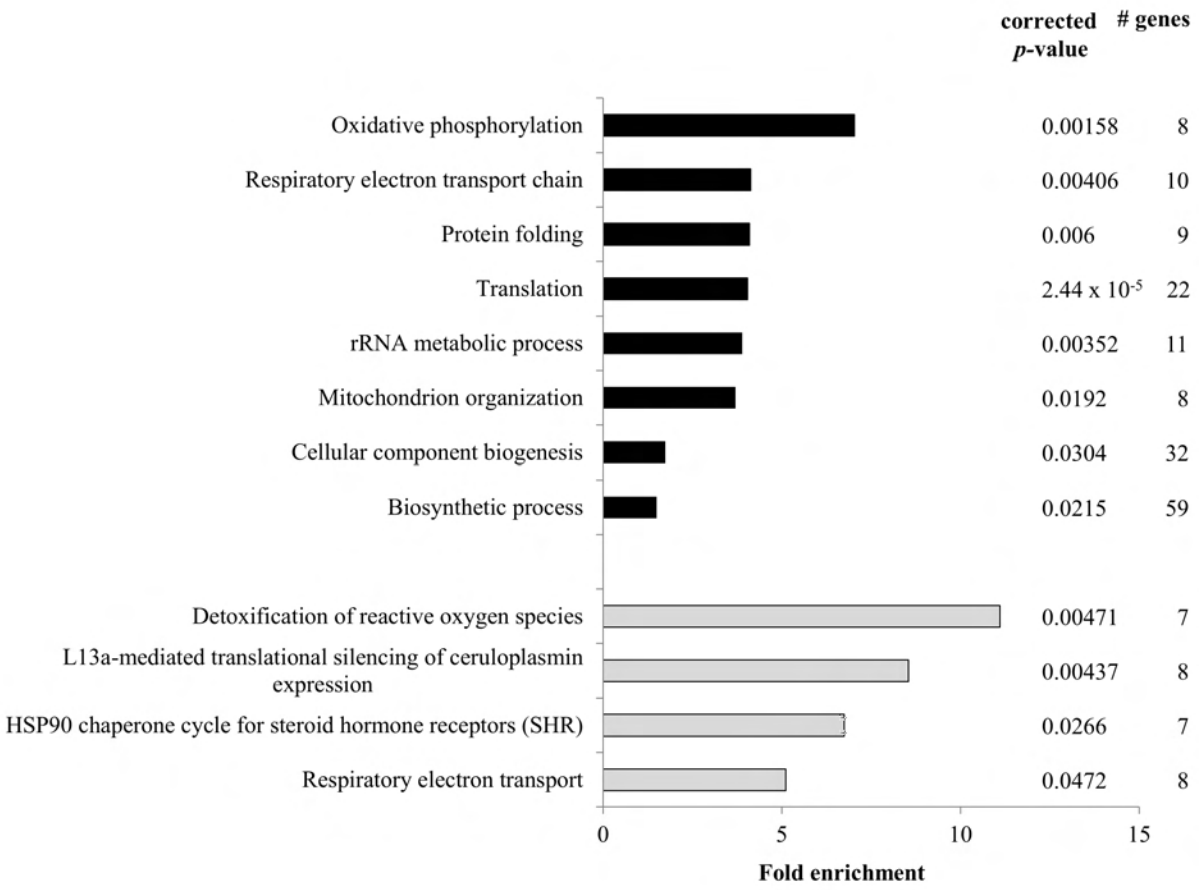

Figure I.2 Enriched GO-Slim terms in the combined average of the visual cortex of killer whale and long finned pilot whale. Significantly enriched GO-Slim terms of the category Biological Process (black) and Reactome pathways (grey) for the gene set significantly higher expressed in the visual cortex of the long-finned pilot whale and the killer whale compared to the visual cortex of cattle according to their Fold Enrichment, with corrected p-values and the number of genes.

A total of 17 transcripts were found annotated in the pathway "detoxification of reactive oxygen species", including known antioxidant enzymes like peroxiredoxin 6, superoxide dismutase 1 and glutathione S-transferase P, which may be candidate genes involved in the adaptation of the whale brain (Kinnula et al. 2004; Mates et al. 1999) (Table I.4).

Table I.4 Candidate genes for functional analysis.

Original gene symbol	Annotated gene symbol	Gene name	Whale mean (RPKM)	Cattle mean (RPKM)	Fold difference
A. Oxidative phosphorylation					
LOC101902002	COX6A1	Cytochrome c oxidase subunit 6A1	123.4	0.2	573.4
LOC112443463	NDUFB4	NADH dehydrogenase [ubiquinone] 1 beta subcomplex subunit 4	28.0	0.2	170.3
LOC100847304	CYCS	Cytochrome c	6.8	0.1	59.9
LOC783502	UQCRC2	Cytochrome b-c1 complex subunit 2	53.8	0.3	176.2
COXP1	COX4	Cytochrome c oxidase subunit 4 isoform 1	40.9	0.2	199.0
COX7ALP1	COX7A1	Cytochrome c oxidase subunit 7A1	39.8	0.2	181.1
LOC101907120	UQCRB	Cytochrome b-c1 complex subunit 7	35.5	0.0	/
LOC783686	NDUFV2	NADH dehydrogenase [ubiquinone] flavoprotein 2	19.2	0.2	113.4
B. Respiratory electron chain					
LOC101902002	COX6A1	Cytochrome c oxidase subunit 6A1	123.4	0.2	573.4
LOC781255	GLRX3	Glutaredoxin-3	6.7	0.0	202.4
LOC112443463	NDUFB4	NADH dehydrogenase [ubiquinone] 1 beta subcomplex subunit 4	28.0	0.2	170.3
LOC100847304	CYCS	Cytochrome c	6.8	0.1	59.9
LOC783502	UQCRC2	Cytochrome b-c1 complex subunit 2	53.8	0.3	176.2
COXP1	COX4	Cytochrome c oxidase subunit 4 isoform 1	40.9	0.2	199.0
COX7ALP1	COX7A1	Cytochrome c oxidase subunit 7A1	39.8	0.2	181.1
LOC101907120	UQCRB	Cytochrome b-c1 complex subunit 7	35.5	0.0	/
LOC783686	NDUFV2	NADH dehydrogenase [ubiquinone] flavoprotein 2	19.2	0.2	113.4
LOC100847677	CYP4X1	Cytochrome P450 4X1	0.2	0.0	/
C. Detoxification of reactive oxygen species					
LOC786533	PRDX6	Peroxiredoxin-6	30.5	0.0	716.3
LOC507743	SOD1	Superoxide dismutase	121.9	0.3	429.4
NCF2	NCF2	Neutrophil cytosol factor 2	13.7	1.5	9.1
GPX2	GPX2	Glutathione peroxidase	2.6	0.1	44.2
LOC100847304	CYCS	Cytochrome c	6.8	0.1	59.9
GSTP1	GSTP1	Glutathione S-transferase P	10.6	0.1	182.8
LOC107132346	TXN2	Thioredoxin	1.2	0.0	619.0

Genes of the enriched PANTHER GO-Slim category Biological Process “oxidative phosphorylation”, “respiratory electron chain” and “detoxification of reactive oxygen species” in the visual cortex of killer whale and long-finned pilot whale compared to the visual cortex of cattle are shown.

Comparative analyses of gene expression in whale and cattle brains

To evaluate lineage-specific adaptations of the whale brain, we compared all available transcriptomes of different whale brains to the brain transcriptomes of cattle. In addition to the transcriptomes of the visual cortex of the killer whale, the visual cortex and the cerebellum of the long-finned pilot whale, which had been generated in this study, we included the transcriptomes of the cerebellum of the bowhead whale and the brain of the minke whale. For the minke whale, no further information on the brain region is given in the annotation. The two transcriptomes of the beluga whale brain were excluded due to large expression differences to the other whale transcriptomes, as evident from PCA (Fig. I.3). Thus, the final whale dataset included five transcriptomes from four species, the cattle dataset consisted of five transcriptomes (Table I.1).

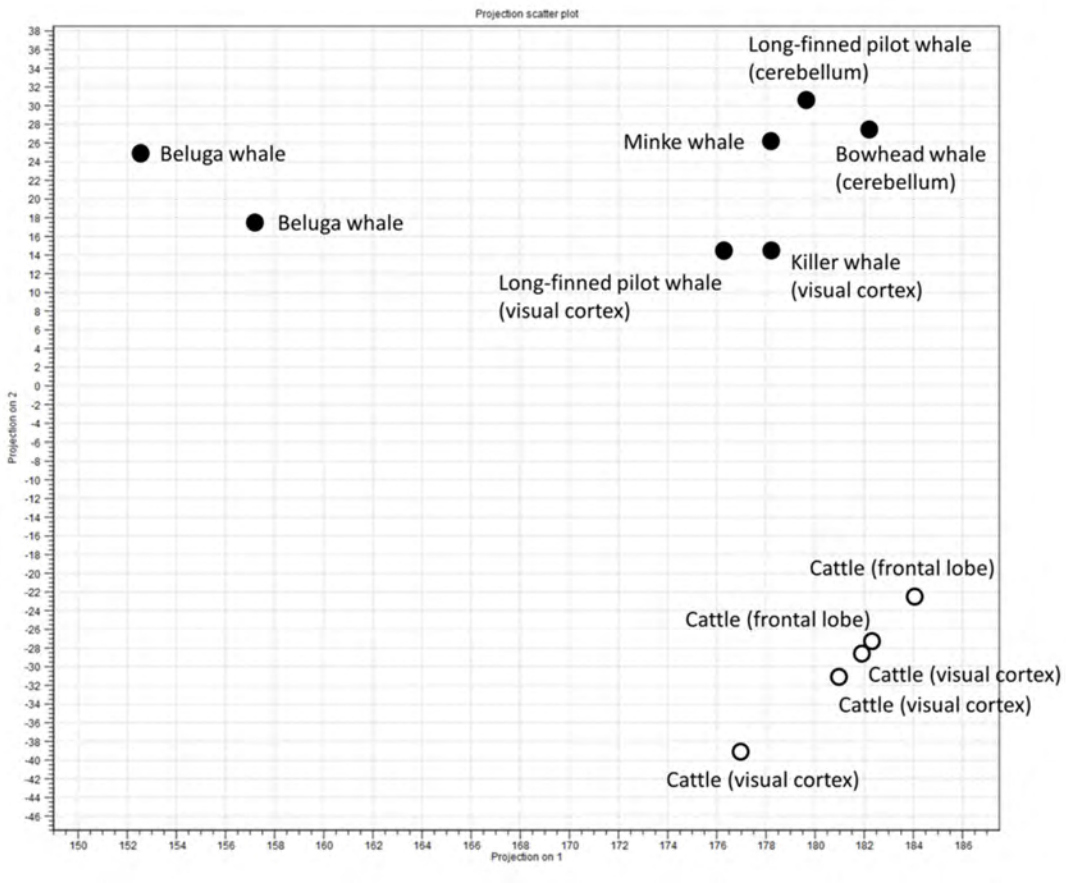

Figure I.3 Principal component analysis of whale and cattle transcriptomes. Principal component analysis (PCA) of RNA-Seq results (transcript expression) of different species of whale (black dots) and cattle (empty dots). PCA was performed to check for possible differences in global transcript expression between whale and cattle samples and to ensure comparability within groups. Note the beluga whale shows a distinctly different transcript expression and thus was not used for the further analysis of whales versus cattle transcriptomes.

For analyses of the transcripts most highly overrepresented (highest RPKM fold-difference) in the whale brain, we used only transcripts with at least 2 RPKM in all samples. The most highly

overrepresented transcript was dehydrogenase/reductase 7 (DHRS7; 14.9-fold), followed by the ribosomal protein S4 y-linked 1 (RPS4Y1; 11.8-fold), the tubulin beta-6 chain (TUBB6; 10.2-fold), which is involved in microtubule cytoskeleton organization, the histone binding nucleosome assembly protein 1-like 3 (NAP1L3; 9.7-fold) (Park et al. 2006), and the uronyl 2-sulfotransferase (UST; 9.2-fold) catalyzing the sulfation of uronyl residues (Kobayashi et al. 1999) (Table I.5).

Table I.5 Most highly overrepresented transcripts in whale vs cattle brain

Gene	**Gene symbol**	**Function**	**Whale mean (RPKM)**	**Cattle mean (RPKM)**	**Fold difference**	**p-value (Bonferroni)**
Dehydrogenase /reductase 7	DHRS7	Oxidoreductase activity	63.1	4.2	14.9	4.2×10^{-11}
Ribosomal protein S4 Y-linked 1	RPS4Y1	Translation	237.9	20.1	11.8	1.7×10^{-5}
Tubulin beta-6 chain	TUBB6	Microtubule cytoskeleton organization	50.9	5.0	10.2	0.00019
Nucleosome assembly protein 1-like 3	NAP1L3	Nucleosome assembly	69.2	7.1	9.7	3.3×10^{-7}
Uronyl 2-sulfotransferase	UST	Sulfotransferase activity	51.7	5.6	9.2	0.01368

Transcripts most highly overrepresented in the whale brain (2 × long-finned pilot whale, killer whale, bowhead whale, minke whale) compared to the cattle brain (n = 5) are shown.

For differential expression analyses, only transcripts that display an at least two-fold difference in normalized unique gene reads, a range (normalized unique gene reads) >5 and a Bonferroni corrected p-value <0.05 were considered. We found 567 transcripts that were significantly higher expressed in the brain of cattle and 603 transcripts significantly higher expressed in the brain of whales (Additional File I.7). No enriched Panther GO terms were found for the genes higher ex-pressed in the cattle brain. For the 603 transcripts higher expressed in whale brain, PANTHER Overrepresentation Test found several terms enriched. In the GO-Slim category Biological Process we found 239 transcripts significantly enriched in ten categories. As previously the highest-fold enrichment was found for the terms “oxidative phosphorylation (GO:0006119)” (5.2-fold, p-value: 0.018), “protein folding (GO:0006457)” (4.04-fold, p-value: 0.0101), “translation (GO:0006412)” (3.8-fold, p-value: 0.0000402), “rRNA metabolic process (GO:0016072)” (3.49-fold, p-value: 0.0124) and “respiratory electron transport chain (GO:0022904)” (3.26-fold, p-value: 0.0339) (Fig. I.4).

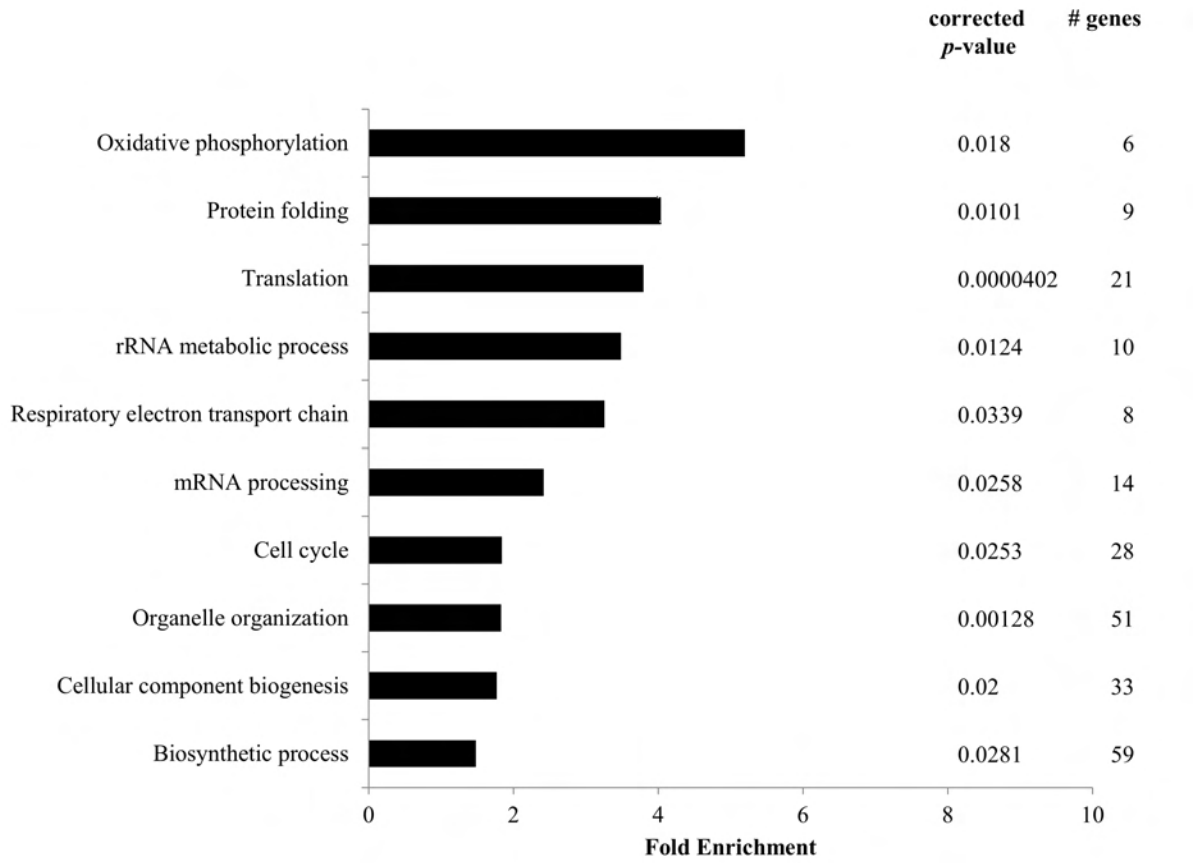

Figure I.4 Enriched GO-Slim terms in the whale brain. Significantly enriched GO-Slim terms for the gene set significantly higher expressed in whale brain compared to the brain of cattle for the category Biological Process according to their Fold Enrichment with corrected p-values and the number of genes.

Discussion

The brain in humans accounts for roughly 20 % of the total oxygen consumption at rest (Harris et al. 2012). While the brains of terrestrial mammals are usually highly susceptible to hypoxia, whales repeatedly perform dives of remarkable duration and depth without obvious damage to their brain. The brain of whales must remain functional during diving and whales like the killer whale or the long-finned pilot whale rely on their ability for hunting and communicating during the dives (Baird 2000; Visser et al. 2017). Analyses of gene expression are more reliable with a high number of replicates (Dugan et al. 1995; Gierlinski et al. 2015). In transcriptomic studies, a high number of replicates is usually used to obtain informative results. Because of ethical, legal and practical consideration, sampling of whale brains has to be conducted opportunistically. Therefore, only a limited number of transcriptomes from whale brains is available and different species and brain regions had to be used. We generated transcriptomes of two brain regions of whales, the visual cortex and the cerebellum and of the visual cortex of cattle. For a more robust insight we furthermore included transcriptomes of brain samples from a minke whale, a bowhead

whale and four cattle from the SRA database in our analyses (Table I.1). Two transcriptomes of the beluga whale brain were excluded, due to general expression differences compared to other whale brain samples (Fig. I.3). The beluga whale samples were sequenced more detailed than the other samples used in this study, which may explain the observed differences in gene expression. Therefore, we have limited our study to samples that were equally generated, for the further statistical analyses. Our results provide insights into the molecular basis of the hypoxia tolerance of the whale brain. To examine the influence of factors besides hypoxia adaptation, we conducted correlation analyses of gene expression between brain samples of additional terrestrial mammals (mouse, pig, dog, sheep, ferret) and whales. The analyses showed correlation between gene expression patterns and species phylogeny as well as brain region used for sampling (see Additional File I.8 Fig. S1). From this, we conclude that there is no evidence in our dataset for obvious influence of allometry, different diet or sampling methods, on gene expression patterns. Due to the lack of a non-diving relative is not possible to compare brain transcriptomes of whales to those of closely related non-diving species with a similar lifestyle, diet and under similar sampling conditions. Therefore, differences in gene expression between cattle and whale need not be ultimately linked to diving. However, our findings indicate an adaptation on the molecular level to hypoxia in the whale brain.

Differential gene expression in the visual cortex vs. the cerebellum of the long-finned pilot whale

To examine brain region-specific gene expression, we compared the transcriptomes of the visual cortex and the cerebellum of the long-finned pilot whale (Fig. I.1, Table I.2). We found 2204 transcripts differentially expressed, with 1184 genes higher expressed in the visual cortex and 1020 genes higher expressed in the cerebellum. In the gene set that was more highly expressed in the visual cortex we found enrichment in the expected category “Visual perception” but also in terms and pathways related to axon guidance, neurotransmitter activity and calcium homeostasis (Fig. I.1). In the cerebellum, fewer categories were found enriched, and these are mainly related to transcriptional regulation (Fig. I.1). Our results indicate higher synaptic plasticity and activity in the visual cortex than in the cerebellum of the long-finned pilot whale. The visual cortex and the cerebellum seem to make use of different GABA receptor types (McKernan et al. 1996). However, GABAeric inhibitory signaling is relevant in both brain regions.

High capacity of aerobic metabolism in the whale brain

Some hypoxia-tolerant animals use extreme hypometabolism to protect their neuronal network. For example, the anoxic freshwater turtle can reduce the most energy demanding processes like excitatory neurotransmitter release, action potentials, and ion flow, thereby entering a coma-like state (Milton et al. 1998; Milton et al. 2002; Thompson et al. 2007). However, the whale brain needs to remain functional, at least at some minimum level, for hunting and communicating when submerged. Marine mammals have evolved a number of mechanisms that allow them to tolerate extended periods of breath-hold diving. Besides elevated hemoglobin and myoglobin concentrations, whales also undergo peripheral vasoconstriction and hypometabolism (Kooyman

et al. 1998; Ramirez et al. 2007; Scholander 1940). This results in a redistribution of the blood flow from the peripheral organs towards the more hypoxia-sensitive tissues, like the brain. However, towards the end of long dives the oxygen tension in arterial blood of diving seals drops to 10–20 mmHg (Kerem et al. 1973a; Meir et al. 2009; Qvist et al. 1986; Williams et al. 1999), corresponding to the threshold for normal brain function in terrestrial mammals (Erecinska et al. 2001), which implies a high intrinsic hypoxia tolerance of the brain. In vitro studies of brain slices from the hooded seal (*Cystophora cristata*), which can dive for >1 h, showed that seal neurons survive much longer under hypoxia than do mouse neurons (Folkow et al. 2008; Ramirez et al. 2011). No such experiments have been conducted in cetaceans, however conformance in physiological adaptations together with similar maximum dive durations in seal and whale species like hooded seal and sperm whale (*Physeter macrocephalus*) imply similar neuronal hypoxia tolerance levels. The balance between metabolic costs and maintaining functional integrity is a major challenge for the brain. In terrestrial mammals acute hypoxia prevents oxidative phosphorylation and anaerobic glycolysis takes over the production of ATP (Kerem et al. 1973a). The brain of the hooded seal shows a specific hypoxia-adaptation of the brain and a reverse astrocyte-neuron lactate shuttle (ANLS) has been proposed, which predicts that astrocytes work largely aerobically while the neurons rely primarily on anaerobic metabolism (Mitz et al. 2009; Schneuer et al. 2012). Transcriptome analyses using hooded seal brain samples suggested a reduced aerobic energy metabolism, possibly implying the existence of a general energy saving mechanism (Fabrizius et al. 2016). No indication of a similar downward shift in the aerobic metabolism was found in the brain of minke whale and harbor porpoise (*Phocoena phocoena*) (Schneuer et al. 2012), again suggesting divergent evolutionary strategies in seals and whales.

We compared transcriptomes of the visual cortex as well as of different brain regions of whale and cattle. Both comparisons showed similar results, with enriched gene expression of transcripts involved in oxidative phosphorylation and respiratory electron chain in the whale brains (Figs. I.2 and I.4). An enhanced cerebral aerobic capacity may possibly reflect an adaptation to cope with the reoxygenation event when the whale resurfaces, at which time it will be presented with a high oxygen availability. The enhanced oxidative capacity might, thus, prepare the brain for rapid energy production after the dive. Recently, a similar adaptation in the brain of hibernating thirteen-lined ground squirrels (*Ictidomys tridecemlineatus*) was found and it was suggested that an increased oxidative capacity of the mitochondria may be needed to meet the high energy requirements during arousal from torpor (Ballinger et al. 2017). The high oxidative capacity in the whale brain might possibly also help neuronal survival under hypoxic conditions by improving the efficiency of ATP production. For example, the high expression of several Cytochrome c oxidase (COX) subunits (Table I.4), the final enzyme in the respiratory electron transport chain, might help to improving efficiency of electron transfer when less oxygen is available (Allen et al. 1995). The regulatory mechanisms of COX expression in mammals are not well understood. However, COX subunit IV has been shown to regulate COX activity and oxygen-dependent expression indicates an oxygen sensing role in the brain (Gnaiger et al. 1998; Horvat et al. 2006; Lau et al. 2017; Vijayasarathy et al. 2003). High expression of specific COX subunits in the whale brain might help to improve the efficiency of ATP production under

hypoxia, and thereby prevent neuronal damage. Further studies of components of the respiratory electron transport chain in the whale brain are required to test such hypotheses.

High expression of antioxidant enzymes in the whale brain

Enhanced oxidative capacity combined with reoxygenation events during resurfacing are likely to lead to an increased ROS production (Boveris et al. 1973; Brand 2010; Murphy 2009). Accordingly, we found the Reactome pathway "detoxification of reactive oxygen species" enriched in the transcripts that were more highly expressed in the visual cortex of whale than in the cattle cortex (Fig. I.2). Three of those transcripts (PRDX6, SOD1 and GSTP1) were also significantly higher expressed in the whale brain when comparing all available whale and cattle transcriptomes (Fig. I.5). The high expression of antioxidant genes in the whale brain could protect the neuronal cells and minimize damage from ROS and these genes may serve as candidates for functional analyses. These findings are consistent with the recent discovery of cetacean-specific amino acid changes in several antioxidant proteins, as well as of enrichment in the functional category antioxidant activity (GO:0016209) in the minke whale genome (Yim et al. 2014).

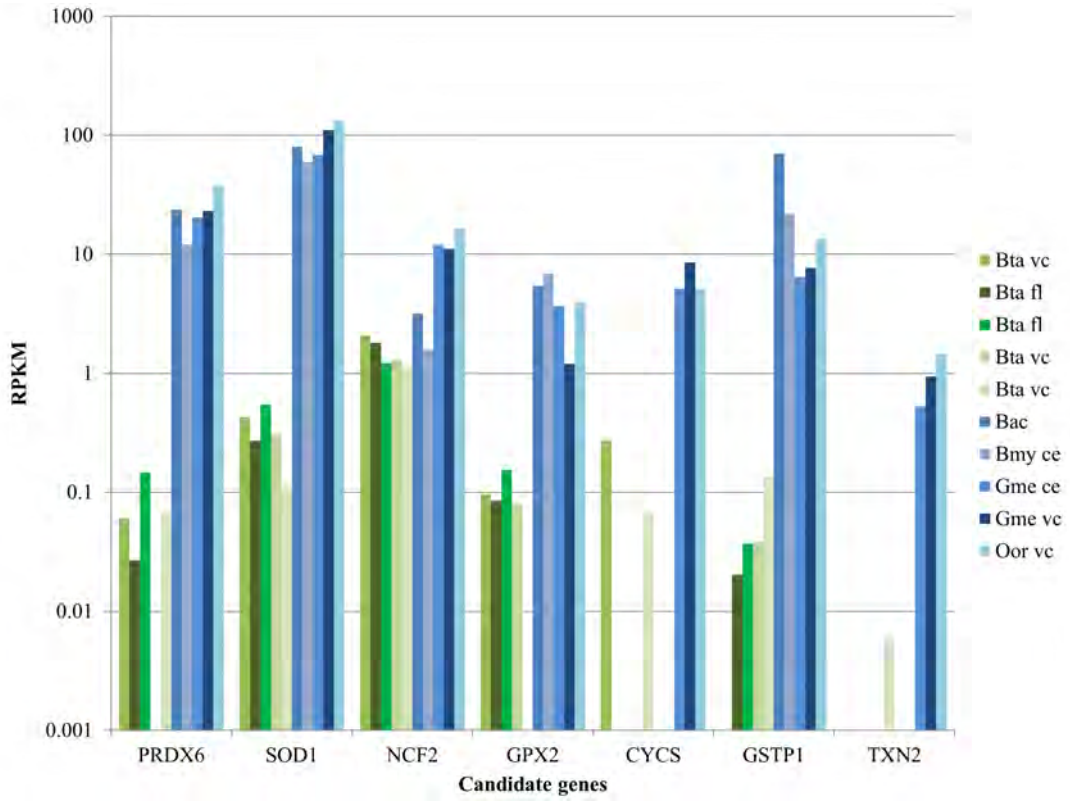

Figure I.5 Candidate genes for functional analysis. RPKM values of transcripts enriched in the visual cortex of whale in the Reactome pathway "detoxification of reactive oxygen species" (Table I.5, Fig. I.2) are shown for all whale and cattle brain samples. Transcripts of peroxiredoxin-6 (PRDX6), superoxide dismutase (SOD1), neutrophil cytosol factor 2 (NCF2), glutathione peroxidase (GPX2), cytochrome c (CYCS), glutathione S-transferase P (GSTP1) and thioredoxin (TXN2) were significantly enriched in the visual cortex of killer whale and long-finned pilot whale. PRDX6, SOD1 and GSTP1 were significantly enriched in all whale samples. Bta=*Bos taurus*; Bac=*Balaenoptera acutorostrata*; Bmy=*Balaena mysticetus*; Gme=*Globicephala melas*; Gme=*Globicephala melas*; Oor=*Orcinus orca*; ce=cerebellum; fl=frontal lobe; vc=visual cortex.

Conclusions

Our results provide a first insight into molecular mechanisms of hypoxia tolerance in the whale brain. The focus of this study was the analysis of its baseline gene expression. The enriched gene expression of transcripts involved in oxidative phosphorylation in the whale brain may reflect an adaptation to varying oxygen availability (diving vs resurfacing) and changing energy demands. However, the gene expression changes of the diving whale brain under hypoxic conditions (i.e. during a dive) remain unknown. Transcriptome analyses of whale brain slices subjected to hypoxia, and functional analysis of candidate genes, could provide further insight into such adaptations.

Availability of data and material

The raw Illumina files of the transcriptomes from the visual cortex of the cattle (SRR8305676) and the killer whale (SRR8305677) and the visual cortex (SRR8305674) and the cerebellum (SRR8305675) of long-finned pilot whale are available from the NCBI SRA database under the Bioproject PRJNA506903. Mammalian brain transcriptomes were retrieved from the NCBI SRA database (accession numbers SRX790347, SRX313597, SRX211675, SRX211674, SRX196362, SRX196353 SRX2585929, SRX2585928). All other data is provided in the Supplemental material on the CD attached to this dissertation.

Acknowledgments: We thank Matthias Preuß (University of Hamburg) for preparation of cattle brain samples. This work has been supported by the Deutsche Forschungsgemeinschaft (BU 956/22-1) and by a fellowship to A. K. by the Studienstiftung des deutschen Volkes.

7 Chapter II

The SOD1 and COMMD6 genes of the killer whale (*Orcinus orca*) protect hippocampal neuronal cells from hypoxia and oxidative stress

Alena Krüger[a], Cornelia Geßner[a], Andrej Fabrizius[a], Bjarni Mikkelsen[b], Ursula Siebert[c], Lars P. Folkow[d], Thorsten Burmester[a]

[a]Institute of Zoology, University of Hamburg, Germany

[b]Natural History Museum, Faeroe Islands

[c]Institute for Terrestrial and Aquatic Wildlife Research, University of Veterinary Medicine Hannover, 25761 Büsum, Germany

[d]University of Tromsø – The Arctic University of Norway, NO-9037 Tromsø, Norway

Abstract

Low oxygen levels in the organism (hypoxia) have immediate effects on the oxidative metabolism of mammals and thus on brain function. While hypoxia causes severe brain damage in most mammals, whales and seals must have developed strategies to tolerate hypoxia that allow them to dive for up to 2 h without surfacing. Physiological adaptations in diving mammals have been examined extensively but little is known about the molecular mechanisms underlying the hypoxia tolerance of the diving brain. In a previous study, transcriptome analyses of the whale brain showed high expression of several antioxidant and neuroprotective genes. We tested the effect of overexpression of two of those genes, SOD1 and COMMD6 on neuronal cells under hypoxic and oxidative stress. SOD1 catalyzes the conversion of superoxide radicals to hydrogen peroxide signifying its role in the detoxification of reactive oxygen species. We found whale-specific substitutions in the SOD1 amino acid sequence which might play a role in the hypoxia adaptation. COMMD6 inhibits the activation of NF-κB signaling, a transcription factor, which is, among others, involved in the regulation of apoptotic processes. We found a neuroprotective effect of the overexpression of both, SOD1 and COMMD6, in HN33 neuronal mouse cells after exposure to hypoxia and oxidative stress and a reduced production of reactive oxygen species under hypoxia. Our data indicate that high expression levels of specific genes are part of the adaptations to hypoxia in the whale brain.

Keywords: Cetacea, Whale, Hypoxia, Oxidative stress, Neuronal cells, SOD1, COMMD6, Brain

Introduction

Marine mammals are known for their impressive diving ability. Whales live a solely aquatic life and rely on periodic dives for hunting and foraging. Due to their frequent breath-hold diving and resurfacing behavior, whales are routinely exposed to hypoxic conditions and oxidative stress caused by reperfusion after the dive. To conduct dives that last for up to 2 hours, as observed in the beaked whale (Schorr et al. 2014), specific physiological adaptations are required. A vast number of studies revealed different specializations to reduce energy consumption, to enhance oxygen storage, transportation and availability and to improve oxygen supply to central organs (for review see: Butler 2004; Butler et al. 1997; Ponganis 2011; Ramirez et al. 2007). However, the molecular mechanisms protecting the whale brain from hypoxic injuries and reoxygenation events are largely unknown. Molecular processes in the defense against ROS might play a key role in the adaptation to hypoxia. During hypoxia and reoxygenation after resurfacing, a high amount of ROS might cause detrimental damage to the brain. The enzymatic detoxification of reactive oxygen species (ROS) prevents cell damage caused by oxidation of proteins, lipids and nucleic acids (Murphy 2009). In the blood and in several tissues of marine mammals, the concentration and activity of antioxidant enzymes was enhanced compared to terrestrial relatives (Vazquez-Medina et al. 2006; Vazquez-Medina et al. 2012; Wilhelm Filho et al. 2002; Zenteno-Savin et al. 2002). The genome of the minke whale exhibits signatures of an increased antioxidant capacity, with gene expansions and whale-specific mutations in antioxidant genes (Yim et al. 2014). However, there is little information about the ROS defense of the neuronal tissue of whales. The detoxification of reactive oxygen species is largely based on an enzymatic cascade reaction: Superoxide dismutase (SOD) catalyzes the degradation of the superoxide radical (O_2^-) into hydrogen peroxide (H_2O_2), which is transformed into oxygen and water by catalase (CAT) and glutathione peroxidase (GPx) (Mann et al. 2007a; Mann et al. 2007b). In Mammals three distinct superoxide dismutase enzymes are known: SOD1 is located in the cytoplasm, SOD2 is found in the mitochondria and SOD3 is present extracellularly. SOD 1 is highly abundant in neurons and plays a protective role during oxidative stress (Pardo et al. 1995; Perry et al. 2010). A high concentration and activity of SOD1 in the heart and in blood plasma of marine mammals suggest an important role in oxidative defense mechanisms (Elsner et al. 1998; Vazquez-Medina et al. 2006; Wilhelm Filho et al. 2002). Transgenic rat models overexpressing SOD1 show a reduced superoxide production after ischemia and spinal cord injury resulting in a reduction of neuronal cell death (Chan et al. 1998; Sugawara et al. 2002a; Sugawara et al. 2002b). These results indicate a neuroprotective role of SOD1 against oxidative stress. In an earlier study, we proposed a high aerobic capacity in the whale brain as an adaptation to varying energy demands and found overexpression of genes involved in stress response and antioxidant defenses (Krüger et al. 2019). Compared to the cattle brain we found an elevated expression for a transcript of SOD1 (RPKM fold difference: 271) in four whale species (see Additional file II.1). Besides SOD1 we focused our study on the gene COMM Domain Containing 6 (COMMD6). Our transcriptome analyses revealed a higher expression of COMMD6 transcripts in whale brain (RPKM fold difference: 1638) (Additional file II.1). In the COMMD (Copper metabolism gene

MURR1 domain) family, the function of COMMD6 and most of the other members is largely uninvestigated. COMMD1 is the most extensively studied member and is linked to several biological processes. For example, COMMD1 is related to copper metabolism (Burstein et al. 2004; de Bie et al. 2007; Narindrasorasak et al. 2007), regulation of intracellular sodium (Biasio et al. 2004) and adaptation to hypoxia via inhibition of the HIF1α transcription factor (van de Sluis et al. 2007). The ten members of the COMMD family were found in several vertebrates and are highly conserved in mammals and fish (Burstein et al. 2005). COMMD2-4 and COMMD7-10 were not higher expressed in whales than in cattle. COMMD proteins are known to inhibit NF-κB signaling by affecting its association with chromatin (for review see: Bartuzi et al. 2013; Maine et al. 2007). NF-κB is a transcription factor conserved in a wide range of taxa and involved in gene regulation in response to inflammation, cell proliferation and apoptosis (Gilmore 2006). Hypoxia induces the activation of NF-κB signaling but the detailed mechanisms are not yet understood. In the brain NF-κB may play a role in synaptic activity (Guerrini et al. 1995; Meberg et al. 1996). Ischemia was shown to activate NF-κB in neurons leading to neuronal cell death (Clemens et al. 1997b; Stephenson et al. 2000). Antioxidants, like N-acetyl-L-cysteine (NAC) were found to block the activation of NF-κB in neurons (Meyer et al. 1993; Schreck et al. 1991) and prevent oxidative stress-induced cell death (Behl et al. 1994; Kaltschmidt et al. 1997). COMMD6 consists of 85 amino acids and is the only member of the COMMD family lacking the variable extended N-terminus. However, it has been shown that COMMD6 inhibits NF-κB to a similar extent as COMMD1 (de Bie et al. 2006). The overexpression of both, SOD1 and COMMD6, in the whale brain may play an important role in the hypoxia tolerance by preventing neuronal cell death. Functional analyses of these candidate genes overexpressed in the whale brain might improve the understanding of their specific functions. Here we evaluated the effect of SOD1 and COMMD6 during hypoxia and oxidative stress in murine neuronal cells.

Materials and methods

Animals

Brain samples of a juvenile killer whale (*Orcinus orca*) and an adult bottlenose dolphin (*Tursiops truncatus*) were dissected and provided by the Institute of Terrestrial and Aquatic Wildlife Research, University of Veterinary Medicine Hannover, Foundation. The killer whale died of live stranding in Sylt, Germany in 2016, the bottlenose dolphin lived in the Duisburg Zoo in Germany and died in 2008. Two long-finned pilot whales (*Globicephala melas*) (male and female, adult) were harvested during traditional whaling at the Faroe Islands and samples from the visual cortex and the cerebellum were taken by a veterinarian. *Regulations of the Convention on Biological Diversity* (CBD) and *Convention on International Trade in Endangered Species of Wild Fauna and Flora* (CITES) were followed, and the appropriate permits were obtained (Permit number: E-01456/17). Two brains of cattle (male, 22 months and female, 23 months) were acquired from a German butchery under an exceptional permission of the German law of *Tierische Nebenprodukte-Beseitigungsgesetz*. The skull was dissected, and the visual cortex was

sampled by the University of Hamburg's taxidermist. Brain samples of the bottlenose dolphin and the long-finned pilot whales were frozen in liquid nitrogen and stored at -80 °C, samples of killer whale and cattle were preserved in RNAlater at -80 °C.

Sequence analysis

To compare SOD1 and COMMD6 amino-acid sequences between diving and non-diving mammals, sequences of the several whales and terrestrial mammals were retrieved from NCBI (Additional file II.2) and aligned using the GeneDoc software (Version 2.7) (http://genedoc.software.informer.com/2.7/). The sequences of the pilot whale were reconstructed using transcriptomic sequence data of the long-finned pilot whale's visual cortex and cerebellum (Krüger et al. 2019) using the SOD1 and COMMD6 sequences of the killer whale (NCBI accession numbers: XM 004264510 and XM 004284280, respectively) as a reference. The mapped reads were used for a de novo assembly of the long-finned pilot whale SOD1 and COMMD6 sequence with CLC Workbench (Version 10.0.1). The coding sequences (CDS) of SOD1 and COMMD6 of the long-finned pilot whale were annotated using ORF-Finder (https://www.ncbi.nlm.nih.gov/orffinder/).

RNA Extraction and cDNA Cloning

To verify gene expression levels of SOD1 and COMMD6 retrieved from transcriptome data, quantitative Real-Time Reverse Transcription OCR was performed. Total RNA of visual cortices samples from killer whale, long-finned pilot whale, bottlenose dolphin and cattle was extracted using the peqGOLD Trifast (PEQLAB, Erlangen, Germany) and the Crystal RNA Mini Kit (Biolab Products, Bebensee, Germany). Quality and quantity analysis was performed using the NanoDrop 1000 Spectrophotometer (Waltham, MA, USA) and formaldehyde agarose gel electrophoresis. One μg of total RNA was applied for first-strand cDNA synthesis using the RevertAid H Minus First Strand cDNA Synthesis kit (Thermo Fisher, Bonn, Germany) according to the manufacturer's instructions.

Gene expression analysis

Quantitative Real-Time Reverse Transcription PCR

Expression levels of *Sod1* and *Commd6* in the visual cortex of cattle, killer whale and long-finned pilot whale, in the brain of the bottlenose dolphin and in the cerebellum of the long-finned pilot whale were estimated by quantitative real-time reverse transcription PCR (qRT-PCR). Amplification was performed on an ABI Prism 7500 Real Time PCR System (Applied Biosystems, Darmstadt, Germany) with the Power SYBR Green master mix (Applied Biosystems, Darmstadt, Germany) using a 40 cycles protocol (95 °C for 15 s, 58 °C for 60 s). Primer for cetacea SOD1 and COMMD6 and cattle are listed in Table II.1. The copy number of *Sod1* and *Commd6* in a cDNA sample was determined using a concentration curve (10^7 -10^3) of the recombinant plasmid as standard, and then normalized to 1 μg of total RNA. Whale and cattle mRNA copy

numbers of *Sod1* and *Commd6* were normalized using the house-keeping gene glyceraldehyde-3-phosphate dehydrogenase (*Gapdh*) as reference (de Jonge et al. 2007).

Table II.1 Primer sets used to amplify the coding sequences of *Sod1* (OorSOD1) and *Commd6* (OorCOMMD6) of the killer whale and for expression analysis of *Sod1* and *Commd6* in killer whale, bottlenose dolphin, long-finned pilot whale (Cet[SOD1/COMMD6]_qRT-PCR) and cattle (Bta[SOD1/COMMD6]_qRT-PCR) via qRT-PCR. Annealing temperature was 58 °C for all primer sets.

Name	Strand	Primer sequence (5′ - 3′)
OorSOD1_cds	sense	CATGAATTCAACATGGTGACGAAGGCC
OorSOD1_cds	antisense	GGATCGCCCAATAAGGGCCCTATA
OorCOMMD6_cds	sense	CATGAATTCAACATGGAGGGGTGTAGC
OorCOMMD6_cds	antisense	CAGTTATTGAAACTGTGTGAGGGCCCTATA
CetSOD1_qRT-PCR	sense	GAGATAATACACAAGGCTGTACC
CetSOD1_qRT-PCR	antisense	GGCCGAAGTGCGTATTGAAG
BtaSOD1_qRT-PCR	sense	ATCCACTTCGAGGCAAAGGG
BtaSOD1_qRT-PCR	antisense	TGAAGAGAGGCATGTTGGAGA
CetCOMMD6_qRT-PCR	sense	CAACCAGCTAATAGATTTTCAGTG
CetCOMMD6_qRT-PCR	antisense	CCACAGTTTCAGAATTTCTACAG
BtaCOMMD6_qRT-PCR	sense	CAATCCCACAGTTTCAGAATTTC
BtaCOMMD6_qRT-PCR	antisense	CAAAGCTGCTTAAGGATCGAAT
GAPDH_qRT-PCR	sense	ATCACCATCTTCCAGGAGCG
GAPDH_qRT-PCR	antisense	GCCAAGAGGGTCATCATCTCT

Functional characterization in cell culture

Cloning of the killer whale SOD1 and COMMD6 sequences

The CDS of the killer whale SOD1 (OorSOD1) and COMMD6 (OorCOMMD6) were amplified from the killer whale cDNA via PCR. The forward (5′) primer included a Kozak sequence ([G/A]NNATGG) and an EcoRI site; the reverse primer had an ApaI site (Table II.1). PCR products were purified using the Crystal Gel-Extraction Kit (Biolab Products, Bebensee, Germany) and cloned into a pGEM-T vector (Promega, Mannheim, Germany) and afterwards in a pcDNA3.1+ vector (Invitrogen, Karlsruhe, Germany). Sequences were verified by a commercial sequencing service (GATC, Konstanz, Germany).

Transfection of HN33 cells

HN33 cells (murine hippocampal neurons x neuroblastoma) (Lee et al. 1990) were cultivated at 37 °C in a humidified atmosphere with 5 % CO_2 in Dulbecco's modified Eagle medium (DMEM) (BioWest, Darmstadt, Germany), supplemented with 10 % fetal bovine serum (BioWest, Darmstadt, Germany) and a mixture of 1 % penicillin/streptomycin (PAA, Pasching, Austria). HN33

cells of passage 37 were stably transfected with the pcDNA3.1+ vectors containing OorSOD1 and OorCOMMD6, as well as the empty vector (mock cells) using Lipofectamin^{TM}2000 (Invotrogen, Karlsruhe, Germany). After transfection and selection with 700 μg/ml geneticin (PAA, Pasching, Austria) in DMEM, the successful overexpression of *Sod1* and *Commd6* were verified via qRT-PCR.

Hypoxia and oxidative stress experiments

For hypoxia experiments transfected cells of passage 48 were transferred in a CB150 incubator (Binder, Tuttlingen, Germany) with 1.2 % O_2, 5 % CO_2 and 93.8 % N_2 for 24 h. All experiments were carried out with at least three replicates per stress experiment and per viability test with 3.75×10^4 cells per well in a 96-flat bottom well plate. Oxidative stress was induced using a final concentration of 275 μM of H_2O_2 in DMEM in normoxia for 24 h. Additionally, all cell lines were kept in normoxia for 24 h without stress as controls.

Cell viability tests

The viability of the cells was assayed by the CellTiter-Glo® Luminescent Cell Viability Assay Kit (CTG test) (Promega, Mannheim, Germany), which measures the ATP content of the cells and the Caspase-Glo® 3/7 Assay System (Promega, Mannheim, Germany), which measures the activity of caspases 3 and 7 that are involved in the disassembly of the cell during apoptosis. Both tests were carried out according to the manufacturer's instructions with 3.75×10^4 cells per well in 96 well plates in triplicates per stress experiment and per viability test. 75 μl of reagent was used for each well. The luminescence was determined with a DTX-880 Multimode Plate Reader (Beckman Coulter, Krefeld, Germany).

Detection of ROS

The production of ROS by the transfected cells after exposure to hypoxia was measured with the 2',7'-dichlorofluorescin diacetate (DCFH-DA) test (Roche, Mannheim, Germany), which is based on the measurement of the ROS-induced oxidation of the non-fluorescent DCFH to the fluorescent DCF (Wang et al. 1999). The detection of the fluorescence signal was carried out using the DTX-880 Multimode Plate Reader using an excitation wavelength of 485 nm and an emission wavelength of 535 nm.

Statistical analysis

Statistical analyses were performed in the R statistics program v. 3.5.1 (Team 2013). Signal intensities of the Caspase test and the DCFH-DA test were normalized to the raw values of the CTG test, which represents the amount of living cells. Comparisons of means of the transfected cell lines with each other and with mock cells were carried out employing one-way ANOVA, followed by the Levene test for variance homogeinity included in the Rcmdr package

(Fox et al. 2019), and the Tukey-Kramer test of the multcomp package (Hothorn et al. 2008). P-values were corrected for multiple testing using the Bonferroni correction implemented in the p.adjust()-function. P-values <0.05 were considered significant.

Results

Sod1 and *Commd6* are higher expressed in the cetacean brain

Expression analysis of *Sod1* and *Commd6* was performed on brain samples of different species of cetacean and on samples of the visual cortex of cattle (Fig. II.1 A).
mRNA levels of *Sod1* were lower in the killer whale visual cortex (1.7×10^8 copies/μg RNA) compared to the cattle (5.8×10^8 copies/μg RNA), but the brain of the bottlenose dolphin (1.4×10^9 copies/μg RNA), the visual cortex and cerebellum of the long-finned pilot whale showed a higher expression of *Sod1* compared to the visual cortex of cattle. The highest expression was found in the cerebellum of the long-finned pilot whale (1.1×10^{11} copies/μg RNA) followed by the visual cortex of the long-finned pilot whale (4×10^{10} copies/μg RNA). Expression of *Commd6* was distinctly higher in the brain samples of whales than in the visual cortex of cattle (Fig. II.1 B). The visual cortex of cattle showed the lowest expression levels of all species tested (2.3×10^4 copies/μg RNA). The highest expression levels were found in the cerebellum (2.1×10^8 copies/μg RNA) and the visual cortex (9.8×10^7 copies/μg RNA) of the long-finned pilot whale. Expression of *Commd6* was higher in the brain of the bottlenose dolphin (4.2×10^6 copies/μg RNA) than in the visual cortex of the killer whale (2.3×10^5 copies/μg RNA).

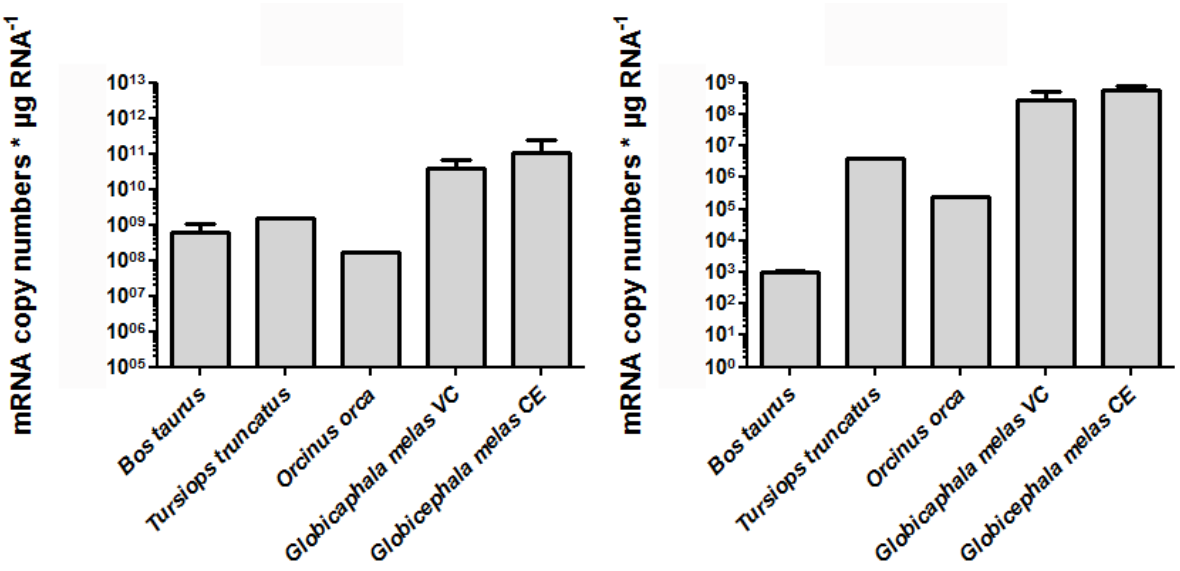

Figure II.1 Expresssion levels of superoxide dismutase 1 (*Sod1*) and COMM Domain Containing 6 (*Commd6*) in brain samples of cattle (*Bos taurus*, N=2), bottlenose dolphin (*Tursiops truncatus*, N=1), killer whale (*Orcinus orca*, N=1), and long-finned pilot whale visual cortex (*Globicephala melas* VC, N=2) and cerebellum (*Globicephala melas* CE, N = 2). Data are expressed in means of mRNA copy number per μg RNA used in cDNA synthesis normalized to the expression of *Gapdh*. Bars represent standard deviation.

SOD1 and COMMD6 appear highly conserved among cetaceans

The Sod1 and Commd6 sequences of cetaceans show 95 – 100 % and 96 – 100 % similarity of the amino acids, respectively (Additional File II.3 and II.4). The Sod1 sequences of the mammals included in this study consist of 152-157 amino acids (Fig. II.2). One cetacean specific amino acid substitution was found (Lys77Glu). Another substitution was found only in whales and in the hypoxia tolerant naked mole rat (*Heterocephalus glaber*) (Asp96Glu). Diving and non-diving mammals shared only 77 – 90 % of the amino acids.

Sequences of killer whale, long-finned pilot whale and bottlenose dolphin were 100 % identical. The biggest difference was found between domestic sheep, horse and florida manatee (71 %). The Commd6 sequences tested consisted of 83 – 116 amino acids (Additional File II.5). The sequences of the beluga whale, the narwhal, the long-finned pilot whale and the bottlenose dolphin were 100 % identical. Minke whale and killer whale shared the fewest identities among the cetaceans (96 %). Diving and non-diving mammals shared 63 – 95 % of the amino acids.

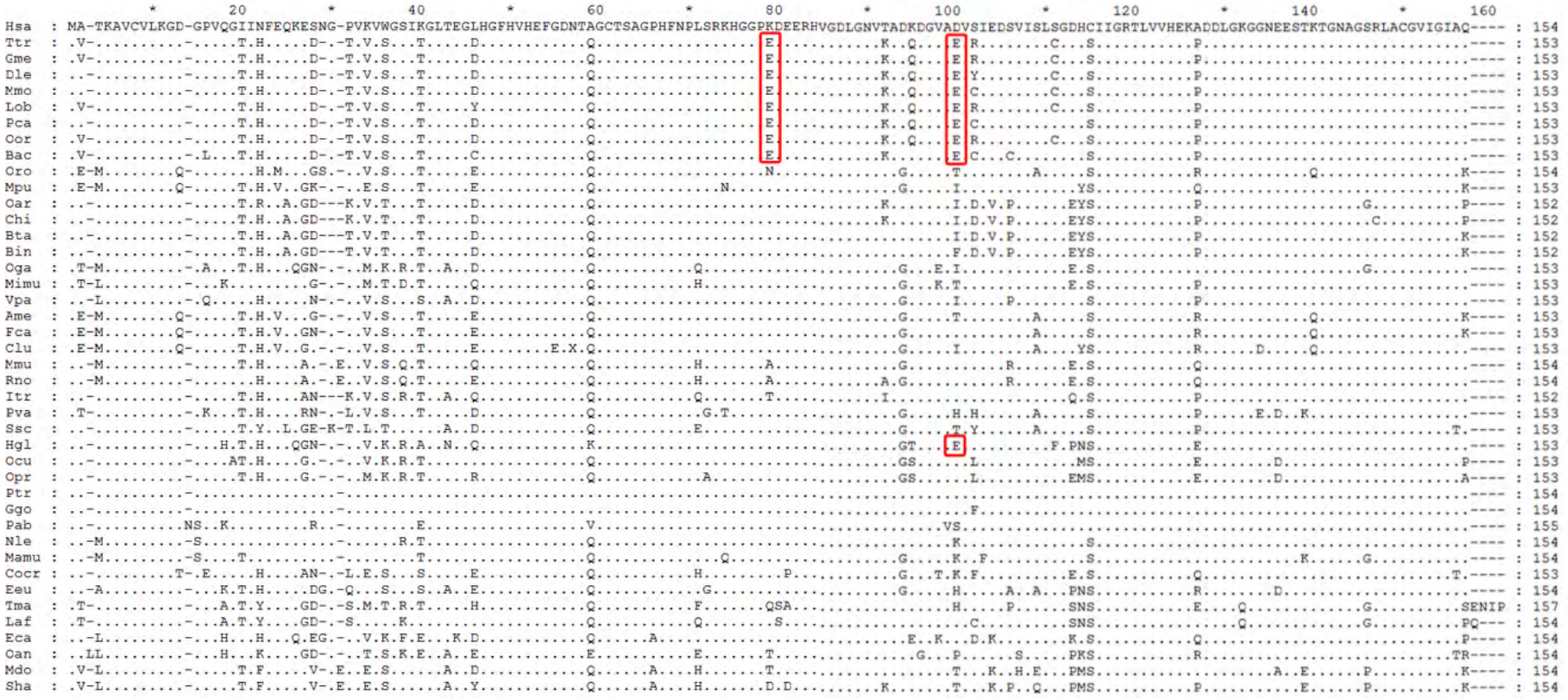

Figure II.2 Multiple alignment of SOD1 amino acid sequences of selected species of diving and non-diving mammals. The species are abbreviated as follows: Hsa: *Homo sapiens* (human), Ttr: *Tursiops truncatus* (bottlenose dolphin), Gme: *Globicephala melas* (long-finned pilot whale), Dle: *Delphinapterus leucas* (beluga whale), Mmo: *Monodon monoceros* (narwhal), Lob: *Lagenorhynchus obliquidens* (pacific white-sided dolphin), Pca: *Physeter catodon* (sperm whale), Oor: *Orcinus orca* (killer whale), Bac: *Balaenoptera acutorostrata* (minke whale), Oro: *Odobenus rosmarus divergens* (pacific walrus), Mpu: *Mustela putorius furo* (ferret), Oar: *Ovis aries* (domestic sheep), Chi: *Capra hircus* (goat), Bta: *Bos taurus* (cattle), Bin: *Bos indicus* (zebu), Oga: *Otolemur garnettii* (bushbaby), Mimu: *Microcebus murinus* (gray mouse lemur), Vpa: *Vicugna pacos* (alpaca), Ame: *Ailuropoda melanoleuca* (panda),), Fca: *Felis catus* (cat), Clu: *Canis lupus familiaris* (dog), Mmu: *Mus musculus* (mouse), Rno: *Rattus norvegicus* (rat), Itr: *Ictidomys tridecemlineatus* (squirrel), Pva: *Pteropus vampyrus* (megabat), Ssc: *Sus scrofa* (pig), Hgl: *Heterocephalus glaber* (naked mole-rat), Ocu: *Oryctolagus cuniculus* (rabbit), Opr: *Ochotona princeps* (pika), Ptr: *Pan troglodytes* (chimpanzee), Ggo *Gorilla gorilla* (gorilla), Pab: *Pongo abelii* (orangutan), Nle: *Nomascus leucogenys* (gibbon), Mamu: *Macaca mulatta* (macaque), Cocr: *Condylura cristata* (star-nosed mole), Eeu: *Erinaceus europaeus* (hedgehog), Tma: *Trichechus manatus latirostris* (Florida manatee), Laf: *Loxodonta Africana* (elephant), Eca: *Equus caballus* (horse), Oan: *Ornithorhynchus anatinus* (Platypus), Mdo: *Monodelphis domestica* (Opossum), Sha: *Sarcophilus harrisii* (Tasmanian devil). The complete sequence of human SOD1 is shown in the upper row. For the other species only replaced amino acids are shown. Consensuses are pictured as dots. Cetacean specific amino acid substitutions are boxed in red.

Transfection of HN33 cells

HN33 cells were stably transfected with pcDNA3.1+ containing OorSOD1 and OorCOMMD6. The sequences of the killer whale were chosen due to the availability of sequence information in online databases. qRT-PCR confirmed high expression of *Sod1* and *Commd6* in the cell lines compared to the mock cells, which were transfected with an empty pcDNA3.1+ vector (Additional Table II.6). *Sod1* expression in the OorSOD1 cell line was 1.1×10^6 copies per μg RNA compared to 133 copies per μg RNA in the mock control. OorCOMMD6 transfected cells had 2.1×10^5 copies of *Commd6* per μg RNA while the mock control had only 97 copies/μg RNA. The cell viability was estimated by measuring the ATP amount and the relative caspase activity of the cells. Transfected cells showed no differences in the basic cell viability under normoxia (Figure II.3, II.4). ROS production was measured using the DCFH-DA assay and revealed no differences in the cell lines under normoxia (Fig. II.5).

SOD1 and COMMD6 protect HN33 cells exposed to hypoxia

To estimate the viability of the different cell lines under hypoxic stress, cells were kept at 1.2 % O_2 for 24 h and were compared to the mock cells (Additional Table II.7). Under normoxia all ATP levels were similar in all cell lines (Fig. II.3). Mock cells showed a significantly lower ATP amount after treatment with hypoxia (50.8 %), while ATP levels in OorSOD1 cells (102.2 %) and OorCOMMD6 cells (86.7 %) were similar in normoxia and hypoxia and significantly higher after treatment with hypoxia compared to mock cells.

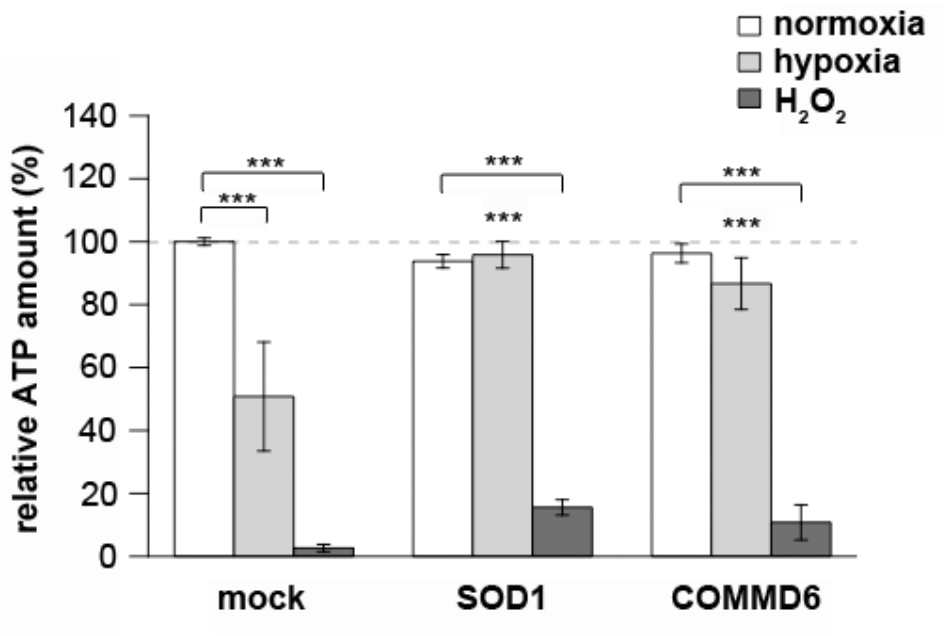

Figure II.3 Relative ATP amount in HN33 cells transfected with an empty pcDNA3.1+ vector (mock), OorSOD1 (SOD1) and OorCOMMD6 (COMMD6), respectively, after treatment with normoxia, 1.2 % O_2 and 275 μM H_2O_2 for 24 h (n$\geq$3 each). Values were normalized to the mock normoxia controls (dotted line). Bars show the standard deviation. Asterisks indicate significance level: p<0.001 (***) compared to the equivalent treatment of mock. Horizontal bars with asterisks indicate significant differences between the different treatments within a cell line.

The caspase activity of the cell lines under normoxia and hypoxia was measured as an indicator for apoptosis. Caspase levels after hypoxia treatment were not significantly different from normoxic levels (Fig. II.4). However, the mock cell line had the highest caspase activity (191.2 %), while the SOD1 and COMMD6 cell line showed a caspase activity similar to normoxia levels (94 % and 145.5 %, respectively).

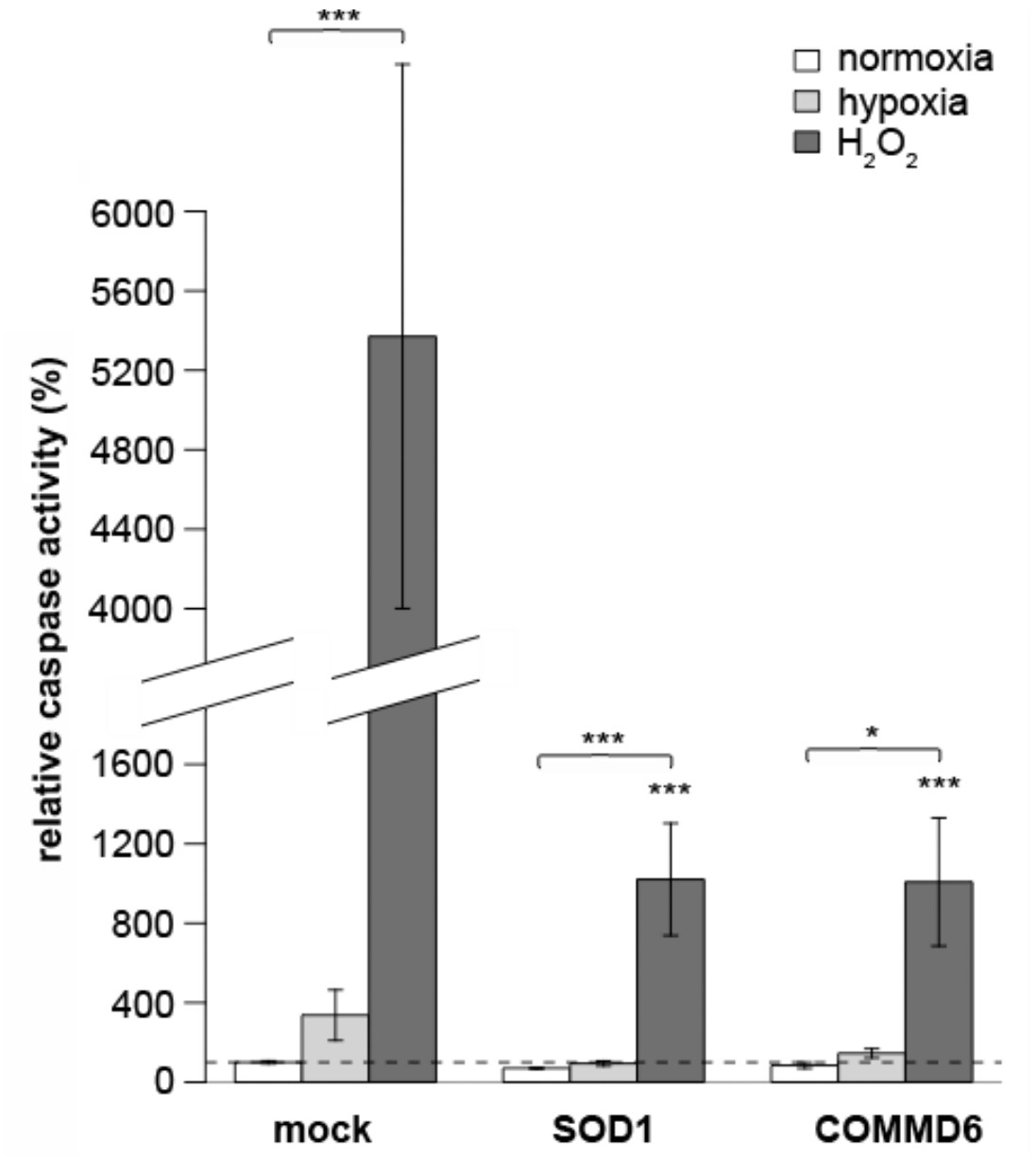

Figure II.4 Relative caspase activity in HN33 cells transfected with an empty pcDNA3.1+ vector (mock), SOD1 and COMMD6 respectively after treatment with normoxia, 1.2 % O_2 and 275 μM H_2O_2 for 24 h (N$\geq$3 each). Values were normalized to the mock normoxia controls (dotted line). Bars show the standard deviation. Asterisks indicate significance level: $p<0.05$ (*), $p<0.01$ (**) and $p<0.001$ (***) compared to the equivalent treatment of mock. Bars with asterisks indicate significant differences between the different treatments within a cell line.

SOD1 and COMMD6 reduce ROS production under hypoxia

The DCFH-DA test was used to measure the ROS production of the transfected cell lines kept at normoxia and hypoxia for 24 h. SOD1 cells and COMMD6 cells had slightly higher ROS levels under normoxia than mock cells (134.3 % and 130 %, respectively) (Fig. II.5). ROS production was significantly increased in all cell lines under hypoxia compared to normoxia. SOD1 cells and COMMD6 cells showed significantly lower ROS levels under hypoxia (526 % and 620 %, respectively) than the mock cells which elevated the ROS production to 895.5% of the normoxia control.

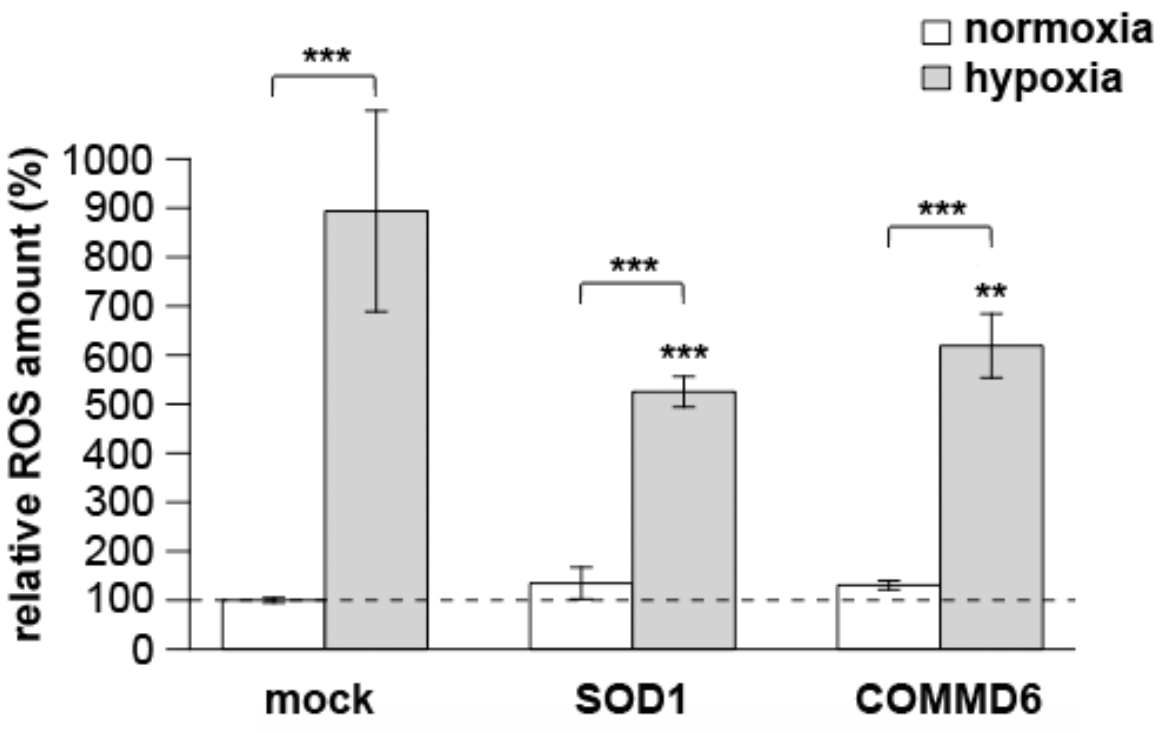

Figure II.5 Relative ROS amount of the transfected HN33 cells after treatment with normoxia and 1.2 % O_2 for 24 h measured by the DCFH-DA test. The cells were transfected with an empty pcDNA3.1+ vector (mock), pcDNA3.1+ vector containing OorSOD1 (SOD1) or OorCOMMD6 (COMMD6). The values were normalized to the mock normoxia control (dotted line). Bars represent standard deviation. Asterisks indicate significance level: $p<0.05$ (*) and $p<0.01$ (**) compared to the equivalent treatment of mock cells. Bars with asterisks indicate significant differences between normoxia and hypoxia within a cell line.

SOD1 and COMMD6 reduce cell death under oxidative stress

Cell viability of the transfected cell lines was evaluated after a 24 h treatment with 275 μM H_2O_2 and was compared to the mock cells. The relative ATP amount between OorSOD1 cells, OorCOMMD6 cells and the mock cell line showed no significant differences (Fig. II.3). The ATP amount of the mock cell line was extremely low after treatment with H_2O_2 (2.2 %) while SOD1 cells and COMMD6 cells had 15.6 % and 10.8 % ATP amount, respectively compared to the mock normoxia control. The caspase assay revealed significant differences between the cell

lines (Fig. II.4). All cell lines showed significantly higher activity of caspase after treatment with H_2O_2 compared to normoxia. SOD1 cells and COMMD6 cells showed significantly lower caspase activity than the mock cell line after treatment with H_2O_2 (Fig. II.4). Mock cells under oxidative stress had a caspase activity 5369.5 % higher than the normoxia controls, while caspase activity in OorSOD1 cells and OorCOMMD6 cells was 1020.6 % and 1007.7 %, respectively.

Discussion

In search of genes involved in the diving adaptation of the whale brain, transcriptome sequencing and RNA-Seq analyses have allowed to identify candidate genes for functional analysis. We found that overexpression of the killer whale genes SOD1 and COMMD6 in hippocampal neuronal mouse cells improved cell viability after 24 hours of hypoxic stress and reduced mortality after treatment with hydrogen peroxide.

High SOD1 concentrations may protect the whale brain during hypoxia and reoxygenation events

We transfected HN33 cells with SOD1 of the killer whale to investigate the effect of elevated expression levels on cell viability under hypoxia and oxidative stress. The SOD1-transfected cells showed a significantly higher amount of ATP under hypoxia (24 h; 1.2 % O_2) (Fig. II.3) as well as a significantly lower caspase activity under oxidative stress (24 h; 275 μM H_2O_2) (Fig. II.4) compared to the mock (control) cells. The production of reactive oxygen species in SOD1-transfected cells was significantly lower than in mock cells after treatment with hypoxia (Fig. II.5). No differences in the ATP amount and the caspase activity were found in the SOD1-transfected cells under hypoxia and normoxia. The higher cell viability and reduced apoptosis rate in the SOD1-transfected cell, compared to the mock cells under hypoxia and oxidative stress indicates a neuroprotective role of high expression of SOD1. Overexpression of SOD1 in transgenic mouse models was shown to protect the adult brain from ischemic injury (Chan 1996; Chan et al. 1996; Chan et al. 1998). Due to the various functions of SOD1 in the cell, for example as modulator of glucose signaling, zinc sensor and in nucleic acid metabolism (for review see: Bunton-Stasyshyn et al. 2015) the exact mechanism behind the protection of the HN33 cells remains unknown. However, SOD1 expression is regulated by H_2O_2 and functions as a transcription factor inducing the expression of antioxidant genes (Hu et al. 2009; Tsang et al. 2014). Therefore, the higher cell viability under hypoxia, the lower apoptosis rate under oxidative stress and the lower production of ROS under hypoxia in SOD1-transfected cells, might derive from the higher concentration of SOD1 and from the upregulation of antioxidant defense mechanisms triggered by SOD1.

Two strategies are known within vertebrates, like anioxia-tolerant fish and turtles or diving mammals to prevent oxidative damage: a constitutively high expression of antioxidant genes or a regulated expression during hypoxia or reperfusion (Hermes-Lima et al. 2002; Zenteno-

Savin et al. 2002). The hypoxia tolerant subterranean mole rat (*Spalax*) was found to have continuously high levels of antioxidant transcripts in the brain (Schülke et al. 2012) which might be advantageous for the permanent hypoxic conditions in their burrows. General high overexpression of SOD1 in the whale brain could not be confirmed in this study. In the killer whale, the SOD1 mRNA levels were lower than in the cattle brain, while in the bottlenose dolphin and in the long-finned pilot whale, expression was higher than in the cattle (Fig. II.1A). Since only mRNA levels of untreated tissues were measured, effects of posttranslational and regulatory mechanisms were not taken into consideration in this work. It is possible that SOD1 levels increase during or after hypoxia in the whale brain. Additionally, the juvenile killer whale has a limited diving ability compared to adult whales, which might explain the relatively low SOD1 level. Therefore, the high SOD1 mRNA levels in the adult long-finned pilot whales might reflect their capacity for long and energy-consuming dives more correctly, indicating that SOD1 might protect the brain from oxidative damage after hypoxic conditions.
We found one whale specific amino acid substitution in the SOD1 sequence (Lys77Glu) and one substitution only present in whales and in the hypoxia-tolerant naked-mole rat (Asp96Glu). The Asp96Glu substitution is located in a region important for SOD1 aggregation (Ida et al. 2016). Intensive research on SOD1 amino acid substitutions has been conducted due to the role of mutant SOD1 in the autosomal dominant neurodegenerative disorder familial amyotrophic lateral sclerosis (ALS) (for review see: Alsultan et al. 2016). Cytoplasmic aggregation of SOD1 is linked to neurotoxicity and altered aggregation properties may lead to a modified antioxidant capacity and altered physiology (for review see: Sheng et al. 2012). The whale-specific amino acid substitution Lys77Glu might play a role in the hypoxia adaptation of whales. Lys77 in human SOD1 is an important sumoylation site (Fei et al. 2006). The posttranscriptional modification via small ubiquitin modification (SUMO) proteins affects protein stability, interaction with other proteins or localization (Gareau et al. 2010). The sumoylation of SOD1 is thought to play a role in the neurodegenerative disease ALS (Fei et al. 2006). Modifications on position 77 lead to SUMO-deficient SOD1 and reduce the formation of harmful aggregates in cells (Dangoumau et al. 2016; Fei et al. 2006). Therefore, the modified SOD1 of whales might represent an adaptation to prevent harmful aggregations caused by oxidative stress (Dangoumau et al. 2016). The role of the specific mutations of SOD1 in hypoxia-tolerant species and their contribution to an improved antioxidant capacity needs to be clarified in future studies.

High expression of COMMD6 in the whale brain might prevent neuronal cell death

COMMD6 is considerably higher expressed in the whale brain, compared to the cattle brain (Fig. II.1B). We transfected HN33 cells with the COMMD6 gene of the killer whale and analyzed the effect of overexpression of COMMD6 on cell viability under hypoxia (24 h; 1.2 % O_2) and oxidative stress (24 h; 275 μM H_2O_2). No effect of hypoxia on ATP amount and caspase activity was observed in COMMD6-transfected cells compared to normoxia levels, whereas hypoxia caused a significant decrease in cell viability of mock cells (Fig. II.3, II.4). A reduced ROS production was found under hypoxia in COMMD6-cells compared to mock cells (Fig. II.5). Oxidative stress caused a significant decrease in ATP and increase in caspase activity in all cell lines compared

to normoxia cells. However, COMMD6-transfected cells showed a significantly lower caspase activity compared to mock cells under oxidative stress. Little information is available of the role of COMMD6 in neurons. COMMD6 was found to inhibit the activation of tumour necrosis factor (TNF)-induced NF-κB signaling (Burstein et al. 2005). NF-κB is a ubiquitous dimeric transcription factor involved in the cellular response to external stimuli, such as inflammation or viral infection (reviewed in: Pahl 1999). The NF-κB transcription factor is known to play a regulatory role in neurological diseases (Clemens et al. 1997a; O'Neill et al. 1997; Schneider et al. 1999) and is activated by hypoxia and oxidative stress (Baldwin 1996; Siebenlist et al. 1994). In neurons, NF-κB activation plays an important role in damage caused by cerebral ischemia (Zhang et al. 2005). Depending on the dimer composition of NF-κB the transcriptional activation of either pro-apoptotic or anti-apoptotic genes is induced in neuronal cells (Sarnico et al. 2009). In our experiments, overexpression of COMMD6 improved viability of neuronal cells under hypoxia and oxidative stress. Therefore, upregulation of anti-apoptotic genes triggered by COMMD6 might play a neuroprotective role. The closely related COMMD1 was studied more extensively than COMMD6 and regulatory functions have been found. For example, COMMD1 is involved in sodium homeostasis, HIF-1 (hypoxia inducible factor 1) signaling and maturation of SOD1 (for review see: Bartuzi et al. 2013). In case of similar functions of COMMD6 these mechanisms could also improve the hypoxia tolerance of the whale brain. Further research is needed to reveal the exact mechanism of neuroprotection via high expression of COMMD6.

Availability of data and material

The raw Illumina files of the transcriptomes from the visual cortex (SRR8305674) and the cerebellum (SRR8305675) of long-finned pilot whale are available from the NCBI SRA database under the Bioproject PRJNA506903. All other data is provided in the Supplemental material on the CD attached to this dissertation.

Acknowledgements: We thank Matthias Preuß (University of Hamburg) for preparation of cattle brain samples and Dustin Krüger for his help with cloning and qRT-PCR analyses. We would like to thank all helpers for collecting, transporting and sampling the orca from Schleswig-Holstein, Germany. This work has been supported by the German Research Foundation (BU 956/22-1) and by a fellowship to A. K. by the Studienstiftung des deutschen Volkes.

8 Chapter III

The composition of lactate dehydrogenase isoenzymes in the cetacean brain may reflect adaptation to diving

Alena Krüger[a], Eda Dönmez[a], Andrej Fabrizius[a], Bjarni Mikkelsen[b], Ursula Siebert[c], Lars P. Folkow[d], Thorsten Burmester[a]

[a]Institute of Zoology, University of Hamburg, Germany

[b]Natural History Museum, Faeroe Islands

[c]Institute for Terrestrial and Aquatic Wildlife Research, University of Veterinary Medicine Hannover, 25761 Büsum, Germany

[d]University of Tromsø – The Arctic University of Norway, NO-9037 Tromsø, Norway

Submitted to Journal of Comparative Physiology B (Dec 02 2019)

Abstract

Cetaceans are well adapted to a marine life and some species may conduct breath-hold dives of remarkable depth and duration, but which may render them hypoxic. While most mammals show severe depression of neuronal functions and neuronal damage within minutes of hypoxia, the brain of whales is apparently unaffected by long-duration dives and remains functional despite low oxygen availability. The mechanisms underlying this unusual hypoxia tolerance are still largely unknown. Here we have investigated the role of lactate dehydrogenase (LDH), a key enzyme in anaerobic metabolic pathways, in the brain of killer whales, long-finned pilot whales and bottlenose dolphins, and its potential adaptations to hypoxia. We found whale-specific amino-acid substitutions in the protein sequences of LDHA and LDHB that may affect kinetic properties and stability of the LDH tetramer. Moreover, LDH activity under high concentrations of lactate as substrate was higher in the whale brain than in cattle brain. Analysis of isoenzyme composition (LDH1-5) showed differences between the whale and the cattle brain. LDH2/LDH3 displayed the highest expression levels in the whale brain, while in cattle LDH1 was most abundant. LDH1 primarily catalyzes the conversion of lactate to pyruvate, LDH5 preferably catalyzes the reverse reaction and LDH2 and LDH3 have intermediate affinities. Therefore, dominance of hybrid isoenzymes may reflect the ability to switch between both reactions. These findings suggest an important role of lactate dehydrogenase in conveying hypoxia tolerance to the whale brain, by allowing rapid switch between aerobic and anaerobic pathways.

Keywords: Brain, Cetacea, Diving, Hypoxia tolerance, Isoenzymes, Lactate dehydrogenase

Introduction

The mammalian brain is dependent on continuous supply of oxygen. Reduced oxygen availability may have a devastating impact on brain function and neuronal survival (Choi et al. 1990; Dirnagl et al. 1999; Lipton 1999; Peers et al. 2007; Walton et al. 1999). Unlike most terrestrial mammals, diving mammals like whales and seals are routinely exposed to low oxygen availability when submerged. Whales can dive for two hours or more, evidently without any brain damage (Joyce et al. 2017; Schorr et al. 2014).

Physiological adaptations of diving mammals have been investigated extensively (Blix et al. 1983; Butler 2004; Butler et al. 1997; Ponganis 2011; Ramirez et al. 2007). They include enhanced oxygen storage capacity due to high levels of the respiratory proteins hemoglobin, myoglobin and neuroglobin (Noren et al. 2000; Schneuer et al. 2012; Soegaard et al. 2012) and the ability to reduce oxygen use during diving, through cardiovascular adjustments, i.e., bradycardia and peripheral vasoconstriction (Blix et al. 1983; Folkow et al. 2010; Ponganis 2011; Scholander 1940; Zapol et al. 1979). When the vasoconstrictor response is fully activated, most organs and tissues experience a shortage of oxygen, while the much-reduced cardiac output of blood is distributed mainly to the brain. Despite these measures, arterial PO_2 may fall below 20 mg Hg (Torr) (Elsner et al. 1970; Meir et al. 2009; Qvist et al. 1986; Ridgway et al. 1969) which is lower than the critical oxygen tension threshold for ischemic brain damage in non-diving mammals (Doppenberg et al. 1998; Elsner et al. 1970; Ridgway et al. 1969).

To survive such low O_2 levels without impairment of cerebral function, additional adaptations are required. A shift to anaerobic metabolism in the brain during long dives has been proposed (Kerem et al. 1973a). During hypoxic conditions lactate dehydrogenase (LDH) catalyzes the conversion of pyruvate to lactate and its activity counts as an indicator of the level of the anaerobic metabolism (Holbrook et al. 1975). Murphy et al. (1980) found a higher activity of lactate dehydrogenase in the brain of the deep diving weddell seal (*Leptonychotes weddellii*) when compared to the brain of cattle and similar results were obtained in the beaver (*Castor fiber*), by Messelt et al. (1976). In a study by Castellini et al. (1981), however, no enhanced glycolytic capacity was found in the brains of diving mammals, when compared to terrestrial mammals. The only cetacean species included were the shallow-diving spotted porpoise (*Stenella attenuata*) and the gray whale (*Eschrichtius robustus*). Moreover, no information concerning the brain region investigated was provided and the enzyme activity of the gray whale differed from that of other, diving and non-diving, mammals. Apparently, more data on the relationship between LDH enzyme activity and cerebral hypoxia tolerance in marine mammals are needed.

Another factor of interest is the link between LDH isoenzyme distribution and anaerobic capacity in the brain. The tetrameric enzyme LDH consists of the two subunits A (muscle type) and B (heart type), encoded by the genes LDHA and LDHB, respectively. Correlating with the predominant type of metabolism, the subunits form five different isoenzymes: LDH1 ($LDHB_4$), LDH2 ($LDHB_3LDHA_1$), LDH3 ($LDHB_2LDHA_2$), LDH4 ($LDHA_3LDHB_1$), and LDH5 ($LDHA_4$) (Cahn et al. 1962; Kaplan et al. 1968; Krieg et al. 1967; Markert et al. 1962; Markert 1963). These isoenzymes differ in their catalytic properties and their sensitivities to substrate inhibition. In

terrestrial mammals, LDH1 is found mainly in aerobic tissues like heart and brain, while LDH5 predominates in skeletal muscle tissues which intermittently rely on anaerobic metabolism. A study by Shoubridge et al. (1976) suggested a higher proportion of LDH5 subunits in the cetacean brain as an adaptation to diving. However, the brain tissue used in that study was sampled 14-24 hours after the death of the animals, which might have resulted in degradation of isoenzymes. Isoenzyme activity is relatively stable for several days. However, LDH isoenzymes 2-5 degrade at a slightly faster rate than LDH1 (Jacobs et al. 1986). Contrasting results were found for the beaver brain, in which LDH2 and LDH3 dominated (Messelt et al. 1976) and for the brain of the hooded seal (*Cystophora cristata*), in which LDH1 and LDH2 dominated (Blix et al. 1971; Hoff et al. 2016). The high hypoxia tolerance of the hooded seal brain (Folkow et al. 2008) may be linked to an unusual distribution of lactate dehydrogenase isoenzymes, with a high proportion of LDH1 and LDH2 in astrocytes (Hoff et al. 2016). These glia cells also express neuroglobin more strongly than do neurons, which implies that they, in fact, have a higher aerobic capacity than the neurons (Mitz et al. 2009). Little is known about the mechanisms of hypoxia tolerance in the whale brain. Although neuroglobin is more highly expressed in the cetacean than in the seal brain (Schneuer et al. 2012), seals and whales may otherwise have evolved similar strategies to cope with cerebral hypoxia. In a transcriptome study we found a high aerobic capacity in the whale brain and suggested this to represent an adaptation to varying oxygen availability (diving vs resurfacing) and changing energy demands (Krüger et al. 2019). In a strictly bioinformatic study, Yim et al. (2014) suggested an expansion of LDHA homologue genes in the minke whale (*Balaenoptera acutorostrata*) and the bottlenose dolphin (*Tursiops truncatus*) to represent an adaptation to hypoxia.

In order to shed more light on such enzymatic adaptations, we have here investigated different properties of lactate dehydrogenase isoenzymes of whales, compared to cattle, a close terrestrial relative of cetaceans. We determined the mRNA expression levels of lactate dehydrogenase a/b transcripts, as well as the genomic copy numbers. An earlier study found a whale-specific amino acid substitution in the LDHA sequence, but not in the LDHB sequence (Tian et al. 2017). We expanded the alignments of LDHA and LDHB with the sequences of the long-finned pilot whale (*Globicephala melas*) and the hooded seal. Furthermore, the LDH isoenzyme distribution and the enzyme activity for pyruvate reduction and lactate oxidation were analyzed.

Materials and methods

Animals

The brain samples of all animals used in this study were obtained opportunistically. The brains of two cattle (*Bos taurus*) were acquired from a German butchery under exceptional permission of the German law of *Tierische Nebenprodukte-Beseitigungsgesetz*. Dissection of the skull and sampling of the visual cortex was performed by the University of Hamburg taxidermist within 3 hours of the animal being killed using a captive bolt gun. The brain of a juvenile killer whale (*Orcinus orca*) that died of live stranding was removed by the Institute of Terrestrial and

Aquatic Wildlife Research, University of Veterinary Medicine Hannover, Foundation and the visual cortex was sampled after approximately 12 hours of death. One unspecified brain sample of an adult bottlenose dolphin that died in the Duisburg Zoo was also dissected within hours by the Institute of Terrestrial and Aquatic Wildlife Research, University of Veterinary Medicine Hannover, Foundation. Samples of the visual cortex and the cerebellum of three long-finned pilot whales were obtained from animals that were harvested during traditional subsistence whaling off the Faroe Islands. Samples were taken by a veterinarian within 4 hours of death. Regulations of the *Convention on Biological Diversity* (CBD) and *Convention on International Trade in Endangered Species* (CITES) were followed, and the appropriate permits were obtained (Permit number: E-01456/17). Brain samples were preserved at -80 °C in RNAlater and solely by freezing at -80 °C. Due to limited sample material from the long-finned pilot whale and the bottlenose dolphin, some analyses were performed only with the material of the killer whale and cattle.

Sequencing and expression analysis

Total RNA was extracted using peqGOLD Trifast (PEQLAB, Erlangen, Germany) and Crystal RNA Mini Kit (Biolab Products, Bebensee, Germany). Quality and quantity analyses were performed using spectrophotometry and gel electrophoresis. Two μg of total RNA from the visual cortex of the cattle (male, 2 years old), 9 μg from one killer whale (juvenile, male) and 2.5 μg from visual cortex and cerebellum of one long-finned pilot whale (male, adult) was used to generate a library for paired end sequencing of 150 nt with an estimated output of 50 million reads. Sequencing was performed with NextSeq 500 (StarSEQ, Mainz, Germany). Sequence quality was analyzed via CLC-Genomics Workbench (Version 10.0.1). For quality trimming, the first 15 nucleotides from the 5′ end were removed. Additionally, all reads with more than two ambiguous nucleotides and reads with a mean Phred quality of below 15 were discarded. Mapping of the quality-trimmed reads was performed using the RNA-seq algorithm of the CLC-Genomics Workbench (Version 10.0.1). The NCBI LDHA (NM_174099) and LDHB (BT021009) sequences of cattle were used for the mapping of cattle reads. Mapping of cetacean reads was performed with the LDHA sequence of the bottlenose dolphin (NM_001280640) and the LDHB sequence of killer whale (XM_004270929) as reference. Brain transcriptome datasets freely available at Sequence Read Archives (SRA) from NCBI of the minke whale (SRX313597), the bowhead whale (*Balaena mysticetus*) (SRX790347) and four cattle (SRX211675, SRX211674, SRX196362, SRX196353) were included in the analyses. Only reads that matched 90 % of the read length and 90 % of nucleotides of the reference were included in the mapping. Reads with non-specific matches were ignored in the mapping. Gene expression was calculated as transcript reads normalized to total reads of each sample.

Quantitative real time reverse transcriptase polymerase chain reaction (qRT PCR)

Total RNA was purified from brain samples samples using peqGOLD Trifast (PEQLAB, Erlangen, Germany) and Crystal RNA Mini Kit (Biolab Products, Bebensee, Germany). An on-column DNA digestion with RNase-Free DNase (Qiagen) was performed. The quantity and

quality of the RNA were verified by spectrophotometry and via gel electrophoresis. First-strand cDNA was synthesized from 1 μg of total RNA using Fermentas RevertAid H- reverse transcriptase kit (Thermo Scientific, Germany) according to manufacturer's protocol. qRT-PCR was performed on the ABI PRISM 7500 Sequence Detection System with the Power SYBR Green master mix (Applied Biosystems, Darmstadt, Germany) using a 40 cycles protocol (95 °C for 15 s, 58 °C for 60 s). The following *Ldha* primers were used for cetaceans and cattle: 5′- TCAGTATCTTAATGAAGGACTTGG-3′ and 5′- GGCAGCCTTTTCCTTAGAACA-3′. *Ldhb* primers for cetaceans and cattle were: 5′- AGCATTCTGGGAAAGTCTCTGA-3′ and 5′- GTGGTGGTAACTGCAGGAG-3′. The copy number of *Ldha* and *Ldhb* in a cDNA sample was determined using a standard curve (10^7 - 10^3) approach of the recombinant plasmid as standard, and then normalized to 1 μg of total RNA. mRNA copy numbers of *Ldha* and *Ldhb* were normalized using *Gapdh* as reference (de Jonge et al. 2007). *Gapdh* primers were: 5′-ATCACCATCTTCCAGGAGCG-3′ and 5′- GCCAAGAGGGTCATCATCTCT-3′.

Determination of genomic copy numbers of LDHA and LDHB

The Quiagen DNeasy Blood and Tissue Kit (Quiagen, Hilden, Germany) was used to extract DNA from 20 mg of brain tissue from cattle, killer whale and bottlenose dolphin according to the manufacturer's protocol. Concentration and quality of the extracted DNA were determined by spectrophotometry. Two primer sets were designed for LDHA and LDHB each. One primer set was used to detect exclusively processed genes, with one primer at the 3′ end of an exon and the other primer at the 5′ end of the following intron. The other primer set was used to detect pseudogenes and processed genes with both primers within an exon. The nucleotide sequences are shown in Table III.1. Quantitative real-time PCR was performed using the ABI PRISM 7500 Sequence Detection System (Applied Biosystems) with 1 μl of genomic DNA, 10 μl of PowerUP SYBR Green Master Mix (Applied Biosystems), 1 μl of Primer mix and 8 μl of water per sample. Three technical replicates were used for each sample. The amplification protocol consisted of an initial denaturation step of 10 minutes at 95 °C followed by 40 cycles of 95 °C for 15 s and 58 °C for 60 s. The efficiency (E) of the assay was determined with a standard curve produced by a series of 10-fold dilutions (0.0213 ng, 0,213 ng, 2.13 ng and 21.3 ng for cattle; 0.042 ng, 0.42 ng, 4.2 ng and 42 ng for killer whale; 0.0458 ng, 0.458 ng, 4.58 ng and 45.8 ng for bottlenose dolphin) and was calculated as:

$$E = 10^{(\frac{-1}{slope})} - 1 \qquad (eq.1)$$

The relative gene copy number was determined using CREBBP (CREB binding protein) as a single copy reference. Relative copy numbers of LDHA and LDHB in cattle, killer whale and bottlenose dolphin were calculated with an efficiency-adapted relative quantification model (Pfaffl 2001) as:

$$Relative\,copy\,number = \frac{E^{\Delta Ct}CREBBP}{E^{\Delta Ct}LDH} \qquad (eq.2)$$

Table III.1 Nucleotide sequences of primers used to determine the genomic copy number via qRT-PCR

Gene	Species	Name	Position	Sequence 5′ - 3′
LDHA	Bta	Bta_LDHA3Ex_For	exon 3	ATAATGTGACAGCAAACTCCAGG
	Bta	Bta_LDHA3Ex_Rev	exon 3	GTAAAATACAGCCCAAATTGCAAG
	Oor, Ttr	Whale_LDHA3Ex_For	exon 3	ATAGTGTGACAGCAAACTCCAAG
	Oor, Ttr	Whale_LDHA3Ex_Rev	exon 3	GTAAAATACAGCCCACACTGCAA
	Bta	Bta_LDHA3In_Rev	intron 3	TCCTGAGAGTGAATTTGTGTTTTTG
	Oor	Oor_LDHA3In_Rev	intron 3	GATGAGCTAGAGTAAAACTGATAG
	Ttr	Ttr_LDHA3In_Rev	intron 3	CTCCTGGGAGTGAGTTTGTG
	Bta	Bta_LDHA3Ex_Rev	exon 3	GTAAAATACAGCCCAAATTGCAAG
	Oor, Ttr	Whale_LDHA3Ex_Rev	exon 3	GTAAAATACAGCCCACACTGCAA
LDHB	Bta	Bta_LDHB3Ex_For	exon 3	TCTCTGACTGACGAGCTTGC
	Bta	Bta_LDHB3In_Rev	intron 3	CTGGTGAATCTAATGTCAGCAG
	Oor, Ttr	Whale_LDHB3Ex_For	exon 3	GTC TCTGACTGATGAGCTTGC
	Oor, Ttr	Whale_LDHB3In_Rev	intron 3	CTGGTGAATCTAGTGTTGGTAGT
	Bta	Bta_LDHB_ Ex_For	exon 3	CAGTGTTATCAACCAGAAGCTG
	Bta	Bta_LDHB_ Ex_Rev	exon 4	ACTACAGTGTGATTAACCACAAG
	Oor, Ttr	Wal_LDHB4Ex_For	exon 4	ATTACTCTGTGACCGCCAATTC
	Oor, Ttr	Wal_LDHB4Ex_Rev	exon 4	CTGCATCATAATTGTGGTTTCTAAC
CREBBP	Bta, Oor, Ttr	Cet_CREBBP_For	exon 26	TGCCAGAAGATGAAGCGGG
	Bta, Oor, Ttr	Cet_CREBBP_Rev	exon 26	TGCTACCACGCCAAACACTG

Sequence analysis and protein-structure visualization

The *Ldha* mRNA sequences of the killer whale and the pilot whale were reconstructed using a de novo assembly with *Ldha* and *Ldhb* specific reads with the *Ldha* sequence of the bottlenose dolphin and the *Ldhb* sequence of the killer whale available at the NCBI nucleotide database (NM_001280640 and XM_004270929, respectively) as reference. The de novo as-

sembly was conducted with the CLC Workbench de novo assembly tool (Version 10.0.1). The coding sequences were annotated using ORF-Finder (https://www.ncbi.nlm.nih.gov/orffinder/). The LDH amino acid sequences of the killer whale, the long-finned pilot whale and the sequences obtained from the NCBI protein database of killer whale (LDHB: XP_004270977.1), bottlenose dolphin (LDHA: NP_001267569.1, LDHB: NP_001267564.1), baiji (*Lipotes vexillifer*, LDHA: XP_007465813.1 corrected, LDHB: XP_007449431.1), the sperm whale (*Physeter catodon*, LDHA: XP_007104972.1, LDHB: XP_007124838.1), minke whale (*Balaenoptera acutorostrata*, LDHA: XP_007174905.1, LDHB: XP_007194889.1), cattle (LDHA: AAI46211.1, LDHB: NP_776525.2), pig (*Sus scrofa*, LDHA: NP_001165834.1, LDHB: NP_001106758.1), hooded seal (*Cystophora cristata*, LDHA: AMC39375.1, LDHB: AMC39376.1), mouse (*Mus musculus*, LDHA: AAH94019.1, LDHB: NP_032518.1) and human (*Homo sapiens*, LDHA: CAG33056.1, LDHB: AKI70389.1) were aligned using the GeneDoc software (Version 2.7) (http://genedoc.software.informer.com/2.7/). To confirm the whale-specific amino acid substitutions, we expanded the dataset used from Tian et al. (2016) with the pilot whale sequence of LDH (Additional file III.1). To visualize the whale-specific amino acid substitutions of LDHA and LDHB, polyview-3d (Porollo et al. 2007) (http://polyview.cchmc.org/polyview3d.html) was used with the human LDHA and LDHB 3D structure obtained from the RCSB Protein Data Bank (LDHA: P00338, LDHB: P07195) as input file.

Enzyme activity assays

Deep-frozen (-80 °C) samples of the visual cortex of cattle and killer whale were homogenized in the proper assay buffer (1/15, w/v) and centrifuged for 30 min at 16,000 g and 4 °C. The total protein concentration of supernatants was determined using the RotiQuant Protein Quantitation Assay (Roth, Karlsruhe, Germany) and BSA as standard, following the manufacturer's guide. The protein concentration in the supernatants was then adjusted for each assay using the specific buffer. Three independent protein isolations per sample were performed, as described. Either pyruvate or lactate was used as substrate to determine the specific activity of LDH in the samples. For the pyruvate assay, a protocol was adapted from Bergmeyer et al. (1965). The samples were homogenized in 0.05 M potassium phosphate buffer (pH 7.4) and the supernatant adjusted to 50 μg/ml total protein. For the lactate assay, an adaptation of the protocol of Markert and Ursprung (1962) was used. The samples were homogenized in Tris buffer (0.01 M Tris–HCl, pH 9.0) and adjusted to 500 μg/ml total protein. The LDH specific activity was measured by either the reduction of NAD^+ or the oxidation of NADH monitored as the chance of absorption at 340 nm. The results are expressed as μmol $\times$ min^{-1} $\times$ mg $protein^{-1}$.

Native protein gel electrophoresis

Frozen samples (-80 °C) of visual cortex from two cattle, from one killer whale and of visual cortex and cerebellum of three long-finned pilot whales were homogenized in Tris-glycine buffer (0.02 M Tris, 0.02 M glycine, 0.002 M EDTA, pH 8.6). For the killer whale, only one biological sample and three technical samples were used. For cattle, two biological samples and two technical replicates were used. Technical and biological samples together were summarized as

three replicates in the analysis. Homogenized samples were centrifuged for 30 min at 16,000 g and 4 °C. The total protein concentration of supernatants was measured using the RotiQuant Protein Quantitation Assay (Roth Karlsruhe, Germany) with BSA as standard, following the manufacturer's instructions. A total of 5 μg protein was loaded and run at 120 V for 70 min. Tris-glycine buffer was used as reservoir buffer. The gel was stained with an LDH activity staining solution (0.1 M Tris, 1 % lactate, 0.05% NAD^+, 0.0005 % PMS, and 0.005 % NBT, pH 9.2) for 60 min at 37 °C. The samples on the gel were separated into five bands correlating the five LDH isoenzymes. The intensity of the bands was determined by densitometry via ImageJ 1.51 t (https://imagej.nih.gov/ij, NIH USA). Isoenzyme composition was defined as a percentage of the total intensity in each sample.

Statistics

Interspecific differences observed in qRT-PCR, genomic copy numbers and isoenzyme composition were considered statistically significant when $p \leq 0.05$ in two-way analysis of variance (ANOVA) and Dunnett's multiple comparisons test. Differences in enzyme activity were analyzed using two-tailed t-test and were considered statistically significant when $p \leq 0.05$.

Results

Lactate dehydrogenase expression values are similar in the brain of cattle and whales

Expression levels were estimated by RNA-seq from the visual cortices of the cattle, killer whale, and long-finned pilot whale and from the cerebellum of the long-finned pilot whale as well as from transcriptomes available at the NCBI SRA database of the brain of the bowhead whale, minke whale and four cattle, with the LDHA and LDHB sequences as reference. In all samples analyzed, lactate dehydrogenase b (*Ldhb*) mRNA copy numbers were higher than lactate dehydrogenase a (*Ldha*) copy numbers (Fig. III.1). Expression values of *Ldha* were slightly, but not statistically significantly higher in whales than in cattle with a mean expression value of 229,585 transcript reads in whales (range: 178,760 in the killer whale to 259,245 in the bowhead whale) and 171,233 transcript reads in cattle (range: 81,772 - 347,416). *Ldhb* expression values were higher in cattle than in whale, with 770,415 transcript reads in whales (range: 740,755 in bowhead whale to 821,240 in killer whale) and 828,767 transcript reads in cattle (range: 652,584 - 918,228). The mean *Ldha* expression value was 1.3 fold higher in whale, while the *Ldhb* expression value was 1.1 fold higher in cattle, but mean expression values of *Ldha* and *Ldhb* in whale and cattle brain samples were not statistically significant (p=1). Mean Ldha/Ldhb ratios were 0.3 in whale (SD=0.04) and 0.21 in cattle (SD=0.16) (see Additional file III.2).

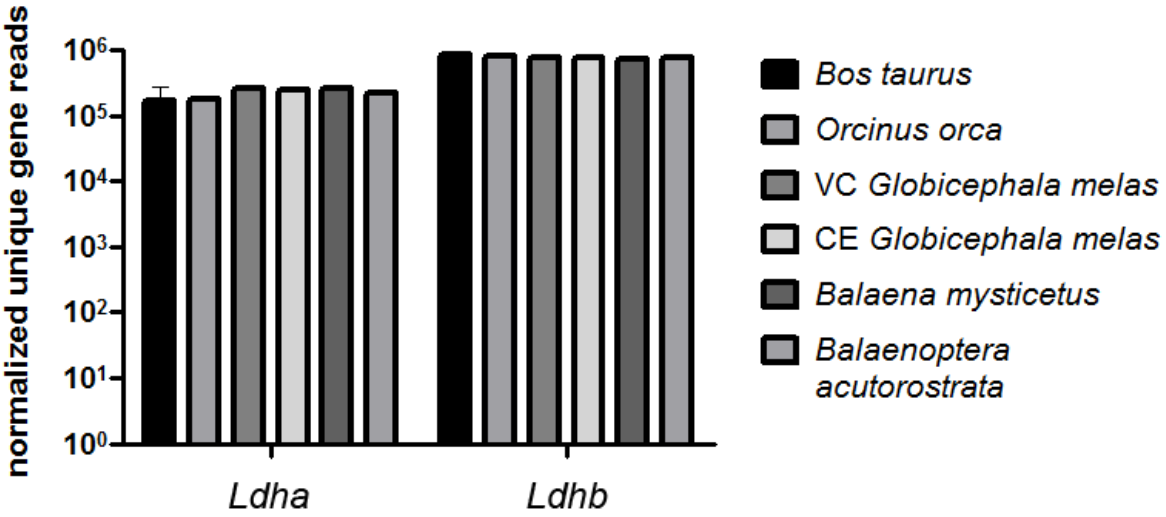

Figure III.1 Expression levels via RNA-seq analysis in normalized unique gene reads of lactate dehydrogenase a (*Ldha*) and lactate dehydrogenase b *Ldhb*) in brain samples of cattle (*Bos taurus*, N = 5), killer whale (*Orcinus orca*, N=1), long-finned pilot whale visual cortex (*Globicephala melas* VC N=1) and cerebellum (*Globicephala melas* CE, N=1) bowhead whale (*Balaena mysticetus*, N=1) and minke whale (*Balaenoptera acutorostrata*, N=1). Data are expressed as means of unique gene reads normalized to total reads of each sample. Error bars represent standard deviations.

Additionally, the mRNA levels of *Ldha* and *Ldhb* in the brain of two cattle, one killer whale, one bottlenose dolphin and in the visual cortex and the cerebellum of six long-finned pilot whales, were determined using qRT-PCR. Similar to the mRNA levels determined by RNA-Seq, *Ldhb* levels were higher in all species tested (Fig. III.2). The highest mRNA levels of *Ldha* and *Ldhb* were found in the brain of long-finned pilot whale. No significant differences were found in the mRNA levels of *Ldha* and *Ldhb* between whale (mean *Ldha*: 156,516,046 copy number per μg RNA; mean *Ldhb*: 3,941,453,207 copy number per μg RNA) and cattle (mean *Ldha*: 43.697.384 copy number per μg RNA; mean *Ldhb*: 570,549,768 copy number per μg RNA), though (*Ldha*: p=0.75; *Ldhb*: p=0.73).

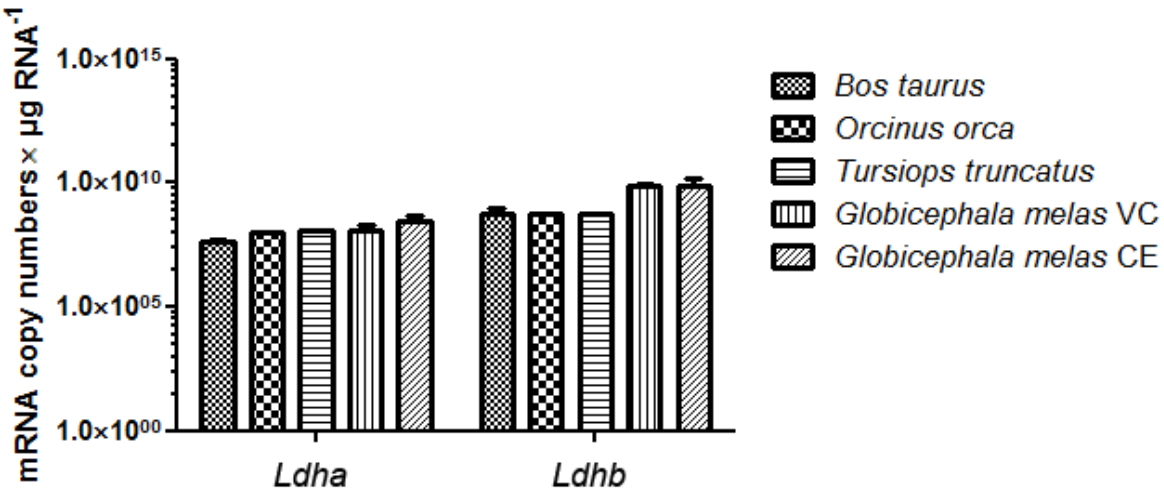

Figure III.2 Expression levels via qRT-PCR of lactate dehydrogenase a (*Ldha*) and lactate dehydrogenase b (*Ldhb*) mRNA in brain samples of cattle (*Bos taurus*, N=2), killer whale (*Orcinus orca*, N=1), and bottlenose dolphin (*Tursiops truncatus*, N=1), and of long-finned pilot whale visual cortex (*Globicephala melas* VC, N=6) and cerebellum (*Globicephala melas* CE, N=6). Mean expression values (mRNA copy number/μg RNA) normalized to the expression of *Gapdh*. Error bars represent standard deviations. No significant differences were found between samples.

Killer whales and bottlenose dolphins have one genomic copy of LDHA and LDHB

Gene copy numbers of LDHA and LDHB were estimated in genomic samples of cattle, killer whale and bottlenose dolphin using a qRT-PCR assay. For the discrimination between processed pseudogenes and coding genes, two primer sets (one set spanning exon/intron boundaries to determine coding genes and one set within exons to measure pseudogenes) were used for each gene (Table III.1). Copy numbers were calculated in relation to the single copy gene CREB Binding Protein (CREBBP). Significant differences were found in all assays between the cetaceans and cattle (Fig. III.3). In the genome of cattle, two copies of LDHA and LDHB were detected, while in the genome of the killer whale and the bottlenose dolphin only one copy of LDHA/B was detected. No significant difference was found in the distinction between coding genes and processed pseudogenes, indicating that no processed pseudogenes were present in the analyzed genomes.

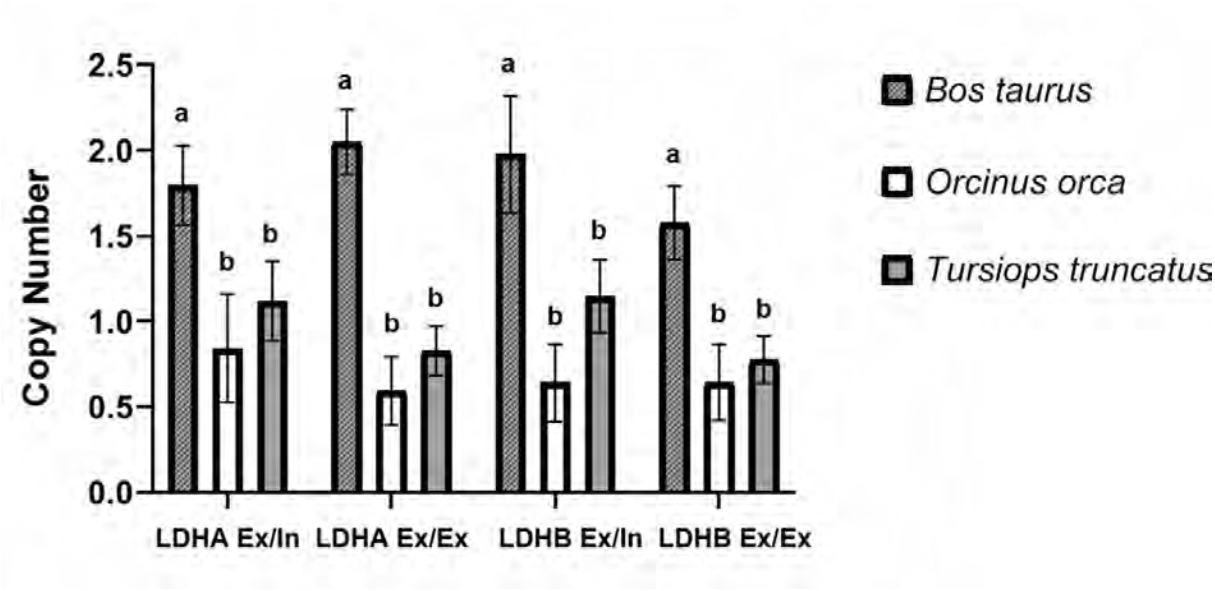

Figure III.3 Genomic gene copies of LDHA and LDHB normalized to the single copy gene CREBBP in cattle (*Bos taurus*, N=3), killer whale (*Orcinus orca*, N=3) and bottlenose dolphin (*Tursiops truncatus*, N=3). LDHA/B Ex/In primers are located in an exon and the following intron to detect processed genes; LDHA/B Ex/Ex primers are located in one exon to detect both, processed genes and pseudogenes. Error bars represent standard deviations of technical replicates. Statistical significance was assessed by two-way ANOVA and Dunnett's multiple comparison test; different letters indicate statistically significant differences between samples ($p<0.05$).

LDHA and LDHB sequences are highly conserved in mammals

The amino acid sequences of LDHA and LDHB in whales consist of 332 and 334 amino acids, respectively, as in terrestrial mammals (Fig. III.4). The LDH amino acid sequences of the species analyzed showed high conservation. The LDHA sequence of cattle and killer whale, and cattle and pilot whale, were both 96 % identical. The sequence of LDHB in cattle and killer whale, pilot whale, bottlenose dolphin, baiji and sperm whale shared 97 % of the amino acid residues. The LDHA sequence of killer whale and long-finned pilot whale and the LDHB sequence of killer whale, long-finned pilot whale, bottlenose dolphin and baiji were 100 % identical (Additional file III.3). The sequence alignment of LDHA (Fig. III.4a) and LDHB (Fig. III.4b) showed one whale-specific amino acid substitution in each sequence. LDHA in whales has a glutamine (Q) in position 313 instead of a glutamate (E) and LDHB in whales has a serine (S) instead of an asparagine (N) in position 306.

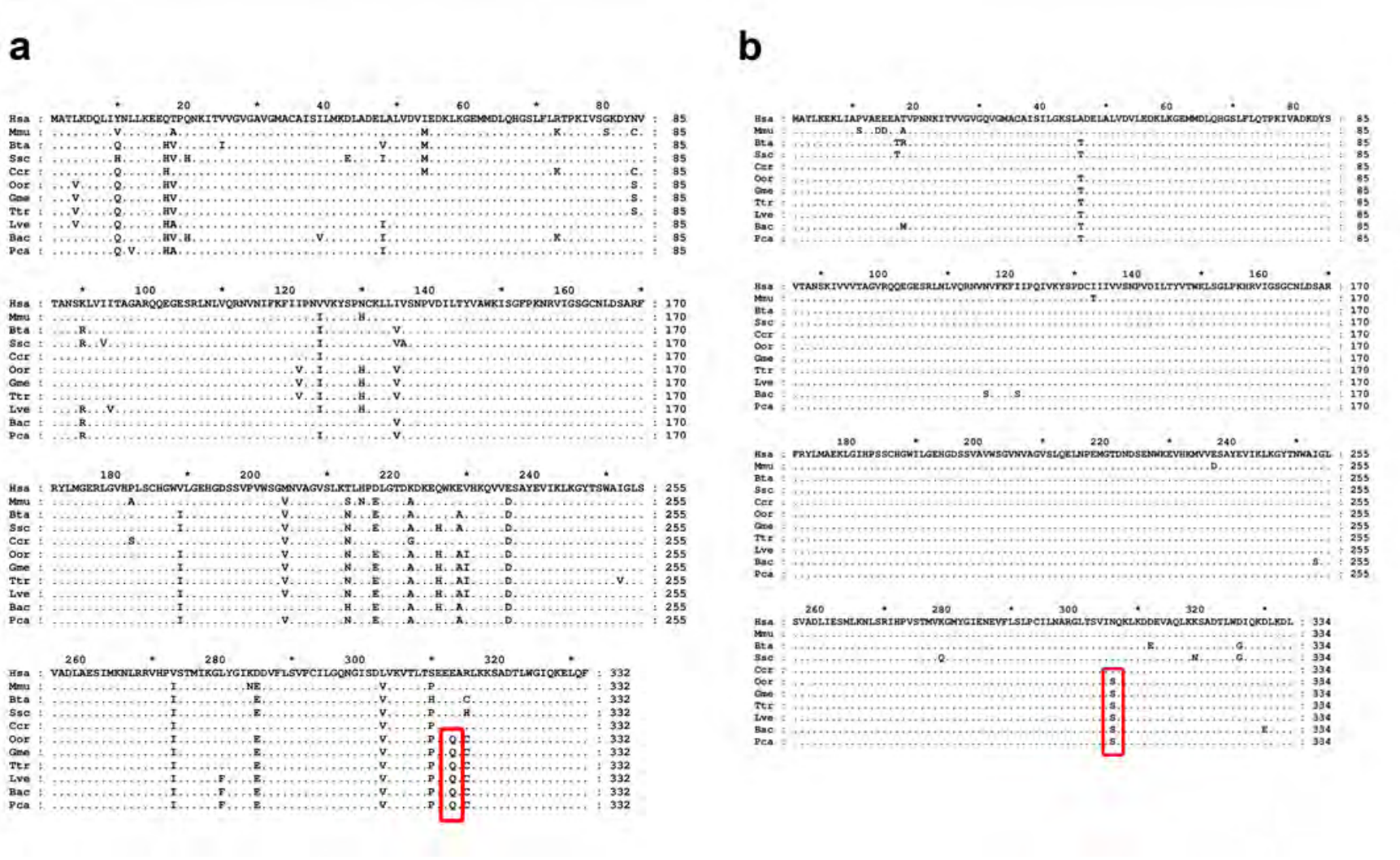

Figure III.4 Multiple alignment of LDHA (a) and LDHB (b) amino acid sequences of selected species of diving and non-diving mammals. The species are abbreviated as follows: Hsa: *Homo sapiens* (human), Mmu: *Mus musculus* (mouse), Bta: *Bos taurus* (cattle), Ssc: *Sus scrofa* (pig), Ccr: *Cystophora cristata* (hooded seal), Oor: *Orcinus orca* (killer whale), Gme: *Globicephala melas* (long-finned pilot whale), Ttr: *Tursiops truncatus* (bottlenose dolphin), Lve: *Lipotes vexillifer* (baiji), Bac: *Balaenoptera acutorostrata* (minke whale), Pca: *Physeter catodon* (sperm whale). The complete sequence of human LDHA and LDHB is shown as reference. For the other species, only replaced amino acids are shown. Consensuses are pictured as dots. The whale-specific amino acid substitutions in LDHA and LDHB are boxed red.

The whale-specific substitution in LDHB has interchain contact

All species of whales tested in this study exhibit a specific amino acid substitution in the protein sequences of LDHA and LDHB, when compared to the sequences of other species (man, mouse, cattle, pig, hooded seal). While terrestrial mammals and the hooded seal all have a glutamate in position 313 in LDHA, the residue is glutamine in the whale LDHA (Fig. III.5). The whale-specific substitution is located at the protein surface, without known ligand or interchain contact.

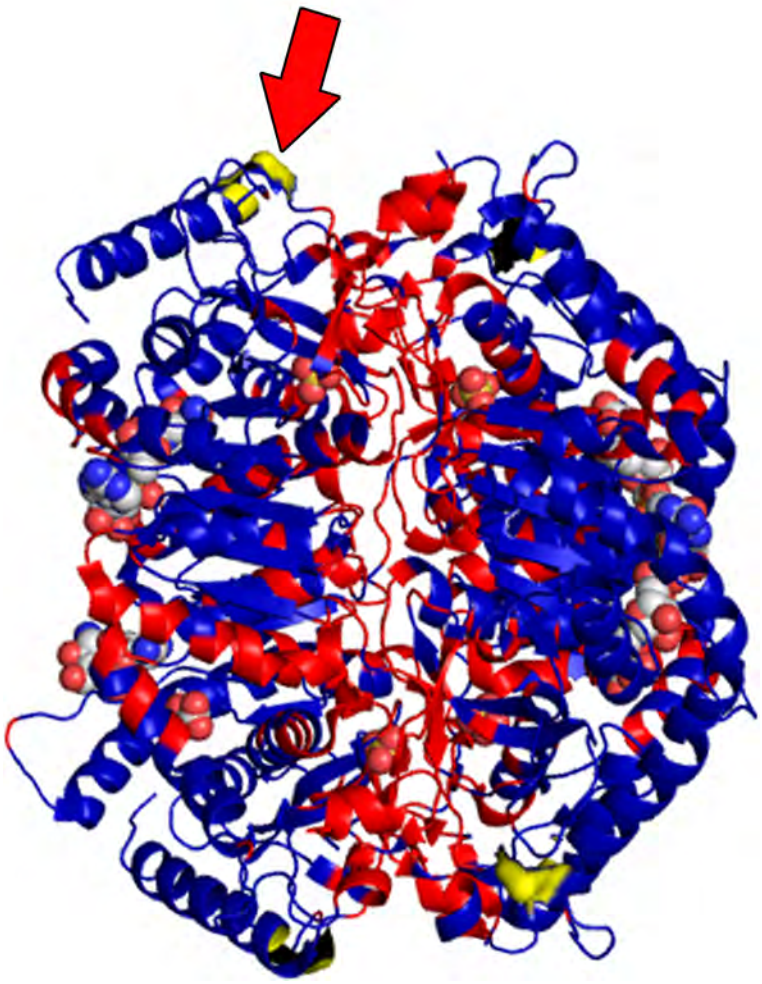

Figure III.5 Structure of human lactate dehydrogenase a (LDHA) in blue, complexed with the ligands NADH and oxalate in red/grey as spheres, with the whale-specific amino acid substitution on position 313 from glutamate to glutamine marked with an arrow and all residues with interchain contact in red.

The amino acid sequence of LDHB shows a whale-specific amino acid substitution in position 306 (Fig. III.6). The protein sequences of non-diving mammals and the hooded seal show an asparagine in position 306 whereas in the protein sequence of whales, asparagine is replaced by serine. The substitution in whales is located at the protein surface, with known interchain contact.

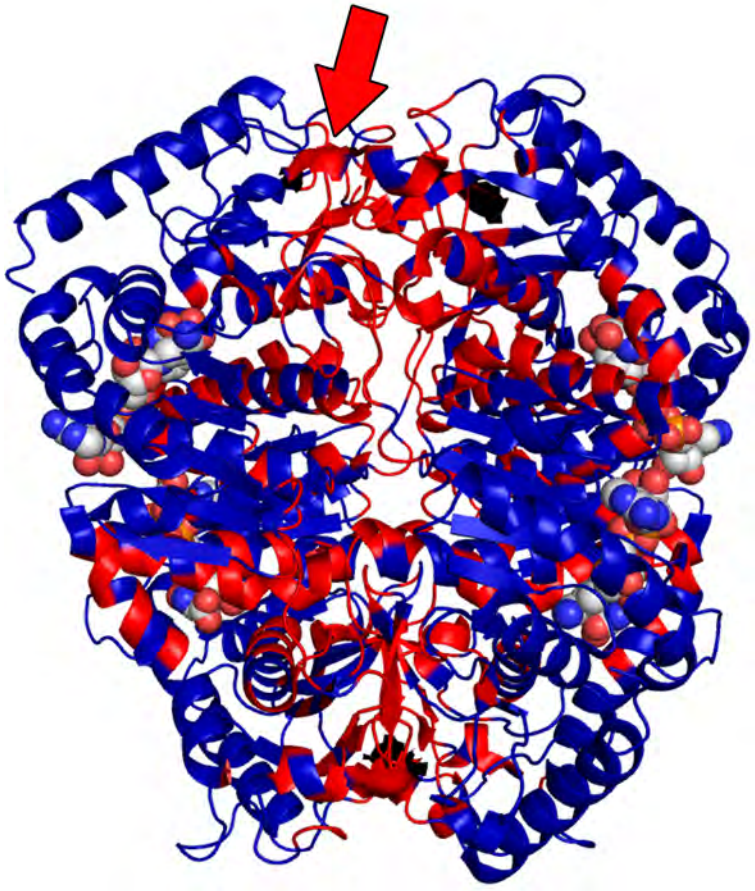

Figure III.6 Structure of human lactate dehydrogenase b (LDHB) in blue, complexed with the ligands NAD^+ and 4-hydroxy-1,2,5-oxadiazole-3-carboxylic acid in red/grey as spheres, with the whale-specific amino acid substitution on position 306 from asparagine to serine marked with an arrow and all residues with interchain contact in red.

LDH activity with lactate as substrate was higher in the whale brain than in the cattle brain

LDH activity was estimated using pyruvate and lactate assays. In the cattle and killer whale brain, LDH activity was higher with pyruvate than with lactate as substrate (Fig. III.7). With lactate concentrations between 10^{-2} and 5×10^{-1} M LDH activities were significantly higher in the killer whale brain than in cattle brain (Fig. III.7a). The maximum LDH activity with lactate was 8.52 μmol $NAD^+ \times min^{-1} \times$ mg $protein^{-1}$ in the visual cortex of killer whale and 4.93 μmol $NAD^+ \times min^{-1} \times$ mg $protein^{-1}$ in the visual cortex of cattle. No significant differences were found between LDH activity in cattle and whale brain with pyruvate as substrate (Fig. III.7b). The highest LDH activity with pyruvate as substrate was 78.43 μmol NADH $\times min^{-1} \times$ mg $protein^{-1}$ and 94.3 μmol NADH $\times min^{-1} \times$ mg $protein^{-1}$ in killer whale and cattle, respectively.

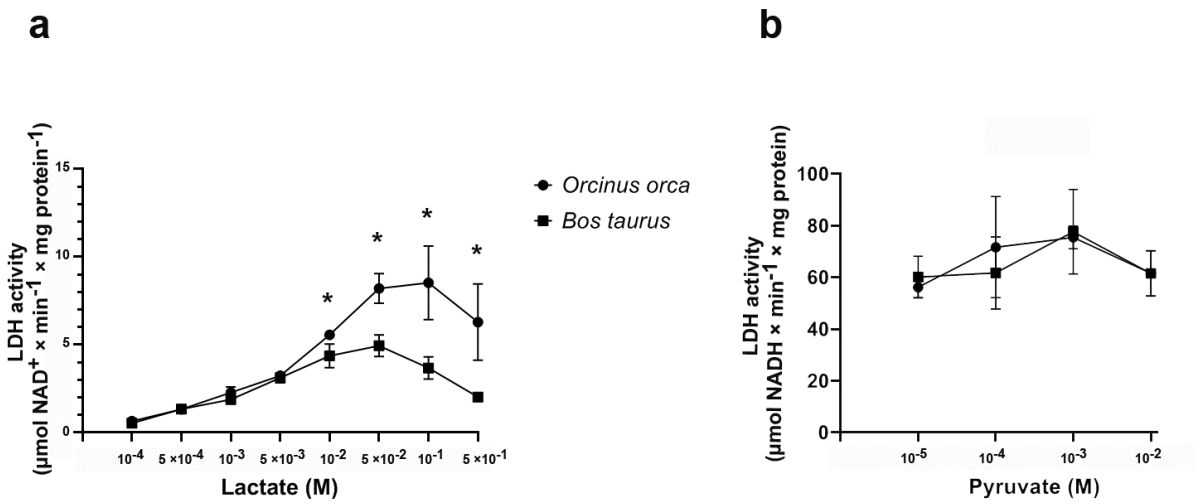

Figure III.7 Lactate dehydrogenase (LDH) activity in brain samples of cattle (square, N=3) and killer whale (circle, N=3). Data are expressed as means of μmol of NAD^+ (a), or NADH (b) consumed per minute per milligram protein. Error bars represent standard deviations of technical replicates. Statistical significance was indicated by one-way ANOVA and Dunnet's multiple comparison test; differences of enzyme activity between species at a given substrate concentration are marked with an asterix ($p<0.05$).

The LDH isoenzyme composition is different in the cattle and whale brains

The five homo- or heterotetrameric LDH isoenzymes are formed by four LDHA and/or LDHB subunits: LDH1 ($LDHB_4$), LDH2 ($LDHB_3$ $LDHA_1$), LDH3 ($LDHB_2$ $LDHA_2$), LDH4 ($LDHA_3$ $LDHB_1$) and LDH5 ($LDHA_4$) (Markert 1963). The electrophoretogram (Fig. III.8) showed a different electrophoretic mobility of LDH isoenzymes of cattle and whale, caused by differing isoelectric points (PI) of LDHA and LDHB. The PI of LDHA of the long-finned pilot whale was 8.41; the PI of LDHA of the killer whale ranged from 8.88 to 9.8; the PI of LDHA of cattle ranged from 8.12 to 8.18. PI of LDHB was 6.2 for cattle, 5.58 for the killer whale and 6.79 for the pilot whale.

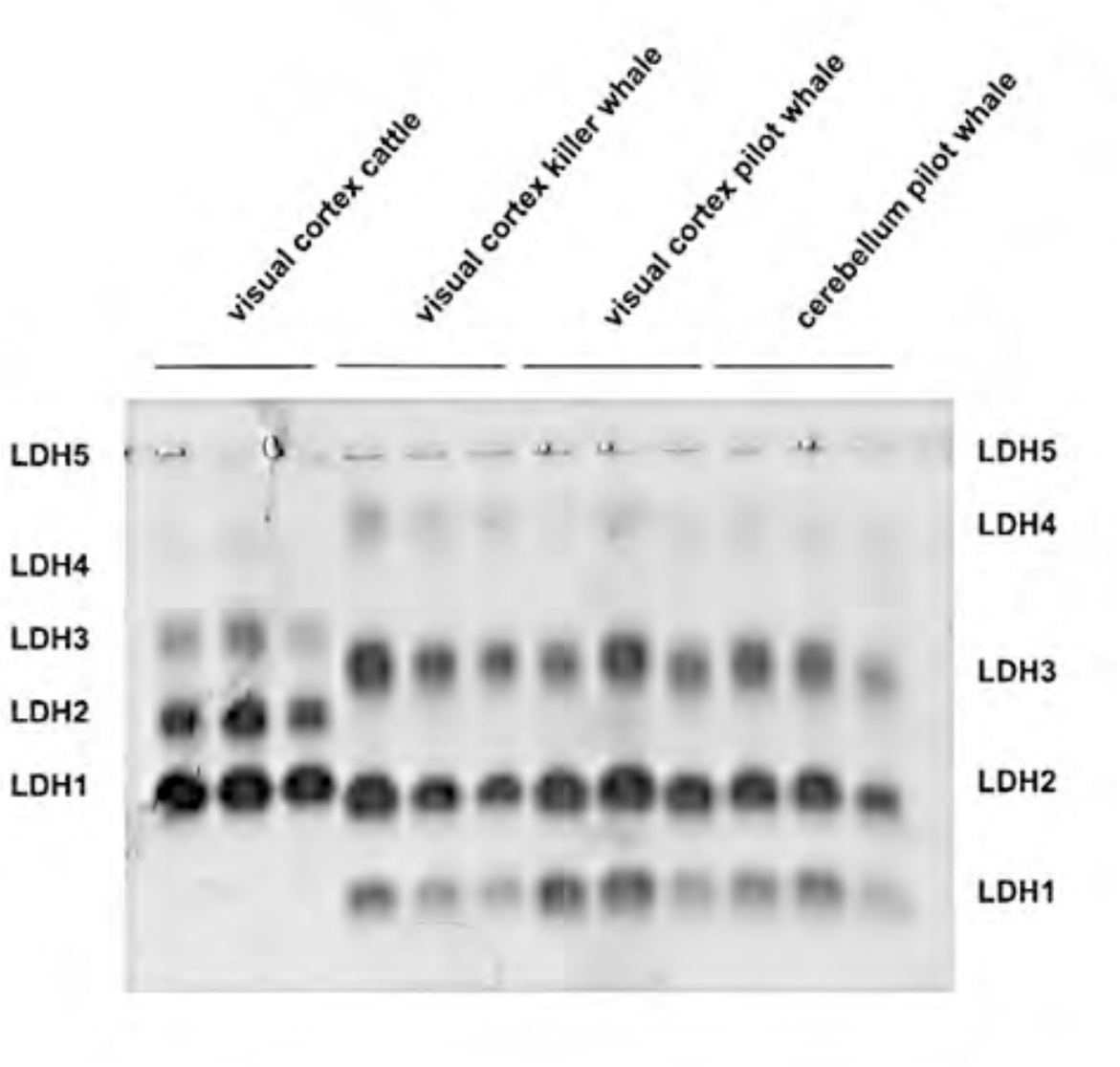

Figure III.8 Lactate dehydrogenase (LDH) isoenzyme composition in visual cortex samples of cattle, killer whale and pilot whale and in cerebellum samples of pilot whale. Differences in electrophoretic mobility are caused by different isoelectric points (PI) of LDH of whales (PI LDHA 8.41 - 9.8, PI LDHB 5.58 - 6.79) and cattle (PI LDHA 8.12-9.18, PI LDHB 6.2).

The brain samples of whales and cattle had different LDH isoenzyme compositions (Fig. III.9). In cattle, LDHB isoenzymes (LDH1 and LDH2) accounted for 74.2 % of total electrophoretic intensity (from Fig. III.8). In whales, LDH2 and LDH3 had the highest proportions with 35.4 % and 32.8 % of total intensity, respectively. In brain samples of cattle, the highest activity was attributed to LDH1; in brain samples of whale, LDH2 showed the highest intensity. Significant differences between samples of whale and cattle were found for LDH1 ($p=5.6 \times 10^{-7}$), LDH2 ($p=5 \times 10^{-6}$) and LDH3 ($p=3.7 \times 10^{-6}$), respectively. LDH4 ($p=0.041$) and LDH5 ($p=0.352$) showed no significant differences in intensity between whale and cattle.

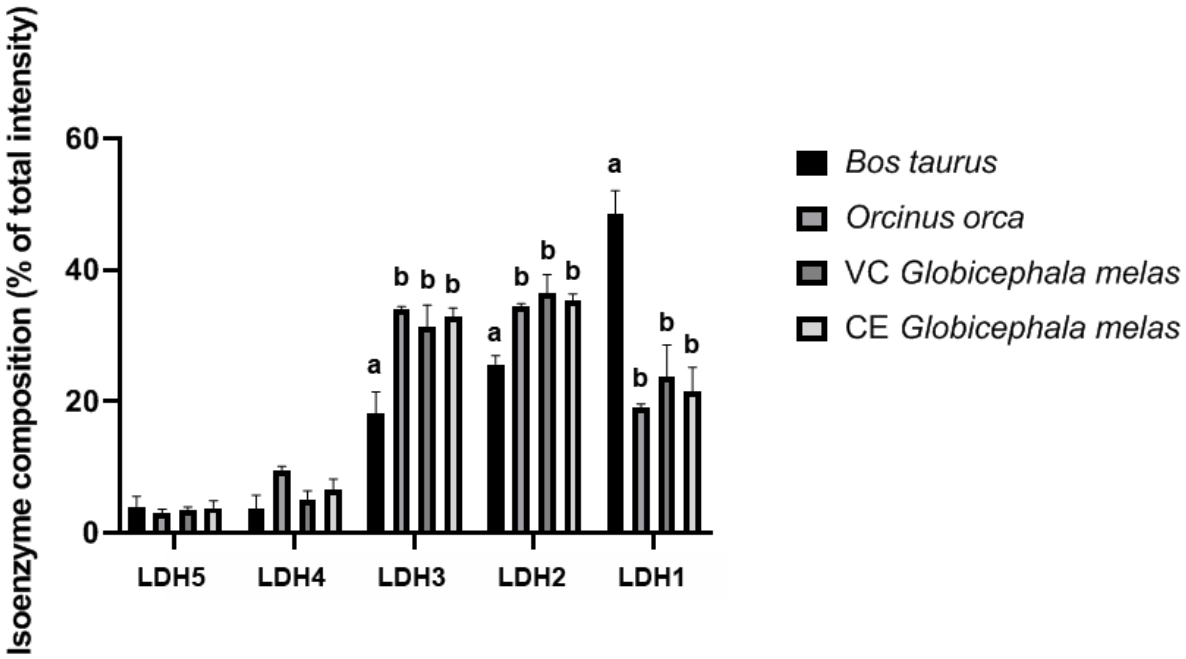

Figure III.9 Lactate dehydrogenase (LDH) isoenzyme composition in brain samples of cattle (N=3), killer whale (N=3) and in cerebellum (N=3) and visual cortex samples (N=3) of long-finned pilot whale. Bars indicate means of biological replicates and/or technical replicates (cerebellum and visual cortex of long finned pilot whale: 3 biological replicates, killer whale: 3 technical replicates; cattle: 2 biological replicates, 1 technical replicate) and are expressed as percentages (%) of the total electrophoretic intensity (from Fig. III.8) of a given sample. Standard deviations are shown by error bars. Statistical significance was indicated by one-way ANOVA and Dunnet's multiple comparison test and significant differences ($p<0.05$) in the relative content of the given isoenzyme between species are indicated by different letters.

Discussion

The brain is one of the most sensitive organs in mammals and is typically highly vulnerable to hypoxia. Without constant oxygen supply, the aerobic energy production via oxidative phosphorylation is impaired. However, diving mammals survive low oxygen conditions when submerged, apparently without fatal damage to nerve cells (Qvist et al. 1986). A higher anaerobic capacity in the whale brain could pose a benefit in maintained ATP production under hypoxic conditions. Hoff et al. (2016) found no evidence for an enhanced anaerobic capacity in the brain of the hooded seal, when compared to the ferret (*Mustela putorius furo*). Instead, they found an atypical distribution of LDH isoenzymes, with LDHB being more strongly expressed in astrocytes than in neurons. This observation supports the hypothesis of a shift in the aerobic energy metabolism from neurons to astrocytes in seals that has been launched previously (Mitz et al. 2009; Schneuer et al. 2012). The expression of other proteins that are linked to aerobic metabolism (e.g., neuroglobin, cytochrome) does not suggest a similar shift in the whale brain

(Schneuer et al. 2012). On this basis, we hypothesized that cetaceans may have a divergent strategy enhancing the aerobic capacity, to improve efficiency of O_2 usage in mitochondria. To test this hypothesis, we analyzed the sequence composition, RNA expression, genomic copy number, substrate affinity and isoenzyme composition of lactate dehydrogenase (LDH), a key enzyme in anaerobic glycolysis, in various species of whales and compared it with cattle, being a non-diving relative of whales.

Whales have no genomic gene expansion and no enhanced cerebral mRNA levels of LDH

A high anaerobic capacity might help the brain to survive hypoxic periods (Kerem et al. 1973a). However, we found no differences in the expression of *Ldha* and *Ldhb* in the brains of cattle and whale (Fig. III.1, III. 2). Similar results were found comparing brain samples of the hooded seal with a terrestrial relative, the ferret (Hoff et al. 2016), indicating convergent strategies in seals and whales. Since skeletal muscles of marine mammals shift to anaerobic metabolism during long dives producing large amounts of lactate (e.g., Blix 2018; Scholander 1940), Yim et al. (2014) suggested an expansion of the LDHA gene in whales to cope with high lactate concentrations after long dives. Although gene duplications do not necessarily double the expression, it mostly leads to increased protein levels (Schuster-Böckler et al. 2010; Stranger et al. 2007; Zhou et al. 2011). Gene expansion as an adaptation to environmental stress is widely known (Magadum et al. 2013). For example, in the Atlantic cod, gene duplications of anti-freezing genes together with the upregulation of these genes play a significant role in the cold adaptation (Chen et al. 1997; Chen et al. 2008). In our study, we analyzed the genomic copy numbers of LDHA and LDHB and found two copies of each gene in the cattle genome, while the killer whale and the bottlenose dolphin genome contain only one copy of each gene (Fig. III.3). The possible role of the LDHA/ LDHB gene duplication in cattle is unknown but the duplication event seems to be evolutionary old, near the origin of vertebrates and in the early mammalian history (Li et al. 2002). However, the single gene copy in whales may facilitate the transcriptional regulation of LDH to match fluctuating metabolic demands. The only hint we found for an adaptation to periodically elevated levels of lactate in the whale brain was the higher activity of lactate dehydrogenase using high levels of lactate as substrate (Fig III.7a). While our findings do not suggest an elevated anaerobic capacity in the whale brain, a periodic reliance on anaerobic metabolism is possible. The samples tested in this study originate from non-diving whales and do not reflect the condition of the brain metabolism during the dive. For seals, it has been proposed that during long dives, cerebral oxygen demand may be reduced via regional hypometabolism, while other regions remain active and may have to partially resort to anaerobic ATP production (Ramirez et al. 2007). While brain slices of both diving ducks (eider ducks (*Somateria mollissima*); Ludvigsen et al. 2009) and hooded seals (Larson et al. 2014) have been demonstrated to have a high tolerance towards hypoxia, no similar data are available for the cetacean brain.

The whale-specific amino acid substitution may influence tetramer forming, stability and kinetics

Tian et al. (2016) found a whale-specific amino acid substitution in the protein sequence of LDHA, with glutamine replacing the glutamate that is typical of terrestrial mammals. We confirmed this observation also in the long-finned pilot whale. The substituted amino acid is located at the solvent-exposed protein surface, comprises the substrate-binding site (Read et al. 2001) (Fig. III.5) and reduces the negative charge of the protein surface. In each chain of LDHB there are over hundred residues with inter-chain contact, with one of these residues exhibiting a whale-specific amino acid substitution (Fig. III.6). One residue (Asn30Ser) is highly conserved in all whale species under investigation. The substitution in whales may lead to a weakening of the bonds between subunits and therefore allow a more flexible adjustment of changing isoenzyme patterns. Single amino acid substitutions may enhance the function and efficiency of proteins. For example, one mutation from glutamine 102 to arginine in the lactate dehydrogenase of *Bacillus stearothermophillus* converts the protein into a malate dehydrogenase (Wilks et al. 1988). Further research is needed to decipher the physiological consequences of amino acid substitutions in LDHA and LDHB in cetaceans, but it is possible that the unique amino acid sequence of whale LDHB represents an adaptation to hypoxia in their brain.

The whale brain LDH isoenzyme pattern is conserved in marine mammals

The two distinct subunits of lactate dehydrogenase LDHA and LDHB combine to form five isoenzymes: LDH1 ($LDHB_4$), LDH2 ($LDHB_3$ $LDHA_1$), LDH3 ($LDHB_2$ $LDHA_2$), LDH4 ($LDHA_3$ $LDHB_1$) and LDH5 ($LDHA_4$) (Markert et al. 1962). The relative distribution of these isoenzymes is tissue-specific (Cahn et al. 1962; Plagemann et al. 1960). LDH5 is found predominantly in glycolytic tissue, like skeletal muscle, while LDH1 is enriched in oxidative tissues like the heart (Cahn et al. 1962; Markert et al. 1975). When examining the LDH isoenzyme distribution in the brain of whale and cattle, significant differences were found in the representation of LDH1, LDH2 and LDH3 (Fig. III.9). The highest proportion in the cattle brain was found for LDH1, with 48.5 %, while in whale LDH2 and LDH3 were the most abundant, with 35.4 and 32.8 %, respectively. LDH1 and LDH2 have a high affinity for lactate and are inhibited by high levels of pyruvate to a greater extent than LDH4 and LDH5 (Dawson et al. 1964; Kopperschläger et al. 1996). Several studies found a cell-specific pattern of LDH isoenzymes in vertebrate brains (Bittar et al. 1996; Laughton et al. 2000; Tholey et al. 1981). Although all five isoforms are present in all brain cells, LDH1 is the predominant form in neurons, while LDH5 is more abundant in glia (Bagley et al. 1989; Bittar et al. 1996; Laughton et al. 2000). Fin whales (*Balanoptera physalus*) and minke whales exhibit a glia/neuron index (proportion) of 3.59 to 7.7 (Eriksen et al. 2007; Hawkins et al. 1957), which is significantly higher than an index of 1.22 in cattle (Herculano-Houzel 2014). The higher proportion of glia cells in baleen whales could explain lower levels of LDH1. However, the glia/neuron index has also been examined in the visual cortex of the bottlenose dolphin, in which ratios between 1.6 and 3 were found (Garey et al. 1986). The species examined in this study are closely related to the bottlenose dolphin, suggesting a similar glia/neuron ratio. Transcriptomic analysis of the glia marker “glial fibrillary

acidic protein" (GFAP) and the neuronal marker "RNA Binding Fox-1 Homolog 3" (RBFOX3) revealed an even higher glia/neuron ration in cattle than in whale (mean of 5.6 in different species of whale and 21.5 in cattle) (see Additional file III.4). Therefore, the high proportion of LDH2 in the odontocete brain cannot be explained in terms of a higher ration of glial cells.
No significant difference in the activity level of LDH5, which was the isoenzyme with the lowest activity in all species, was found between the whale and the cattle brain. LDH2, LDH3 and LDH4 were elevated in cetaceans compared to cattle. These findings are consistent with earlier studies in diving mammals. In brain samples of the hooded seal, as well as in beavers, LDH2 was also more abundant when compared to terrestrial mammals (Blix et al. 1971; Hoff et al. 2016). The high levels of the hybrid isoenzymes consisting of both subunits of LDHA and LDHB may suggest a biochemical adaptation to diving. It can be proposed that the cetacean brain has a high capacity for lactate oxidation since the LDH1 and LDH2 isoenzymes showed a higher activity than did LDH4 and LDH5 (Fig. III.9). However, a rapid switch between lactate oxidation and anaerobic glycolysis is enabled by enhanced levels of LDH2 and LDH3. Moreover, adjustable switching between different mechanisms of energy production in the whale brain may help to manage lactate concentrations. An earlier study found a high proportion of LDH2, LDH3 and LDH4 in sperm whale brain, in which LDH3 was the most abundant isoenzyme, while in humpback whale, sei whale and fin whale LDH1 showed the highest proportion of total activity (Shoubridge et al. 1976). However, sei whales, fin whales and humpback whales typically perform relatively short dives, between 14 and 20 minutes (Goldbogen et al. 2008; Lockyer et al. 1986), while the maximum recorded dive duration for sperm whale was 73 minutes (Watkins et al. 1993). The species used in the present study, killer whales and long-finned pilot whales, conduct mostly short time dives (Heide-Jørgensen et al. 2002; Miller et al. 2010). However, given their hunting strategies, often characterized by intense swimming (de Soto et al. 2008), these whales are still likely to experience severe hypoxemia, at the same time as they must maintain high cognitive functionality (Baird 2000; Gannon et al. 1997). It is therefore not unlikely that the odontocete brain may have higher levels of hybrid isoenzymes, to enable rapid switch between energy production pathways. All samples in this study have been taken within a relatively short time after the death of the animal. The longest time between death and sampling was approximately 12 h for the killer whale. However, no significant differences were found in the isoenzyme composition between the brain of the killer whale and the brain of the long-finned pilot whales, which were sampled within 4 hours after death. Therefore, significant differences between whale brain and cattle brain are most likely not caused by a varying degree of degradation of the isoenzymes. The physiological role of LDH isoenzymes has been debated lately. Under steady-state conditions the total LDH activity, rather than isoenzyme patterns, influences the tissue lactate concentration (Downer et al. 2006). However, in case of a burst of anaerobic metabolism, the lactate concentration is affected by the isoenzyme distribution (Quistorff et al. 2011). Hypoxic conditions during dives could trigger such a burst of anaerobic metabolism and the distinct isoenzyme distribution of cetaceans, as also observed in pinnipeds and other diving mammals, may well be important in maintaining adequate ATP production in the diving brain (Blix et al. 1971; Hoff et al. 2016; Messelt et al. 1976; Shoubridge et al. 1976).

Conclusions

In the present study we examined the *Ldha* and *Ldhb* expression, LDH activity, the genomic copy number and LDH isoenzyme distribution in whale brain, compared to a terrestrial relative, the cattle. We further investigated the LDHA and LDHB protein sequences and the protein structures of whale LDHA and LDHB. The LDHA and LDHB proteins are fairly similar in diving and non-diving mammals. Whales exhibit one specific amino acid substitution in LDHA and one in LDHB, which are located at the c-terminal tail comprising the substrate-binding site. The substitution in the sequence of LDHA is exposed to the solvent, while the substitution in LDHB has contact to other subunits. These substitutions may alter the stability and kinetics of the LDH tetramer and facilitate the switch between energy production pathways. The isoenzyme pattern in the whale brain is similar to seals and beavers and suggests a convergent evolution of LDH in the adaptation to diving, with an adjustable switching of the energy production between oxidative phosphorylation and anaerobic glycolysis and a high capacity to oxidize high concentrations of lactate to pyruvate. These findings provide essential information needed to understand lactate and energy metabolism in the whale brain.

Availability of data and material

The raw Illumina files of the transcriptomes from the visual cortex of the cattle (SRR8305676) and the killer whale (SRR8305677) and the visual cortex (SRR8305674) and the cerebellum (SRR8305675) of long-finned pilot whale are available from the NCBI SRA database under the Bioproject PRJNA506903. Mammalian brain transcriptomes were retrieved from the NCBI SRA database (accession numbers SRX790347, SRX313597, SRX211675, SRX211674, SRX196362, SRX196353 SRX2585929, SRX2585928). All other data is provided in the Supplemental material on the CD attached to this dissertation.

Acknowledgements: We thank Matthias Preuß (University of Hamburg) for preparation of cattle brain samples and Christopher Schnoor for his help with the enzyme activity assays. We would like to thank helpers for collecting, transporting and sampling the orca from Schleswig-Holstein, Germany. This work has been supported by the Deutsche Forschungsgemeinschaft (BU 956/22-1) and by a fellowship to A. K. by the Studienstiftung des deutschen Volkes.

9 Discussion

Marine mammals routinely experience severe hypoxic conditions when submerged (e.g.: Meir et al. 2009; Qvist et al. 1986). Although many physiological adaptations have been reported, the extreme diving capabilities of marine mammals raise the question, how their brain survives long periods without continuous oxygen supply. The molecular mechanisms underlying the hypoxia tolerance of the diving brain are still poorly understood. The brain relies mainly on aerobic energy production via oxidative phosphorylation, which is impaired by hypoxia (e.g. Haddad et al. 1993; Larson et al. 2014). It has been suggested, that the diving brain possesses a high capacity for anaerobic energy production (Larson et al. 2014). However, Fabrizius et al. (2016) found no evidence for a permanently increased anaerobic capacity in the brain of the hooded seal. Instead, anaerobic metabolism is thought to increase only under hypoxic conditions (Hoff et al. 2017). A shift of the aerobic metabolism from neurons to astrocytes might contribute to the neuronal hypoxia tolerance in the brain of deep diving seals, but was not found in whales, indicating divergent strategies in seals and whales (Mitz et al. 2009; Schneuer et al. 2012). Here first insights into the molecular mechanisms of the hypoxia tolerance of the whale brain are provided and are discussed focusing on the aspect of divergent evolution in marine mammals.

9.1 Increased aerobic capacity in the whale brain

The comparison of transcriptomes from whale and cattle brain showed enhanced aerobic capacities in the whale brain (Chapter I). The study thus aimed to identify genes and pathways which show a general higher expression in the whale brain unraveling molecular signatures of hypoxia tolerance. To support a reliable statistical basis all samples of whale and cattle brains available in the NCBI SRA database were included in the analyses. In the resulting experiment two samples of the visual cortex from killer whale and long-finned pilot whale, two samples of the cerebellum from long-finned pilot whale and bowhead whale and one unspecified brain sample from minke whale were compared to three samples of visual cortex and two samples of the frontal lobe of cattle. Analyzing transcripts that were significantly higher expressed in the five samples of whale brain compared to the five samples of cattle brain, revealed an overrepresentation of transcripts involved in oxidative phosphorylation and respiratory electron chain

(Fig. I.4). An even stronger overrepresentation of these biological processes was found in the second approach of this study, when comparing only samples of the visual cortex of whale and cattle (Fig. I.2). The comparison of samples originating from the same brain region was used to minimize differential gene expression caused by varying functions of different brain regions. The overrepresentation of the terms oxidative phosphorylation and respiratory electron chain in both approaches, comparison of samples from different brain regions and comparison of the samples originating from visual cortex only, is a strong indicator for a high aerobic capacity as a global adaptation of the whale brain.

The aerobic energy metabolism of the brain uses glucose and oxygen to match energy demands of the cells. Energy requirements are dependent on the composition of neurons and glia cells, since neurons consume 75 – 80 % of the energy produced in the brain (Hyder et al. 2013). Oxidative metabolism in neurons is even enhanced during neuronal activation (Kasischke et al. 2004). In the process of oxidative phosphorylation, electrons are transferred from NADH and $FADH_2$ to O_2. NADH and $FADH_2$ are produced via glycolysis and tricarboxylic acid cycle and are oxidized in complex I and II of the respiratory electron transport chain, respectively. The electron transport is used to generate a proton gradient across the inner mitochondrial membrane. The proton gradient powers the final complex of oxidative phosphorylation, which is the ATP-synthase. Catalyzed by the movement of protons through the ATP synthase, ADP is phosphorylated to ATP. O_2 is the final electron acceptor in the respiratory electron chain and is fundamental for the process (for review see: Papa et al. 2012).

Aerobic capacity and its enhancement after hypoxia have been studied extensively in skeletal muscle of human athletes. Endurance training in human is known to increase the respiratory capacity by elevating mitochondrial density (Hoppeler et al. 1985). Exercise in hypoxic conditions was shown to promote the biogenesis of mitochondria in muscle leading to an improved performance and to uncouple TCA and respiratory chain to minimize the formation of ROS (Desplanches et al. 2014; Schmutz et al. 2010). An increased aerobic metabolism in hypoxia tolerant animals was found for example in muscles of the bar headed goose (*Anser indicus*) (Scott et al. 2009). This animal migrates over the Himalayas reaching altitudes of up to 9000 m and experiences extremely low O_2 levels (Swan 1970). High proportions of mitochondria in muscle of the bar headed goose were redistributed to the cell membrane suggesting a reduced diffusion distance of blood-borne O_2 and the respiration rate was enhanced as an adaptation to flights in low oxygen conditions (Scott et al. 2009). Also in hypoxia tolerant mammals adapted to high

altitudes, a high density and respiration rate of mitochondria has been found as an adaptation to low oxygen conditions (Li et al. 2001; Sheafor 2003). High-altitude-adapted animals respond to exercise under low oxygen conditions with an increase in respiration and cardiac output (Scott 2011). In contrast, marine mammals are cut off from atmospheric O_2 and have to manage a limited amount of oxygen. No redistribution of mitochondria to the sarcolemma was found in the muscles of seals, probably due to their reduced reliance on oxygenated blood. However, a high density of mitochondria and high activities of oxidative enzymes indicate a high intrinsic aerobic capacity in seal muscle (Kanatous et al. 1999).

While aerobic capacity and the effects of hypoxia on mitochondria are well studied in muscle, the transferability of the results to the brain is not assured. In the brain, mitochondrial biogenesis and an increase in oxidative phosphorylation triggered by impacts like exercise are still debated (Herbst et al. 2015; Steiner et al. 2011). However, the brain of mice was shown to increase mitochondrial biogenesis as a neuroprotective response to transient global hypoxia (Gutsaeva et al. 2008). Mitochondria in the brain of the hibernating thirteen-lined ground squirrel (*Ictidomys tridecemlineatus*) show an enhanced oxidative capacity during hibernation, which is thought to enable a fast and efficient ATP production for arousal (Ballinger et al. 2017). In the comparison of whale and cattle brain transcriptomes, several genes were found in the gene set higher expressed in whale brain, that were related to biosynthetic processes and mitochondrion organization (Fig I.3, I.4) supporting the hypothesis of an elevated mitochondrial density in the whale brain.

Nuclear respiratory factor-1 (NRF-1) is a transcriptional key regulator of mitochondrial biogenesis (Rasbach et al. 2007; Suliman et al. 2003) and RPKM values in whale brain are 3.3 times higher than in cattle (Additional file I.1). The high expression of NFR-1 together with a high oxidative capacity in the whale brain might represent an increased mitochondrial density and respiration rate. An increased capacity for mitochondrial respiration including high amounts of aerobic enzymes could increase the O_2 gradient in the brain tissue, facilitating O_2 diffusion and enhance the cells ability to utilize oxygen.

Additionally, a high expression of several Cytochrome c oxidase (COX) subunits was found in the whale brain (Table I.4). COX is the terminal oxidase of the respiratory electron transport chain and consists of 14 subunits in mammals which are partly encoded in the mitochondrial DNA and partly in the nuclear DNA (Balsa et al. 2012; Timon-Gomez et al. 2018). The nuclear expressed subunit 4 (COX4) which is significantly higher expressed in the whale brain (Table I.4)

has been shown to alter the enzyme efficiency and to be regulated by oxygen availability (Allen et al. 1995; Fukuda et al. 2007). Two isoforms of COX4 are distinguished and are known to be antagonistically regulated depending on oxygen availability. Hypoxia induces the induction of COX4-2 and the reduction of COX4-1 for an optimization of respiratory efficiency (Fukuda et al. 2007). In the whale brain, COX4-2 is 4.3 times higher expressed than in cattle brain (Additional file I.1). The differential expression of COX subunit genes in whale and cattle brain might represent an adaptation of the whale brain to diving via an improved ATP production and an efficient respiration under hypoxia. The strategy of maintaining high respiratory rates might increase the amount of ATP produced per oxygen, which would directly enhance the hypoxia tolerance and it might help to replenish ATP fast and efficiently after hypoxic periods when oxygen supply is restored.

In contrast to the findings in the whale brain, Fabrizius et al. (2016) found a reduced aerobic capacity in the brain transcriptome of the hooded seal, compared to the ferret. A general energy saving strategy was suggested in the seal brain, including reduction of ATP demanding processes like protein translation. In the whale brain, genes related to protein folding and translation were higher expressed than in cattle (Fig. I.2, I.4), indicating divergent strategies between seals and whales. While seals seem to reduce their oxygen consumption in the brain via permanent low brain metabolism, whales maintain a high rate of energy production in the brain.

The comparative approach of whale and cattle brain transcriptomes cannot ultimately define the differences in steady-state metabolism as an adaptation to diving or hypoxia. Whales and cattle separated around 56 million years ago (Thewissen et al. 2007) and exhibit entirely different lifestyles. The domesticated, herbivore cattle oppose the fish, krill or mammal-eating whales with complex social structures and sometimes tremendous body and brain masses. However, to address differences in gene expression caused by encephalization level, domestication, diet and allometric scaling, a correlation of gene expression in the brain of several terrestrial animals, as well as in different species of seals and whales, with brain/body mass was conducted (Fig. 9; Supplemental File I.8). A set of 3746 genes that were expressed in either species was correlated. A correlation according to the evolutionary distance of the species and the sampled brain region, rather than to allometric scaling was found. Therefore, differences in gene expression between whale and cattle brain are unlikely caused by their different brain size, intelligence, diet or allometry and could, in fact, indicate adaptations of the whale brain to diving on the molecular level.

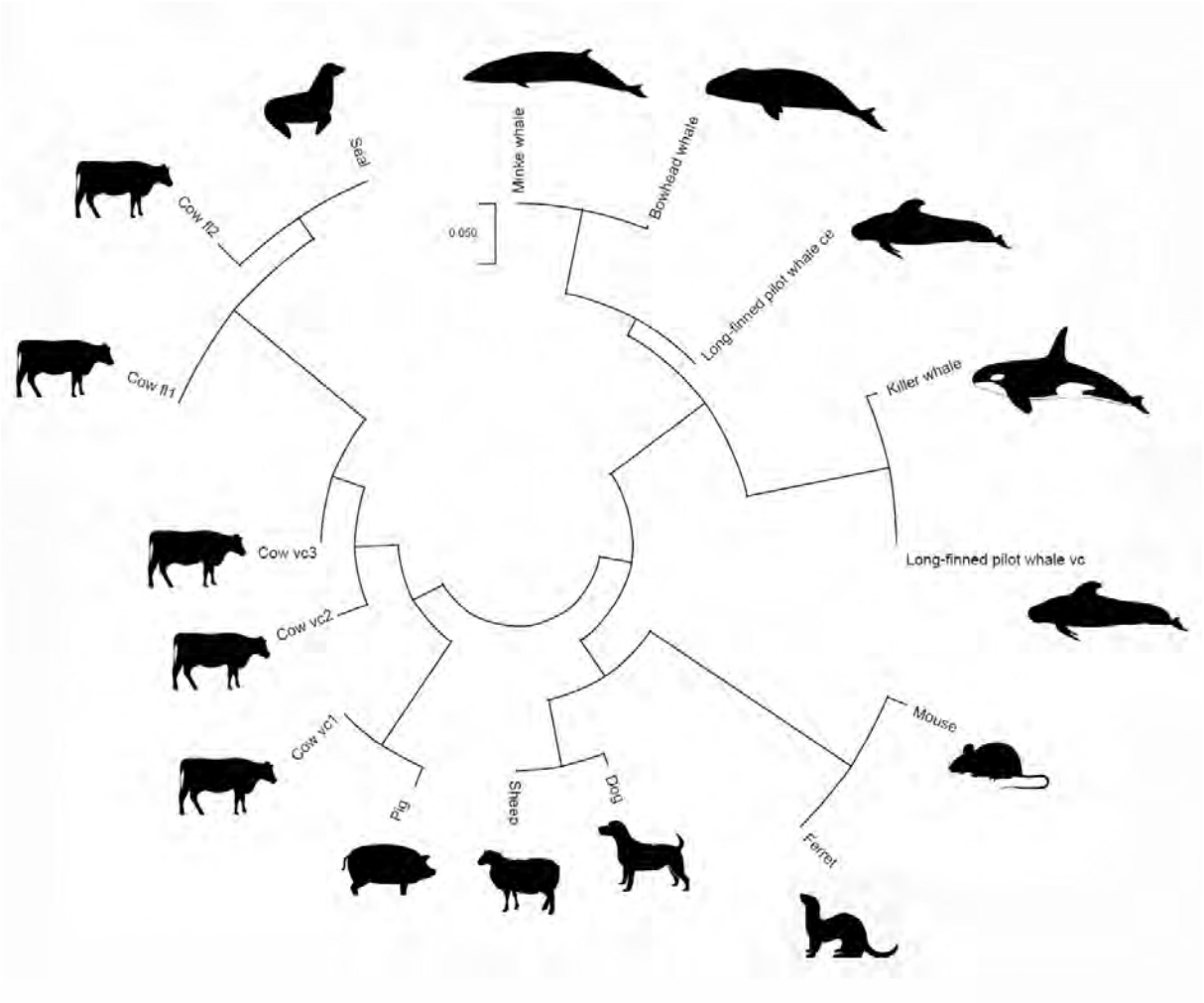

Figure 9 Correlation of gene expression between mammalian brain transcriptomes. The correlation coefficients of 3746 genes expressed in all samples were converted into distances and visualized by a neighbor-joining tree.

9.2 Enhanced antioxidant defense in the whale brain compared to the cattle brain

In the respiratory electron transport chain reactive oxygen species (ROS) are continuously produced as a byproduct (Birben et al. 2012). The amount of ROS and therefore oxidative stress produced by mitochondrial respiration is linked to the metabolic rate and levels are controlled by enzymatic and nonenzymatic antioxidant systems. Periods of hypoxia and reoxygenation events increase the oxidative stress in the brain and especially in neurons (Halliwell et al. 2015; Niizuma et al. 2009; Ramanathan et al. 2005). Due to its increased aerobic capacity and its repeated exposure to hypoxia and reoxygenation, the whale brain requires an efficient antioxidant defense system to avoid cellular damage (Murphy 2009). The generation of ROS is counteracted

by a first line of defense including antioxidant enzymes like superoxide dismutase (SOD), catalase (CAT), glutathione peroxidase (GPX) or thioredoxin (TRX), which convert ROS into less harmful compounds. Under hypoxia or reoxygenation events the ROS production is enhanced and defense mechanisms of SOD, CAT, GPX and TRX are overwhelmed. As a result, lipid, protein and DNA oxidation products emerge in the cell and cause additional damage (Burton et al. 2011). A second line of defense is necessary to avoid degradation of cellular components and cell death and is composed for example of enzymes like glutathione S-transferase (GST) or glutathione peroxidase (GPX). The transcriptomes of the visual cortex of whales indicated a high antioxidant capacity. In the gene set significantly higher expressed in the visual cortex of killer whale and long-finned pilot whale, an enrichment of genes related to detoxification of reactive oxygen species was found (Fig. I.2). A total of 7 antioxidant genes were significantly higher expressed in the visual cortex of whale compared to cattle with RPKM fold changes ranging from 9.1 to 716.3 (Fig. 10; Table I.4).

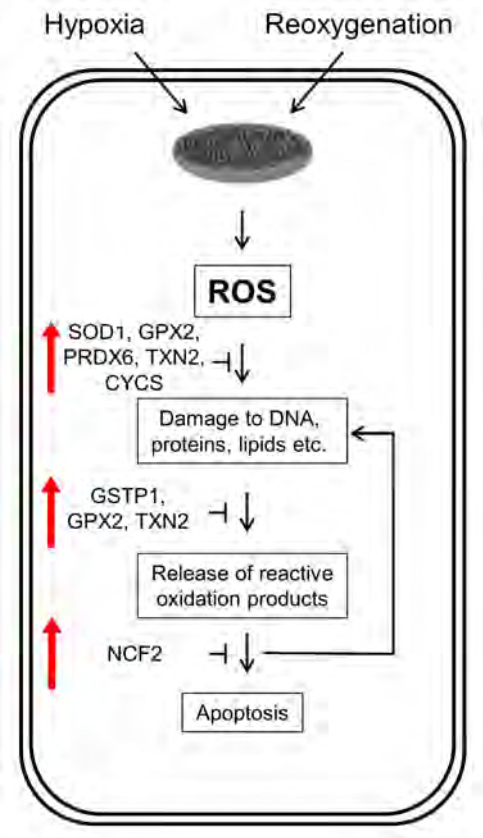

Figure 10 Summary of differentially expressed genes in the antioxidant defence mechanisms in the visual cortex of killer whale and pilot whale compared to the visual cortex of cattle. All genes shown here were significantly higher expressed in the visual cortex of whale and were found in the Reactome pathway "Detoxification of reactive oxygen species" (modified from Hayes et al. 1999).

The highest fold change (FC: 716.3) of antioxidant genes was found for a peroxiredoxin-6 (PRDX6) transcript, a thiol-specific peroxidase, which uses reduced glutathione (GSH) to reduce oxidants like H_2O_2 (Manevich et al. 2005; Park et al. 2016). The PRDX6 protein functions in several physiological roles, including detoxification of oxidants, the repair of peroxidized cell membranes and cellular signaling mediated by ROS (Fisher 2017; Vazquez-Medina et al. 2016). The role of PRDX6 expression levels has been evaluated in numerous studies. A high expression of PRDX6 in cell culture, isolated organs, as well as whole animals has been shown to protect cells against lipid peroxidation, protein peroxidation, membrane damage and apoptosis caused by oxidative stress (Manevich et al. 2002; Manevich et al. 2005; Singh et al. 2016; Walsh et al. 2009; Wang et al. 2004b; Wang et al. 2006;). PRDX6 knockout mice showed increased sensitivity to oxidative injury in several tissues and organs (Lien et al. 2012; Liu et al. 2010; Ozkosem et al. 2016; Wang et al. 2003; Wang et al. 2004). The exact defense mechanisms of PRDX6 against oxidative stress are not yet understood. However, the repair of peroxidized cell membranes is a crucial survival task during oxidative stress, since lipid peroxidation affecting cell membranes leads to cell death and is a major part of the detrimental effects of ROS (Ayala et al. 2014; Cao et al. 2016). The peroxidase activity of PRDX6 to catalyze the reduction of H_2O_2 is activated by homodimerization with glutathione S-transferase P (GSTP1) (Manevich et al. 2004; Manevich et al. 2005), which is also significantly higher expressed in the visual cortex of whale, compared to cattle (FC: 182.8). GSTP1 plays an important role in the cellular protection from oxidative damage, by catalyzing the conjugation of electrophiles to glutathione (Hayes et al. 1999). GSTP1 belongs to the enzymes detoxifying breakdown products of macromolecules like lipid and nucleic-acid hydroperoxides produced during oxidative stress (Berhane et al. 1994; Hayes et al. 1999). For example conjugation of GSH with α,β-unsaturated aldehydes formed during lipid peroxidation is mediated by GSTP1 (Berhane et al. 1994; Chien et al. 1994). Besides its function in detoxification of electrophiles, GSTP1 is involved in redox regulation (Zhang et al. 2018) and modulates stress response cascade via inhibition of JNK signaling (Tew 2007). The JNK pathway is activated by environmental stresses like oxidative stress and promotes cell death (Bogoyevitch et al. 2010; Dhanasekaran et al. 2008; Johnson et al. 2007).

Additionally, Tian et al. (2018) found a positive selection in the GSTP1 gene of whales, supporting its critical role in the detoxification of ROS, caused by hypoxia/reoxygenation events in the diving whale. A high expression of GSTP1 in the whale brain might, therefore, serve a neuroprotective purpose by reducing oxidants and inhibit apoptosis during oxidative stress.

Several genes directly involved in the reduction of oxygen derivates were also significantly higher expressed in the visual cortex of whale compared to cattle, namely superoxide dismutase 1 (SOD1; FC: 429.4), glutathione peroxidase 2 (GPX2; FC: 44.2) and thioredoxin-2 (TXR2; FC: 619). The cytosolic SOD1 is associated with copper/zinc (Cu/Zn) and catalyzes the conversion of superoxide anions ($O_2^{\cdot-}$), which are the primary product in the production of ROS, to hydrogen peroxide (H_2O_2) (Sea et al. 2015). High expression of SOD1 has been associated with an enhanced cerebral hypoxia tolerance in mammals. For example, in transgenic mice, overexpressing SOD1, oxidative stress caused by focal reperfusion following ischemia, neuronal cell death was reduced (Fujimura et al. 2000; Kokubo et al. 2002). Upregulation of SOD1 levels and enzyme activities has been shown to protect the rat brain when oxygen supply is impaired (Loh et al. 2010; Qiao et al. 2012). In whales SOD1 activities have been measured in red blood cells of minke whale, Clymene dolphin (*Stenella clymene*) and La Plata dolphin (*Pontoporia blainvillei*) and were higher than in terrestrial relatives (Wilhelm Filho et al. 2002). The high RPKM values of SOD1 in the whale brain suggest an improved capacity for removal of toxic superoxide anions after oxidative stress. A whale specific amino acid substitution was found in the SOD1 protein, as well as one amino acid substitution present only in whales and the hypoxia tolerant naked-mole rat (Fig.II.2). The substitutions might prevent harmful aggregation of SOD1 when high concentrations are present in the cell.

Overexpressing the SOD1 gene isolated from the killer whale in HN33 neuronal mouse cells, enhanced the survival of the cells under hypoxia and oxidative stress (Fig.II.3, II.4). As expected, overexpression of SOD1 caused a reduced production of ROS in HN33 cells under hypoxia (Fig. II.5). Therefore, a constitutively high expression, which might be even upregulated in case of oxidative stress together with adaptations in the amino acid sequence, might play an important role in the resistance to oxidative stress of the whale brain.

Following the enzymatic reduction via SOD1, H_2O_2 is detoxified by Cat or GPX. GPX2, which showed a 44 times higher RPKM value in the visual cortex of whale than in cattle (Table I.4), might be more relevant for H_2O_2 removal in the whale brain than CAT, which showed only slightly higher RPKM values in whale compared to cattle (FC: 1.6; see Additional file I.1). However, since CAT enzymes have one of the fastest turnover rates (Chelikani et al. 2004; Nicholls et al. 2000), the 1.6 times higher expression in whales might as well be sufficient for an enhanced antioxidant defense.

Expression of GPX2 is tissue specific in mammals with highest levels in the gastrointestinal

tract, where it is thought to play a role in the detoxification of ROS derived from inflammation in the gut (Chu et al. 1993; Chu et al. 2004). A preferential expression of GPX2 was also found in the developing central nervous system (Baek et al. 2011; Brigelius-Flohé et al. 2013). In the brain of rat, GPX2 is upregulated after ischemia (Schmidt-Kastner et al. 2002; Sukhanova et al. 2019) and overexpression of GPX2 protects cells against oxidative stress (Yan et al. 2006). Besides its function in the breakdown of H_2O_2, GPX2 reduces fatty acid hydroperoxides and lipid peroxides and is therefore involved in protection of cell membranes under oxidative stress (Ighodaro et al. 2018).

The detoxification of H_2O_2 is supported by additional enzymatic antioxidants which are higher expressed in the whale brain. Thioredoxin-2 (TRX2) plays an important role in the scavenging of H_2O_2 by supplying reducing equivalents to other antioxidants which reduce ROS (Pérez et al. 2008). It is also involved in the regulation of the mitochondrial membrane potential and through its ability to reduce disulfide bonds, maintains the function of enzymes repairing DNA and proteins (Damdimopoulos et al. 2002; Kudin et al. 2012; Sugano et al. 2013). TXN2 is upregulated in the brain of rodents under hypoxic preconditioning (Gilchrist et al. 2013) and knockdown in mice leads to an increased oxidative stress in the brain (Pérez et al. 2008).

Besides the well-known antioxidant enzymes, two more genes were higher expressed in the visual cortex of whale compared to cattle, neutrophil cytosolic factor 2 (NCF2; FC: 9.1) and cytochrome c (CYCS; FC: 59.9). CYCS is a component of the respiratory electron transport chain and when released into the intermembrane space is well known to oxidize superoxide to O_2 produced by complexes I and III (Korshunov et al. 1999; Skulachev 1998). Additionally, CYCS has been found to activate caspases in response to DNA damage leading to apoptosis (Liu et al. 1996).

No information is available so far about the role of CYCS expression in cerebral hypoxia tolerance. However, the high expression of CYCS in the whale brain might reflect its high oxidative capacity as well as the higher mitochondrial density and detoxify superoxide anions in case of high ROS concentrations.

NCF2 codes for a subunit of nicotinamide adenine dinucleotide phosphate (NADPH) oxidase (NOX) and activates NOX2 (Italiano et al. 2012). Although NOX generates superoxide anions NCF2 is thought to play a role in the protection of cells under oxidative stress. NCF2 is a target for antiapoptotic p53 signaling and a knockdown in human cell lines resulted in increased cell death (He et al. 2013; Italiano et al. 2012). The exact role of a constitutively high expression of

NCF2 remains unknown. However, in the whale brain, it might play a role in redox signaling, improving the antioxidant capacity.

In summary, a high expression of genes involved in a variety of antioxidant mechanisms was observed in the whale brain, which can be interpreted as an improved scavenging of ROS and prevention of damage to macromolecules. Similar observations were made in the hypoxia tolerant naked-mole rat (*Spalax spec.*). Schülke et al. (2012) found constitutively high expression of antioxidant genes like CAT and GPX in the brain of the naked-mole rat and suggested a more effective protection against oxidative insults. In contrast to whales and naked-mole rat, no enhanced antioxidant capacity was found in the brain of the hooded seal. Only one antioxidant gene (paraoxonase 2; PON2) was higher expressed in visual cortex of the hooded seal compared to ferret (Fabrizius et al. 2016). Brain slices of the hooded seal exposed to hypoxia also showed no upregulation of antioxidant defense genes (Hoff et al. 2017), indicating a divergent strategy in seals and whales.

9.3 High expression of COMMD6 might protect the whale brain from hypoxia induced apoptosis

Indicative from the high antioxidant capacity of the whale brain, it is likely that despite the energy saving and oxygen storage adaptations the whale experiences periodical cerebral hypoxia. The cellular response to hypoxia is mediated by a variety of transcription factors (for review see: Bickler et al. 2002). Among these hypoxia responsive transcription factors is nuclear factor-κB (NF-κB) (Cummins et al. 2005; Kenneth et al. 2008). NF-κB is formed by the dimeric assembly of five proteins and the composition of the subunits specify the DNA binding activity (Hoffmann et al. 2003). The different subunits have been shown to mediate opposite physiological effects. For example, while activation of the p50/c-Rel dimer protects neuronal cell from injury (Pizzi et al. 2005; Valerio et al. 2009), activation of p50/RelA dimers induces apoptotic signaling (Pizzi et al. 2002; Sarnico et al. 2009). It has been shown, that cerebral ischemia activates NF-κB and promotes cell death (Schneider et al. 1999; Crack et al. 2006). Knockdown of RelA in mice significantly reduced neuronal cell death (Sarnico et al. 2009).

When comparing differentially expressed transcripts in the transcriptomes of whale and cattle brain, COMM domain containing 6 (COMMD6) was found among the transcripts with the highest fold difference (RPKM fold difference: 1638) (Additional File I.1; Additional file II.1).

COMMD proteins are a family consisting of 10 members that are characterized by an interface domain enabling protein-protein interactions (Burstein et al. 2005; Maine et al. 2007). COMMD6 has been shown to inhibit NF-κB activation through an association with the RelA subunit of NF-κB (Fig. 11; de Bie et al. 2006).

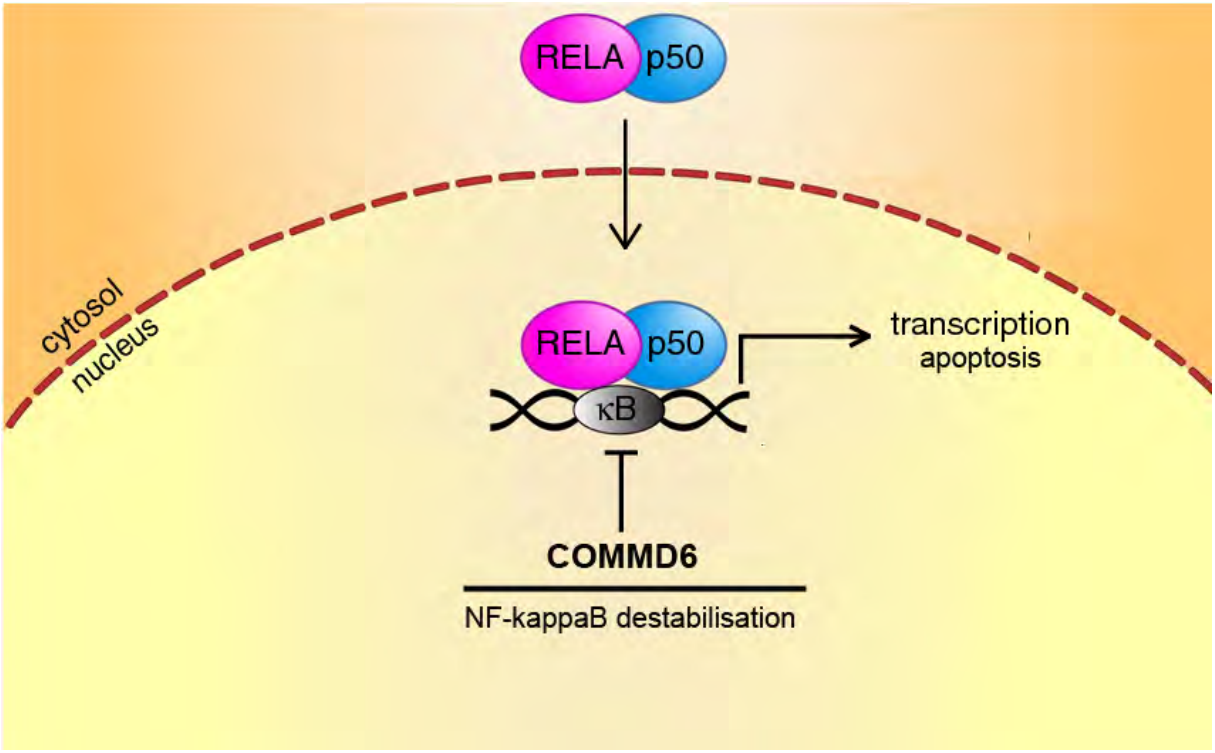

Figure 11 Simpified model of NF-κB down-modulation via COMMD6. After activation, NF-κB dimer, RELA/p50, translocates into the nucleus. COMMD6 inhibits NF-κB induced transcription via association with RelA (modified from Sugawara et al. 2002a).

To examine the effects of high COMMD6 expression as was found in the whale brain, cell culture experiments were conducted. HN33 transfected with the COMMD6 sequence of the killer whale were exposed to 24 h of hypoxia and oxidative stress (Chapter II). Compared to control cells, overexpression of COMMD6 significantly reduced cell death and improved ATP production under hypoxia and oxidative stress (Fig. II.3, II.4). Additionally, overexpression of COMMD6 in HN33 cells reduced the production of ROS under hypoxia, compared to control cells (Fig. II.5). The mechanism behind the reduction of ROS production mediated by COMMD6 is not known. However, COMMD1 which is the best studied COMMD protein, is closely related to COMMD6 and has been shown to play a role in sodium and copper homoeostasis, SOD1 maturation and hypoxia-inducible factor 1α (HIF1α) signaling (Bartuzi et al. 2013). Therefore, a regulatory activity of COMMD6 in the antioxidant defense can be assumed. The exact role of COMMD6

in cells exposed to hypoxia and oxidative stress requires further attention. However, suppression of pro-apoptotic NF-κB activation in neurons mediated by high expression of COMMD6 might represent a neuroprotective mechanism in the whale brain. Derous et al. (2019) recently demonstrated positive selection in several NF-κB genes in whales, which was interpreted as adaptation toward a reduced inflammatory response in adipose tissue expansion, thus a role in the hypoxia adaptation cannot be excluded. The suppression of apoptotic pathways in marine mammals is poorly investigated. However, Fabrizius et al. (2016) found a remarkably high expression of clusterin (CLU) in the brain of the hooded seal. CLU acts as an extracellular chaperone and a truncated protein product has been found to interfere with the BAX-mediated apoptosis pathway (Giannakopoulos et al. 1998; Pucci et al. 2008). Thus, high expression of genes inhibiting apoptotic pathways might be a convergent mechanism in diving mammals.

9.4 Flexible switch between aerobic and anaerobic metabolism might contribute to hypoxia tolerance in the whale brain

Despite the enhanced aerobic capacity of the whale brain, long dives with a high proportion of physical and neurological activity might exhaust the oxygen stores and inhibit oxidative metabolism. Anaerobic metabolism displays a short-term alternative for cellular energy production using intracellular glycogen stores for substrate (for review see: Ames III 2000; Schurr 2002). To examine the anaerobic capacity of the whale brain, several parameters of lactate dehydrogenase (LDH) were compared in the brain of killer whale, long-finned pilot whale, common bottlenose dolphin and cattle. LDH is a key enzyme in the anaerobic metabolism and interconverts pyruvate and lactate (Holbrook et al. 1975). An expansion of the LDHA gene in whales enhancing expression levels as an adaptation to high lactate levels after the dive has been proposed (Yim et al. 2014). However, no genomic duplication of the LDHA gene was found in the genome of killer whale and bottlenose dolphin and expression levels of LDHA and LDHB did not differ in whale and cattle brain, indicating a similar anaerobic capacity (Chapter III). However, similar baseline levels of LDH in whale and cattle brain do not exclude a function in the anaerobic metabolism during the dive. Analyzing the isoenzyme distribution of LDH in whale and cattle, significant differences were found, favoring a flexible switch between aerobic and anaerobic metabolism in the whale brain. The LDH enzyme consists of four subunits of LDHA and LDHB assembled in different combinations. The resulting five distinct tetrameric

LDH isoenzymes are LDH1 ($LDHB_4$), LDH2 ($LDHB_3LDHA_1$), LDH3 ($LDHB_2LDHA_2$), LDH4 ($LDHA_3LDHB_1$), and LDH5 ($LDHA_4$) (Markert 1963). The distribution of LDH isoenzymes in tissues correlates with their catalytic properties (Cahn et al. 1962; Plagemann et al. 1960). LDH1 preferentially catalyzes lactate oxidation and is predominantly found in the highly aerobic cardiac muscle, while LDH5 is found in skeletal muscle tissue with a high anaerobic capacity and preferentially uses pyruvate as substrate (Cahn et al. 1962; Markert et al. 1975). In aerobic tissues of mammals, isoenzymes show a steady decline in their percentage from LDH1 to LDH5 (Heinová et al. 2018). Therefore, the brain of cattle showed the expected LDH isoenzyme pattern with the highest percentage found for LDH1.

The predominant isoenzymes in the whale brain were LDH2 and LDH3 representing together 68.2 % of the total isoenzymes. Surprisingly, the highest percentage was found for LDH2 (35.4 %) (Fig. III.9). A high percentage of hybrid isoenzymes (LDH2, LDH3, LDH4) as found in the whale brain has previously been found in tissues exposed to alternating aerobic and anaerobic conditions (Antonova et al. 2018; de Quiroga et al. 1980). The intermediate isoenzymes are thought to function in both, aerobic and anaerobic conditions and are therefore an indicator for a periodic metabolic switch in the whale brain. The higher percentage of LDH1 compared to LDH5 in all brain samples is representative for the predominance of aerobic metabolism in the brain. However, in contrast to the cattle brain, the whale brain with a high percentage of LDH2 and LDH3 is better equipped to switch to an anaerobic metabolism in periods of hypoxia. A high percentage of LDH2 and a low amount of LDH1 were also found in the visual cortex of seal, indicating a similar strategy in seal and whale brain (Fig. 12; Hoff et al. 2016). In contrast to the whale brain, LDH3 in seal brain showed similar levels to the cattle brain. The high percentage of LDH3 in addition to LDH2 in the whale brain might indicate an even higher capacity for metabolic switching in whale brain under hypoxia than in seal brain.

The native gel electrophoresis showed distinct relative electrophoretic mobilities of LDH isoenzymes in whale and cattle brain (Fig. III.8). Those differences resemble the amino acid substitutions found in the protein sequences of whale LDHA and LDHB. LDH sequences are highly conserved among mammals and killer whale, pilot whale, bottlenose dolphin and cattle share 96 % and 97 % of amino acid residues in LDHA and LDHB, respectively (Additional File III.3). However, substitutions of amino acids change the isoelectric point of the protein, causing different mobility patterns (Hou et al. 2017). While the physiological consequences of the whale specific amino acid substitutions in LDHA and LDHB sequences need further investigation, a

role in the hypoxia adaptation via optimized stability and kinetics facilitating the switch between energy production pathways is entirely possible. For example, Reidarson et al. (1999) suggested an increased stability of whale LDH in changing milieus compared to human LDH. The single genomic copy of LDHA and LDHB in the whale compared to two copies of each in the cattle might display another indicator for the adaptation towards a flexible metabolic switch (Fig. III.3). In evolution, gene duplication plays an important role and is able to create novel gene functions via sub-or neofunctionalization (Ohno 1970). However, conversely, there are also deleterious effects of gene duplication, as evident in several human diseases (Conrad et al. 2007; Makino et al. 2010; Seeger et al. 1985; Singleton et al. 2003). The advantage of the single copy LDH in the whale genome might implicate a facilitated transcriptional regulation adjusted to the actual metabolic demands during aerobic or anaerobic periods. In support of a flexible switch between aerobic and anaerobic metabolism in the whale brain, LDH in the killer whale brain showed a higher activity with high lactate concentrations (Fig. III.7a). This might represent an adaptation to rising lactate concentrations during the dive. The rapid removal of accumulated lactate caused by anaerobic energy metabolism under hypoxic conditions is essential, since elevated lactate levels impair neuronal activity and lead to necrotic cell death (Nabekura et al. 2003; Okada et al. 2009).

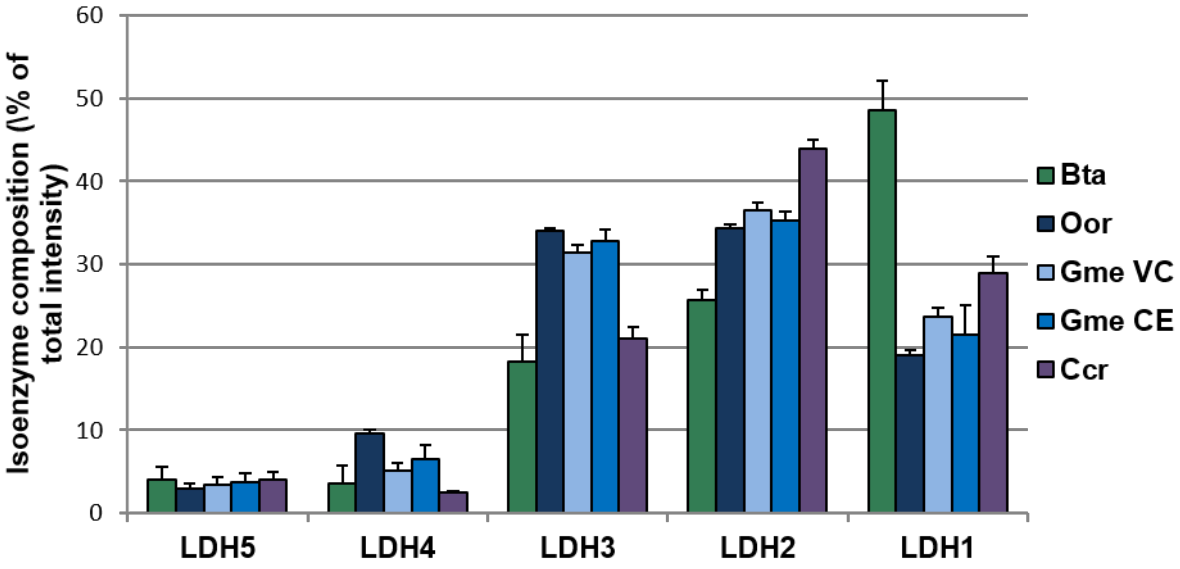

Figure 12 Lactate dehydrogenase (LDH) isoenzyme distribution in brain samples of cattle (Bta), killer whale (Oor), long-finned pilot whale visual cortex (Gme VC) and cerebellum (Gme CE) and hooded seal (Ccr). Data are expressed as means of the percentage (%) of the total activity of each sample. Error bars represent standard deviations (modified from Hoff et al. 2016 and Fig. III.9).

Evidence for an elevated anaerobic metabolism in the brain of a marine mammal under hypoxia was found in transcriptomic analyses of brain slices of the hooded seal exposed to hypoxia. A downregulation of the pyruvate dehydrogenase complex and an upregulation of genes involved in glycolysis was accompanied by the upregulation of the monocarboxylate transporter MCT4 (Hoff et al. 2017). MCT4 is important for lactate release from glycolytic cells and a high expression in the brain has been suggested to display an adaptation to hypoxic conditions (Hong et al. 2015; Rosafio et al. 2014). For example, a knockdown of MCT4 reduced the survival rate of astrocytes-neurons mixed-cultures under hypoxia (Gao et al. 2015) and hypoxia preconditioning of rats resulted in the upregulation of MCT4 in astrocytes (Gao et al. 2014).
In the whale brain MCT4 is 4.6 times higher expressed than in the cattle brain (Additional File I.1). One can speculate that a general high expression of MCT4 in the whale brain might display an adaptation to an enhanced anaerobic metabolism. The upregulation of MCT4 in brain slices of the hooded seal under hypoxic conditions indicates a convergent mechanism in seals and whales during periods without sufficient oxygen supply.

10 Conclusions and perspectives

This study provides insights into the molecular mechanisms of cerebral hypoxia tolerance in whales. In contrast to seals that reduce their brain metabolism for energy saving purposes, whales seem to have improved oxygen usage to maintain neuronal activity. Enhanced aerobic capacity in the whale brain might improve the efficiency of cytochrome oxidase subunits in the respiratory electron transport chain, enhancing ATP production efficiency. Furthermore, the mitochondria of whales might be better prepared for a rapid energy production after the dive, when oxygen supply is restored. The increased production of ROS, resulting from a high aerobic capacity, as well as from hypoxic conditions and reoxygenation events is counteracted by a high expression of several antioxidant enzymes, which act on various levels of the antioxidant defense mechanism. High expression of genes inhibiting apoptotic pathways like COMMD6 might help the whale brain to reduce neuronal cell death during hypoxic periods. Due to the protection status and body size of whales, it is nearly impossible to examine the whale brain during actual diving or in vivo in hypoxic conditions. Therefore, no information is available

about the metabolic changes in the brain during a dive. However, indicators for a flexible switch between aerobic and anaerobic metabolism were found in the whale brain, together with the ability to remove high concentrations of lactate. This might indicate a reliance of the whale brain on anaerobic energy production when oxygen supply is impaired. Similar results in the seal brain might indicate a convergent evolution of the cerebral capacity to switch to anaerobic energy production in hypoxic conditions. Therefore, the evolution of the hypoxia tolerance of the brain of diving mammals is partly divergent, regarding general metabolic processes, while rescue mechanisms in low oxygen conditions might have developed convergent.

In future studies, a possible next step would be to compare brain transcriptomes of shallow-diving whales and deep-diving whales. Master divers, like sperm whales or beaked whales might show even more pronounced adaptations on the molecular level. By comparing shallow-diving with deep-diving whales, gene expression differences resulting from the different encephalization levels, lifestyles, varying diets or differences in body and brain size in cattle and whale could be minimized. Transcriptomes of deep-diving whales might also lead to new candidate genes involved in either improvement of the antioxidant defense or in the suppression of apoptotic signaling. Functional analysis in cell culture improves insights into the function of specific genes in the hypoxia adaptation of the whale.

Comparison with transcriptomes of the only extant relative that is closer to whales than cattle, the hippo, might also provide interesting insights into the evolution of the molecular diving adaptations.

Just recently, the first annotated genome of a whale was published (Fan et al. 2019). A transcriptome analysis using this sperm whale genome as a reference would allow more profound comparisons of whale and cattle transcriptomes. In this study only genes higher expressed in the whale brain were examined, while lower expressed genes were ignored. This was due to the fact, that it is not possible to discriminate between an actual lower expression and sequence differences in whale and cattle that lead to a lower amount of mapping reads in whale transcriptomes when the cattle genome is used as reference. However, lower expressed genes in the whale brain might also provide insights into metabolic adaptations in the whale brain. For example, downregulation of pro-apoptotic genes might protect the whale brain from hypoxia induced cell death and reduced expression of specific transporters such as MCT2 might prevent the influx of harmful molecules into brain cells. So far, only homogenous samples from specific brain regions of whales were analyzed. Since the brain is a heterogeneous tissue with specialized cell types,

gene expression in either only neurons or only astrocytes would allow more exact predictions of the metabolic processes in the whale brain. Using the laser capture technique transcriptomes of whale neurons and astrocytes could be compared to those of the cattle.

Additionally, metabolomic and proteomic analyses of the whale brain compared to terrestrial relatives might improve the understanding of metabolic adaptations to hypoxia that can not be explaied by analysing the transcriptome.

11 References

Acker, T., & Acker, H. (2004). Cellular oxygen sensing need in cns function: Physiological and pathological implications. *J Exp Biol*, *207*(Pt 18), 3171–88.

Allen, K. N., & Vazquez-Medina, J. P. (2019). Natural tolerance to ischemia and hypoxemia in diving mammals: A review. *Front Physiol*, *10*, 1199.

Allen, L. A., Zhao, X. J., Caughey, W., & Poyton, R. O. (1995). Isoforms of yeast cytochrome c oxidase subunit v affect the binuclear reaction center and alter the kinetics of interaction with the isoforms of yeast cytochrome c. *J Biol Chem*, *270*(1), 110–8.

Alsultan, A. A., Waller, R., Heath, P. R., & Kirby, J. (2016). The genetics of amyotrophic lateral sclerosis: Current insights. *Degener Neurol Neuromuscul Dis*, *6*, 49–64.

Amano, M., & Yoshioka, M. (2003). Sperm whale diving behavior monitored using a suction-cup-attached tdr tag. *Mar. Ecol. Prog. Ser.*, *258*, 291–295.

Ames III, A. (2000). Cns energy metabolism as related to function. *Brain Res Brain Res Rev*, *34*(1-2), 42–68.

Andrews, R. D., Jones, D. R., Williams, J. D., Thorson, P. H., Oliver, G. W., Costa, D. P., & Le Boeuf, B. J. (1997). Heart rates of northern elephant seals diving at sea and resting on the beach. *J Exp Biol*, *200*(Pt 15), 2083–95.

Andrisic, L., Dudzik, D., Barbas, C., Milkovic, L., Grune, T., & Zarkovic, N. (2018). Short overview on metabolomics approach to study pathophysiology of oxidative stress in cancer. *Redox Biol*, *14*, 47–58.

Angelova, P. R., Kasymov, V., Christie, I., Sheikhbahaei, S., Turovsky, E., Marina, N., Korsak, A., Zwicker, J., Teschemacher, A. G., Ackland, G. L., Funk, G. D., Kasparov, S., Abramov, A. Y., & Gourine, A. V. (2015). Functional oxygen sensitivity of astrocytes. *J Neurosci*, *35*(29), 10460–73.

Antonini, E. (1965). Interrelationship between structure and function in hemoglobin and myoglobin. *Physiol Rev*, *45*, 123–70.

Antonova, E. P., Ilyukha, V. A., Sergina, S. N., Unzhakov, A. R., & Belkin, V. V. (2018). Lactate dehydrogenase isozymes in the tissues of hibernating bats (chiroptera). *Biophysics*, *63*(1), 116–121.

Avivi, A., Gerlach, F., Joel, A., Reuss, S., Burmester, T., Nevo, E., & Hankeln, T. (2010). Neuroglobin, cytoglobin, and myoglobin contribute to hypoxia adaptation of the subterranean mole rat spalax. *Proc Natl Acad Sci U S A*, *107*(50), 21570–5.

Ayala, A., Munoz, M. F., & Arguelles, S. (2014). Lipid peroxidation: Production, metabolism, and signaling mechanisms of malondialdehyde and 4-hydroxy-2-nonenal. *Oxid Med Cell Longev*, *2014*, 360438.

Baek, I. J., Yon, J. M., Lee, S. R., Kim, M. R., Hong, J. T., Lee, B. J., Yun, Y. W., & Nam, S. Y. (2011). Differential expression of gastrointestinal glutathione peroxidase (gi-gpx) gene during mouse organogenesis. *Anat Histol Embryol*, *40*(3), 210–8.

Bagley, P., Tucker, S., Nolan, C., Lindsay, J., Davies, A., Baldwin, S., Cremer, J., & Cunningham, V. (1989). Anatomical mapping of glucose transporter protein and pyruvate dehydrogenase in rat brain: An immunogold study. *Brain Res*, *499*(2), 214–224.

Baird, R. W. (2000). The killer whale. *Cetacean societies: field studies of dolphins and whales*, 127–153.

Baird, R. W., Borsani, J. F., Hanson, M. B., & Tyack, P. L. (2002). Diving and night-time behavior of long-finned pilot whales in the ligurian sea. *Mar Eco Prog Ser*, *237*, 301–305.

Baird, R. W., Hanson, M. B., & Dill, L. M. (2005). Factors influencing the diving behaviour of fish-eating killer whales: Sex differences and diel and interannual variation in diving rates. *Can J Zool*, *83*(2), 257–267.

Baldwin, J., A. S. (1996). The nf-kappa b and i kappa b proteins: New discoveries and insights. *Annu Rev Immunol*, *14*, 649–83.

Ballarin, C., Povinelli, M., Granato, A., Panin, M., Corain, L., Peruffo, A., & Cozzi, B. (2016). The brain of the domestic bos taurus: Weight, encephalization and cerebellar quotients, and comparison with other domestic and wild cetartiodactyla. *PLoS One*, *11*(4), e0154580.

Ballinger, M. A., Schwartz, C., & Andrews, M. T. (2017). Enhanced oxidative capacity of ground squirrel brain mitochondria during hibernation. *Am J Physiol Regul Integr Comp Physiol*, *312*(3), R301–R310.

Balsa, E., Marco, R., Perales-Clemente, E., Szklarczyk, R., Calvo, E., Landazuri, M. O., & Enriquez, J. A. (2012). Ndufa4 is a subunit of complex iv of the mammalian electron transport chain. *Cell Metab*, *16*(3), 378–86.

Banchero, N., Grover, R. F., & Will, J. A. (1971). Oxygen transport in the llama (lama glama). *Respir Physiol*, *13*(1), 102–15.

Bano, D., & Nicotera, P. (2007). Ca2+ signals and neuronal death in brain ischemia. *Stroke*, *38*(2 Suppl), 674–6.

Bartuzi, P., Hofker, M. H., & van de Sluis, B. (2013). Tuning nf-kappab activity: A touch of commd proteins. *Biochim Biophys Acta*, *1832*(12), 2315–21.

Beckman, K. B., & Ames, B. N. (1997). Oxidative decay of dna. *J Biol Chem*, *272*(32), 19633–6.

Behl, C., Davis, J. B., Lesley, R., & Schubert, D. (1994). Hydrogen peroxide mediates amyloid beta protein toxicity. *Cell*, *77*(6), 817–27.

Bentmann, A., Schmidt, M., Reuss, S., Wolfrum, U., Hankeln, T., & Burmester, T. (2005). Divergent distribution in vascular and avascular mammalian retinae links neuroglobin to cellular respiration. *J Biol Chem*, *280*(21), 20660–5.

Berg, J., J. Tymoczko, & Stryer, L. (2002). Biochemistry, 1050.

Bergmeyer, H.-U., Bernt, E., & Hess, B. (1965). Lactic dehydrogenase. In *Methods of enzymatic analysis* (pp. 736–743). Elsevier.

Berhane, K., Widersten, M., Engstrom, A., Kozarich, J. W., & Mannervik, B. (1994). Detoxication of base propenals and other alpha, beta-unsaturated aldehyde products of radical

reactions and lipid peroxidation by human glutathione transferases. *Proc Natl Acad Sci U S A*, *91*(4), 1480–4.

Bernaudin, M., Tang, Y., Reilly, M., Petit, E., & Sharp, F. R. (2002). Brain genomic response following hypoxia and re-oxygenation in the neonatal rat. identification of genes that might contribute to hypoxia-induced ischemic tolerance. *J Biol Chem*, *277*(42), 39728–38.

Berta, A., Sumich, J. L., & Kovacs, K. M. (2005). *Marine mammals: Evolutionary biology*. Elsevier.

Bi, J., Hu, B., Zheng, J., Wang, J., Xiao, W., & Wang, D. (2015). Characterization of the hypoxia-inducible factor 1 alpha gene in the sperm whale, beluga whale, and yangtze finless porpoise. *Mar Biol*, *162*(6), 1201–1213.

Biasio, W., Chang, T., McIntosh, C. J., & McDonald, F. J. (2004). Identification of murr1 as a regulator of the human delta epithelial sodium channel. *J Biol Chem*, *279*(7), 5429–34.

Bickler, P. E., & Donohoe, P. H. (2002). Adaptive responses of vertebrate neurons to hypoxia. *J Exp Biol*, *205*(Pt 23), 3579–86.

Birben, E., Sahiner, U. M., Sackesen, C., Erzurum, S., & Kalayci, O. (2012). Oxidative stress and antioxidant defense. *World Allergy Organ J*, *5*(1), 9–19.

Bittar, P. G., Charnay, Y., Pellerin, L., Bouras, C., & Magistretti, P. J. (1996). Selective distribution of lactate dehydrogenase isoenzymes in neurons and astrocytes of human brain. *J Cereb Blood Flow Metab*, *16*(6), 1079–1089.

Blank, M. C., Grinberg, I., Aryee, E., Laliberte, C., Chizhikov, V. V., Henkelman, R. M., & Millen, K. J. (2011). Multiple developmental programs are altered by loss of zic1 and zic4 to cause dandy-walker malformation cerebellar pathogenesis. *Development*, *138*(6), 1207–1216.

Blix, A. S. (2018). Adaptations to deep and prolonged diving in phocid seals. *J Exp Biol*, *221*(Pt 12).

Blix, A. S., Elsner, R., & Kjekshus, J. K. (1983). Cardiac output and its distribution through capillaries and a-v shunts in diving seals. *Acta Physiol Scand*, *118*(2), 109–16.

Blix, A. S., & From, S. H. (1971). Lactate dehydrogenase in diving animals–a comparative study with special reference to the eider (somateria mollissima). *Comp Biochem Physiol B*, *40*(3), 579–84.

Blix, A. S., Walloe, L., Messelt, E. B., & Folkow, L. P. (2010). Selective brain cooling and its vascular basis in diving seals. *J Exp Biol*, *213*(Pt 15), 2610–6.

Bogoyevitch, M. A., Ngoei, K. R., Zhao, T. T., Yeap, Y. Y., & Ng, D. C. (2010). C-jun n-terminal kinase (jnk) signaling: Recent advances and challenges. *Biochim Biophys Acta*, *1804*(3), 463–75.

Boveris, A., & Chance, B. (1973). The mitochondrial generation of hydrogen peroxide. general properties and effect of hyperbaric oxygen. *Biochem J*, *134*(3), 707–716.

Brand, M. D. (2010). The sites and topology of mitochondrial superoxide production. *Exp Gerontol*, *45*(7-8), 466–472.

Brigelius-Flohé, R., & Maiorino, M. (2013). Glutathione peroxidases. *Biochim Biophys Acta*, *1830*(5), 3289–303.

Bunton-Stasyshyn, R. K., Saccon, R. A., Fratta, P., & Fisher, E. M. (2015). Sod1 function and its implications for amyotrophic lateral sclerosis pathology: New and renascent themes. *Neuroscientist*, *21*(5), 519–29.

Burmester, T., & Hankeln, T. (2014). Function and evolution of vertebrate globins. *Acta physiol*, *211*, 501–14.

Burmester, T., Weich, B., Reinhardt, S., & Hankeln, T. (2000). A vertebrate globin expressed in the brain. *Nature*, *407*(6803), 520–3.

Burns, J. M., Lestyk, K. C., Folkow, L. P., Hammill, M. O., & Blix, A. S. (2007). Size and distribution of oxygen stores in harp and hooded seals from birth to maturity. *J Comp Physiol B*, *177*(6), 687–700.

Burstein, E., Ganesh, L., Dick, R. D., van De Sluis, B., Wilkinson, J. C., Klomp, L. W., Wijmenga, C., Brewer, G. J., Nabel, G. J., & Duckett, C. S. (2004). A novel role for xiap in copper homeostasis through regulation of murr1. *EMBO J*, *23*(1), 244–54.

Burstein, E., Hoberg, J. E., Wilkinson, A. S., Rumble, J. M., Csomos, R. A., Komarck, C. M., Maine, G. N., Wilkinson, J. C., Mayo, M. W., & Duckett, C. S. (2005). Commd proteins, a novel family of structural and functional homologs of murr1. *J Biol Chem*, *280*(23), 22222–32.

Burton, G. J., & Jauniaux, E. (2011). Oxidative stress. *Best pract res cl ob*, *25*(3), 287–299.

Burton, G. W., & Traber, M. G. (1990). Vitamin e: Antioxidant activity, biokinetics, and bioavailability. *Annu Rev Nutr*, *10*(1), 357–382.

Butler, P. J. (2004). Metabolic regulation in diving birds and mammals. *Resp Physiol Neurobi*, *141*(3), 297–315.

Butler, P. J. (2006). Aerobic dive limit. what is it and is it always used appropriately? *Comp Biochem Physiol, Part A Mol Integr Physiol*, *145*, 1–6.

Butler, P. J., & Jones, D. R. (1997). Physiology of diving of birds and mammals. *Physiol Rev*, *77*(3), 837–898.

Butti, C., Sherwood, C. C., Hakeem, A. Y., Allman, J. M., & Hof, P. R. (2009). Total number and volume of von economo neurons in the cerebral cortex of cetaceans. *J Comp Neurol*, *515*(2), 243–59.

Cahn, R. D., Zwilling, E., Kaplan, N. O., & Levine, L. (1962). Nature and development of lactic dehydrogenases: The two major types of this enzyme form molecular hybrids which change in makeup during development. *Science*, *136*(3520), 962–9.

Cai, Z., Wang, L., Song, X., Tagore, S., Li, X., Wang, H., Chen, J., Li, K., Frenkel, Z., Gao, D., Frenkel-Morgenstern, M., Zhang, T., & Nevo, E. (2018). Adaptive transcriptome profiling of subterranean zokor, myospalax baileyi, to high- altitude stresses in tibet. *Sci Rep*, *8*(1), 4671.

Camandola, S., & Mattson, M. P. (2017). Brain metabolism in health, aging, and neurodegeneration. *EMBO J*, *36*(11), 1474–1492.

Cantú-Medellín, N., Byrd, B., Hohn, A., Vázquez-Medina, J. P., & Zenteno-Savín, T. (2011). Differential antioxidant protection in tissues from marine mammals with distinct diving capacities. shallow/short vs. deep/long divers. *C Comp Biochem Physiol A Mol Integr Physiol*, *158*(4), 438–443.

Cao, J. Y., & Dixon, S. J. (2016). Mechanisms of ferroptosis. *Cell Mol Life Sci*, *73*(11-12), 2195–209.

Castellini, M. A., Somero, G. N., & Kooyman, G. L. (1981). Glycolytic enzyme activities in tissues of marine and terrestrial mammals. *Physiol Zool*, *54*, 242–252.

Chan, P. H. (1996). Role of oxidants in ischemic brain damage. *Stroke*, *27*(6), 1124–9.

Chan, P. H., Epstein, C. J., Kinouchi, H., Kamii, H., Chen, S. F., Carlson, E., Gafni, J., Yang, G., & Reola, L. (1996). Neuroprotective role of cuzn-superoxide dismutase in ischemic brain damage. *Adv Neurol*, *71*, 271–280.

Chan, P. H., Kawase, M., Murakami, K., Chen, S. F., Li, Y., Calagui, B., Reola, L., Carlson, E., & Epstein, C. J. (1998). Overexpression of sod1 in transgenic rats protects vulnerable neurons against ischemic damage after global cerebral ischemia and reperfusion. *J Neurosci*, *18*(20), 8292–9.

Chelikani, P., Fita, I., & Loewen, P. C. (2004). Diversity of structures and properties among catalases. *Cell Mol Life Sci*, *61*(2), 192–208.

Chen, L., DeVries, A. L., & Cheng, C.-H. C. (1997). Evolution of antifreeze glycoprotein gene from a trypsinogen gene in antarctic notothenioid fish. *Proc Natl Acad Sci U S A*, *94*(8), 3811–3816.

Chen, Y., & Swanson, R. A. (2003). Astrocytes and brain injury. *J Cereb Blood Flow Metab*, *23*(2), 137–49.

Chen, Z., Cheng, C.-H. C., Zhang, J., Cao, L., Chen, L., Zhou, L., Jin, Y., Ye, H., Deng, C., Dai, Z., Et al. (2008). Transcriptomic and genomic evolution under constant cold in antarctic notothenioid fish. *Proc Natl Acad Sci U S A*, *105*(35), 12944–12949.

Cherubini, A., Ruggiero, C., Polidori, M. C., & Mecocci, P. (2005). Potential markers of oxidative stress in stroke. *Free Radic Biol Med*, *39*(7), 841–52.

Chien, C. I., Kirollos, K. S., Linderman, R. J., & Dauterman, W. C. (1994). Alpha,beta-unsaturated carbonyl compounds: Inhibition of rat liver glutathione s-transferase isozymes and chemical reaction with reduced glutathione. *Biochim Biophys Acta*, *1204*(2), 175–80.

Chikina, M., Robinson, J. D., & Clark, N. L. (2016). Hundreds of genes experienced convergent shifts in selective pressure in marine mammals. *Mol Biol Evol*, *33*(9), 2182–2192.

Choi, D. W., & Rothman, S. M. (1990). The role of glutamate neurotoxicity in hypoxic-ischemic neuronal death. *Annu Rev Neurosci*, *13*(1), 171–182.

Chu, F. F., Doroshow, J. H., & Esworthy, R. S. (1993). Expression, characterization, and tissue distribution of a new cellular selenium-dependent glutathione peroxidase, gshpx-gi. *J Biol Chem*, *268*(4), 2571–6.

Chu, F. F., Esworthy, R. S., & Doroshow, J. H. (2004). Role of se-dependent glutathione peroxidases in gastrointestinal inflammation and cancer. *Free Radic Biol Med*, *36*(12), 1481–95.

Clemens, J. A., Stephenson, D. T., Dixon, E. P., Smalstig, E. B., Mincy, R. E., Rash, K. S., & Little, S. P. (1997a). Global cerebral ischemia activates nuclear factor-kappa b prior to evidence of dna fragmentation. *Brain Res Mol Brain Res*, *48*(2), 187–96.

Clemens, J. A., Stephenson, D. T., Smalstig, E. B., Dixon, E. P., & Little, S. P. (1997b). Global ischemia activates nuclear factor-kappa b in forebrain neurons of rats. *Stroke*, *28*(5), 1073–80, discussion 1080–1.

Conrad, B., & Antonarakis, S. E. (2007). Gene duplication: A drive for phenotypic diversity and cause of human disease. *Annu Rev Genomics Hum Genet*, *8*, 17–35.

Cox-Limpens, K. E., Gavilanes, A. W., Zimmermann, L. J., & Vles, J. S. (2014). Endogenous brain protection: What the cerebral transcriptome teaches us. *Brain Res*, *1564*, 85–100.

Crack, P. J., Taylor, J. M., Ali, U., Mansell, A., & Hertzog, P. J. (2006). Potential contribution of nf-kappab in neuronal cell death in the glutathione peroxidase-1 knockout mouse in response to ischemia-reperfusion injury. *Stroke*, *37*(6), 1533–8.

Cummins, E. P., & Taylor, C. T. (2005). Hypoxia-responsive transcription factors. *Pflugers Arch*, *450*(6), 363–71.

Czech-Damal, N. U., Geiseler, S. J., Hoff, M. L. M., Schliep, R., Ramirez, J.-M., Folkow, L. P., & Burmester, T. (2014). The role of glycogen, glucose and lactate in neuronal activity during hypoxia in the hooded seal (cystophora cristata) brain. *Neuroscience*, *275*, 374–83.

Damdimopoulos, A. E., Miranda-Vizuete, A., Pelto-Huikko, M., Gustafsson, J. A., & Spyrou, G. (2002). Human mitochondrial thioredoxin. involvement in mitochondrial membrane potential and cell death. *J Biol Chem*, *277*(36), 33249–57.

Dangoumau, A., Marouillat, S., Burlaud Gaillard, J., Uzbekov, R., Veyrat-Durebex, C., Blasco, H., Arnoult, C., Corcia, P., Andres, C. R., & Vourc'h, P. (2016). Inhibition of pathogenic mutant sod1 aggregation in cultured motor neuronal cells by prevention of its sumoylation on lysine 75. *Neurodegener Dis*, *16*(3-4), 161–71.

Dasmeh, P., Serohijos, A. W., Kepp, K. P., & Shakhnovich, E. I. (2013). Positively selected sites in cetacean myoglobins contribute to protein stability. *PLoS Comput Biol*, *9*(3), e1002929.

Davis, R. W. (1983). Lactate and glucose metabolism in the resting and diving harbor seal (phoca vitulina). *J Comp Physiol B*, *153*(2), 275–288.

Dawson, D. M., Goodfriend, T. L., & Kaplan, N. O. (1964). Lactic dehydrogenases: Functions of the two types. *Science*, *143*(3609), 929–933.

de Bie, P., van de Sluis, B., Burstein, E., Duran, K. J., Berger, R., Duckett, C. S., Wijmenga, C., & Klomp, L. W. (2006). Characterization of commd protein-protein interactions in nf-kappab signalling. *Biochem J*, *398*(1), 63–71.

de Bie, P., van de Sluis, B., Burstein, E., van de Berghe, P. V., Muller, P., Berger, R., Gitlin, J. D., Wijmenga, C., & Klomp, L. W. (2007). Distinct wilson's disease mutations in atp7b are associated with enhanced binding to commd1 and reduced stability of atp7b. *Gastroenterology*, *133*(4), 1316–26.

de Jonge, H. J., Fehrmann, R. S., de Bont, E. S., Hofstra, R. M., Gerbens, F., Kamps, W. A., de Vries, E. G., van der Zee, A. G., te Meerman, G. J., & ter Elst, A. (2007). Evidence based selection of housekeeping genes. *PLoS One*, *2*(9), e898.

de Quiroga, C. B., Alonso, M., & Fraile, A. (1980). Lactate dehydrogenase adaptation to variations of oxygen tension in discoglossus pictus larvae. In *Animals and environmental fitness* (pp. 69–70). Elsevier.

de Soto, N. A., Johnson, M. P., Madsen, P. T., Diaz, F., Dominguez, I., Brito, A., & Tyack, P. (2008). Cheetahs of the deep sea: Deep foraging sprints in short-finned pilot whales off tenerife (canary islands). *J Anim Ecol*, *77*(5), 936–947.

de Stephanis, R., García-Tíscar, S., Verborgh, P., Esteban-Pavo, R., Pérez, S., Minvielle-Sébastia, L., & Guinet, C. (2008). Diet of the social groups of long-finned pilot whales (globicephala melas) in the strait of gibraltar. *Mar Biol*, *154*(4), 603–612.

de Zwart, L. L., Meerman, J. H., Commandeur, J. N., & Vermeulen, N. P. (1999). Biomarkers of free radical damage applications in experimental animals and in humans. *Free Radic Biol Med*, *26*(1-2), 202–26.

Delfour, F., & Marten, K. (2001). Mirror image processing in three marine mammal species: Killer whales (orcinus orca), false killer whales (pseudorca crassidens) and california sea lions (zalophus californianus). *Behav Processes*, *53*(3), 181–190.

Derous, D., Sahu, J., Douglas, A., Lusseau, D., & Wenzel, M. (2019). Adaptations of energy metabolism in cetaceans have consequences for their response to foraging disruption. *bioRxiv*, 709154.

Desai, B. S., Chadha, A., & Cook, B. (2014). The stum gene is essential for mechanical sensing in proprioceptive neurons. *Science*, *343*(6176), 1256–1259.

Desplanches, D., Amami, M., Dupre-Aucouturier, S., Valdivieso, P., Schmutz, S., Mueller, M., Hoppeler, H., Kreis, R., & Fluck, M. (2014). Hypoxia refines plasticity of mitochondrial respiration to repeated muscle work. *Eur J Appl Physiol*, *114*(2), 405–17.

Desportes, G., Saboureau, M., & Lacroix, A. (1993). Reproductive maturity and seasonality of male long-finned pilot whales, off the faroe islands. *Biology of northern hemisphere pilot whales, Special*, (14), 233–262.

Devasagayam, T. P., Tilak, J. C., Boloor, K. K., Sane, K. S., Ghaskadbi, S. S., & Lele, R. D. (2004). Free radicals and antioxidants in human health: Current status and future prospects. *J Assoc Physicians India*, *52*, 794–804.

Dhanasekaran, D. N., & Reddy, E. P. (2008). Jnk signaling in apoptosis. *Oncogene*, *27*(48), 6245–51.

Ding, Z., Tong, W. C., Lu, X. X., & Peng, H. P. (2014). Hyperbaric oxygen therapy in acute ischemic stroke: A review. *Interv Neurol*, *2*(4), 201–211.

Dirnagl, U., Iadecola, C., & Moskowitz, M. A. (1999). Pathobiology of ischaemic stroke: An integrated view. *Trends neurosci*, *22*(9), 391–397.

Dong, Q., Shi, L., Li, Y., Jiang, M., Sun, H., Wang, B., Cheng, H., Zhang, Y., Shao, T., Shi, Y., & Wang, Z. (2018). Differential responses of lasiopodomys mandarinus and lasiopodomys brandtii to chronic hypoxia: A cross-species brain transcriptome analysis. *BMC Genomics*, *19*(1), 901.

Doppenberg, E. M., Zauner, A., Watson, J. C., & Bullock, R. (1998). Determination of the ischemic threshold for brain oxygen tension. *Acta Neurochir Suppl*, *71*, 166–9.

Downer, J., Sevinsky, J. R., Ahn, N. G., Resing, K. A., & Betterton, M. (2006). Incorporating expression data in metabolic modeling: A case study of lactate dehydrogenase. *J Theor Biol*, *240*(3), 464–474.

Dugan, L. L., Bruno, V. M., Amagasu, S. M., & Giffard, R. G. (1995). Glia modulate the response of murine cortical neurons to excitotoxicity: Glia exacerbate ampa neurotoxicity. *J Neurosci*, *15*(6), 4545–55.

Durukan, A., & Tatlisumak, T. (2007). Acute ischemic stroke: Overview of major experimental rodent models, pathophysiology, and therapy of focal cerebral ischemia. *Pharmacol Biochem Behav*, *87*(1), 179–97.

Elsik, C. G., Tellam, R. L., Worley, K. C., Gibbs, R. A., Muzny, D. M., Weinstock, G. M., Adelson, D. L., Eichler, E. E., Elnitski, L., Guigo, R., Hamernik, D. L., Kappes, S. M., Lewin, H. A., Lynn, D. J., Nicholas, F. W., Reymond, A., Rijnkels, M., Skow, L. C., Zdobnov, E. M., ... Caetano, A. R., Et al. (2009). The genome sequence of taurine cattle: A window to ruminant biology and evolution. *Science*, *324*(5926), 522–8.

Elsner, R., Oyasaeter, S., Almaas, R., & Saugstad, O. D. (1998). Diving seals, ischemia-reperfusion and oxygen radicals. *Comp Biochem Physiol A Mol Integr Physiol*, *119*(4), 975–80.

Elsner, R., Shurley, J. T., Hammond, D. D., & Brooks, R. E. (1970). Cerebral tolerance to hypoxemia in asphyxiated weddell seals. *Respir Physiol*, *9*(2), 287–97.

Elsner, R., Wartzok, D., Sonafrank, N. B., & Kelly, B. P. (1989). Behavioral and physiological reactions of arctic seals during under-ice pilotage. *Can J Zool*, *67*(10), 2506–2513.

Erbsloh, F., Bernsmeier, A., & Hillesheim, H. (1958). The glucose consumption of the brain & its dependence on the liver. *Arch Psychiatr Nervenkr Z Gesamte Neurol Psychiatr*, *196*(6), 611–26.

Erecinska, M., & Silver, I. A. (2001). Tissue oxygen tension and brain sensitivity to hypoxia. *Respir Physiol*, *128*(3), 263–76.

Eriksen, N., & Pakkenberg, B. (2007). Total neocortical cell number in the mysticete brain. *Anat Rec (Hoboken)*, *290*(1), 83–95.

Fabrizius, A., Hoff, M. L., Engler, G., Folkow, L. P., & Burmester, T. (2016). When the brain goes diving: Transcriptome analysis reveals a reduced aerobic energy metabolism and increased stress proteins in the seal brain. *BMC Genomics*, *17*, 583.

Falke, K. J., Hill, R. D., Qvist, J., Schneider, R. C., Guppy, M., Liggins, G. C., Hochachka, P. W., Elliott, R. E., & Zapol, W. M. (1985). Seal lungs collapse during free diving: Evidence from arterial nitrogen tensions. *Science*, *229*(4713), 556–8.

Falkowska, A., Gutowska, I., Goschorska, M., Nowacki, P., Chlubek, D., & Baranowska-Bosiacka, I. (2015). Energy metabolism of the brain, including the cooperation between astrocytes and neurons, especially in the context of glycogen metabolism. *Int J Mol Sci*, *16*(11), 25959–81.

Fan, G., Zhang, Y., Liu, X., Wang, J., Sun, Z., Sun, S., Zhang, H., Chen, J., Lv, M., Han, K., Tan, X., Hu, J., Guan, R., Fu, Y., Liu, S., Chen, X., Xu, Q., Qin, Y., Liu, L., ... Liu, X. (2019). The first chromosome-level genome for a marine mammal as a resource to study ecology and evolution. *Mol Ecol Resour*, *19*(4), 944–956.

Fei, E., Jia, N., Yan, M., Ying, Z., Sun, Q., Wang, H., Zhang, T., Ma, X., Ding, H., Yao, X., Shi, Y., & Wang, G. (2006). Sumo-1 modification increases human sod1 stability and aggregation. *Biochem Biophys Res Commun*, *347*(2), 406–12.

Feng, Z., Davis, D. P., Sasik, R., Patel, H. H., Drummond, J. C., & Patel, P. M. (2007). Pathway and gene ontology based analysis of gene expression in a rat model of cerebral ischemic tolerance. *Brain Res*, *1177*, 103–23.

Ferretti, G., Costa, M., Ferrigno, M., Grassi, B., Marconi, C., Lundgren, C. E., & Cerretelli, P. (1991). Alveolar gas composition and exchange during deep breath-hold diving and dry breath holds in elite divers. *J Appl Physiol*, *70*(2), 794–802.

Fisher, A. B. (2017). Peroxiredoxin 6 in the repair of peroxidized cell membranes and cell signaling. *Arch Biochem Biophys*, *617*, 68–83.

Folkow, L. P., & Blix, A. S. (2010). Air breathers under water: Diving mammals and birds. *Respiratory Physiology of Vertebrates. Life With and Without Oxygen*, 222–264.

Folkow, L. P., Ramirez, J. M., Ludvigsen, S., Ramirez, N., & Blix, A. S. (2008). Remarkable neuronal hypoxia tolerance in the deep-diving adult hooded seal (cystophora cristata). *Neurosci Lett*, *446*(2-3), 147–150.

Foote, A. D., Liu, Y., Thomas, G. W., Vinar, T., Alfoldi, J., Deng, J., Dugan, S., van Elk, C. E., Hunter, M. E., Joshi, V., Khan, Z., Kovar, C., Lee, S. L., Lindblad-Toh, K., Mancia, A., Nielsen, R., Qin, X., Qu, J., Raney, B. J., ... Gibbs, R. A. (2015). Convergent evolution of the genomes of marine mammals. *Nature Genetics*, *47*(3), 272.

Fordel, E., Thijs, L., Moens, L., & Dewilde, S. (2007). Neuroglobin and cytoglobin expression in mice. evidence for a correlation with reactive oxygen species scavenging. *FEBS J*, *274*(5), 1312–7.

Fox, J., Bouchet-Valat, M., Andronic, L., Ash, M., Boye, T., Calza, S., Chang, A., Grosjean, P., Heiberger, R., Pour, K. K., Et al. (2019). Package 'rcmdr'.

Fujimura, M., Morita-Fujimura, Y., Noshita, N., Sugawara, T., Kawase, M., & Chan, P. H. (2000). The cytosolic antioxidant copper/zinc-superoxide dismutase prevents the early release of mitochondrial cytochrome c in ischemic brain after transient focal cerebral ischemia in mice. *J Neurosci*, *20*(8), 2817–24.

Fukuda, R., Zhang, H., Kim, J. W., Shimoda, L., Dang, C. V., & Semenza, G. L. (2007). Hif-1 regulates cytochrome oxidase subunits to optimize efficiency of respiration in hypoxic cells. *Cell*, *129*(1), 111–22.

Gannon, D. P., Read, A. J., Craddock, J. E., Fristrup, K. M., & Nicolas, J. R. (1997). Feeding ecology of long-finned pilot whales globicephala melas in the western north atlantic. *Mar Ecol Prog Ser*, 1–10.

Gao, C., Wang, C., Liu, B., Wu, H., Yang, Q., Jin, J., Li, H., Dong, S., Gao, G., & Zhang, H. (2014). Intermittent hypoxia preconditioning-induced epileptic tolerance by upregulation of monocarboxylate transporter 4 expression in rat hippocampal astrocytes. *Neurochem Res*, *39*(11), 2160–9.

Gao, C., Zhu, W., Tian, L., Zhang, J., & Li, Z. (2015). Mct4-mediated expression of eaat1 is involved in the resistance to hypoxia injury in astrocyte-neuron co-cultures. *Neurochem Res*, *40*(4), 818–28.

Gareau, J. R., & Lima, C. D. (2010). The sumo pathway: Emerging mechanisms that shape specificity, conjugation and recognition. *Nat Rev Mol Cell Biol*, *11*(12), 861–71.

Garey, L., & Leuba, G. (1986). A quantitative study of neuronal and glial numerical density in the visual cortex of the bottlenose dolphin: Evidence for a specialized subarea and changes with age. *J Comp Neurol*, *247*(4), 491–496.

Geiseler, S. J., Larson, J., & Folkow, L. P. (2016). Synaptic transmission despite severe hypoxia in hippocampal slices of the deep-diving hooded seal. *Neuroscience*, *334*, 39–46.

Giannakopoulos, P., Kovari, E., French, L. E., Viard, I., Hof, P. R., & Bouras, C. (1998). Possible neuroprotective role of clusterin in alzheimer's disease: A quantitative immunocytochemical study. *Acta Neuropathol*, *95*(4), 387–94.

Gierlinski, M., Cole, C., Schofield, P., Schurch, N. J., Sherstnev, A., Singh, V., Wrobel, N., Gharbi, K., Simpson, G., Owen-Hughes, T., Blaxter, M., & Barton, G. J. (2015). Statistical models for rna-seq data derived from a two-condition 48-replicate experiment. *Bioinformatics*, *31*(22), 3625–3630.

Giffard, R. G., Monyer, H., Christine, C. W., & Choi, D. W. (1990). Acidosis reduces nmda receptor activation, glutamate neurotoxicity, and oxygen-glucose deprivation neuronal injury in cortical cultures. *Brain Res*, *506*(2), 339–42.

Gilchrist, R. D., & Gidday, J. M. (2013). Hypoxic preconditioning in the cns. In *Innate tolerance in the cns* (pp. 183–212). Springer.

Gilmore, T. D. (2006). Introduction to nf-kappab: Players, pathways, perspectives. *Oncogene*, *25*(51), 6680–4.

Gnaiger, E., Lassnig, B., Kuznetsov, A., Rieger, G., & Margreiter, R. (1998). Mitochondrial oxygen affinity, respiratory flux control and excess capacity of cytochrome c oxidase. *J Exp Biol*, *201*(Pt 8), 1129–39.

Goldbogen, J. A., Calambokidis, J., Croll, D. A., Harvey, J. T., Newton, K. M., Oleson, E. M., Schorr, G., & Shadwick, R. E. (2008). Foraging behavior of humpback whales: Kinematic and respiratory patterns suggest a high cost for a lunge. *J Exp Biol*, *211*(23), 3712–3719.

Grocott, M. P., Martin, D. S., Levett, D. Z., McMorrow, R., Windsor, J., & Montgomery, H. E. (2009). Arterial blood gases and oxygen content in climbers on mount everest. *N Engl J Med*, *360*(2), 140–9.

Groves, B. M., Droma, T., Sutton, J. R., McCullough, R. G., McCullough, R. E., Zhuang, J., Rapmund, G., Sun, S., Janes, C., & Moore, L. G. (1993). Minimal hypoxic pulmonary hypertension in normal tibetans at 3,658 m. *J Appl Physiol*, *74*(1), 312–8.

Guerrini, L., Blasi, F., & Denis-Donini, S. (1995). Synaptic activation of nf-kappa b by glutamate in cerebellar granule neurons in vitro. *Proc Natl Acad Sci U S A*, *92*(20), 9077–81.

Gutsaeva, D. R., Carraway, M. S., Suliman, H. B., Demchenko, I. T., Shitara, H., Yonekawa, H., & Piantadosi, C. A. (2008). Transient hypoxia stimulates mitochondrial biogenesis in brain subcortex by a neuronal nitric oxide synthase-dependent mechanism. *J Neurosci*, *28*(9), 2015–24.

Haddad, G. G., & Jiang, C. (1993). O2 deprivation in the central nervous system: On mechanisms of neuronal response, differential sensitivity and injury. *Prog Neurobiol*, *40*, 277–318.

Halliwell, B., & Gutteridge, J. M. C. (2015). *Free radicals in biology and medicine*. Oxford University Press, USA.

Harris, J. J., Jolivet, R., & Attwell, D. (2012). Synaptic energy use and supply. *Neuron*, *75*(5), 762–77.

Hawkins, A., & Olszewski, J. (1957). Glia/nerve cell index for cortex of the whale. *Science*, *126*(3263), 76–77.

Hayes, J. D., & McLellan, L. I. (1999). Glutathione and glutathione-dependent enzymes represent a co-ordinately regulated defence against oxidative stress. *Free Radic Res*, *31*(4), 273–300.

He, Z., & Simon, H. U. (2013). A novel link between p53 and ros. *Cell Cycle*, *12*(2), 201–2.

Heide-Jørgensen, M. P., Bloch, D., Stefansson, E., Mikkelsen, B., Ofstad, L. H., & Dietz, R. (2002). Diving behaviour of long-finned pilot whales globicephala melas around the faroe islands. *Wildlife Biol*, *8*(4), 307–313.

Heinová, D., Kostecká, Z., & Petrovová, E. (2018). Lactate dehydrogenase isoenzyme electrophoretic pattern in serum and tissues of mammalian and bird origin. *Electrophoresis: Life Sciences Practical Applications*, 81.

Herbst, E. A., Roussakis, C., Matravadia, S., & Holloway, G. P. (2015). Chronic treadmill running does not enhance mitochondrial oxidative capacity in the cortex or striatum. *Metabolism*, *64*(11), 1419–25.

Herculano-Houzel, S. (2014). The glia/neuron ratio: How it varies uniformly across brain structures and species and what that means for brain physiology and evolution. *Glia*, *62*(9), 1377–1391.

Hermes-Lima, M., & Zenteno-Savin, T. (2002). Animal response to drastic changes in oxygen availability and physiological oxidative stress. *Comp Biochem Physiol C Toxicol Pharmacol*, *133*(4), 537–56.

Higdon, J. W., Bininda-Emonds, O. R., Beck, R. M., & Ferguson, S. H. (2007). Phylogeny and divergence of the pinnipeds (carnivora: Mammalia) assessed using a multigene dataset. *BMC Evol Biol*, *7*, 216.

Hindell, M. A., Slip, D. J., & Burton, H. R. (1991). The diving behavior of adult male and female southern elephant seals, mirounga-leonina (pinnipedia, phocidae). *Aust J Zool*, *39*(5), 595–619.

Hochachka, P. W. (1981). Brain, lung, and heart functions during diving and recovery. *Science*, *212*(4494), 509–14.

Hochachka, P. W. (2000). Pinniped diving response mechanism and evolution: A window on the paradigm of comparative biochemistry and physiology. *Comp Biochem Physiol, Part A Mol Integr Physiol*, *126*, 435–458.

Hochachka, P. W., Liggins, G. C., Qvist, J., Schneider, R., Snider, M. Y., Wonders, T. R., & Zapol, W. M. (1977). Pulmonary metabolism during diving: Conditioning blood for the brain. *Science*, *198*(4319), 831–4.

Hoelzel, A. R. (2009). *Marine mammal biology: An evolutionary approach*. John Wiley & Sons.

Hoff, M. L., Fabrizius, A., Czech-Damal, N. U., Folkow, L. P., & Burmester, T. (2017). Transcriptome analysis identifies key metabolic changes in the hooded seal (cystophora cristata) brain in response to hypoxia and reoxygenation. *PLoS One*, *12*(1), e0169366.

Hoff, M. L., Fabrizius, A., Folkow, L. P., & Burmester, T. (2016). An atypical distribution of lactate dehydrogenase isoenzymes in the hooded seal (cystophora cristata) brain may reflect a biochemical adaptation to diving. *J Comp Physiol B*, *186*(3), 373–86.

Hoffmann, A., Leung, T. H., & Baltimore, D. (2003). Genetic analysis of nf-kappab/rel transcription factors defines functional specificities. *EMBO J*, *22*(20), 5530–9.

Holbrook, J. J., Liljas, A., Steindel, S. J., & Rossmann, M. G. (1975). Lactate dehydrogenase. In *The enzymes* (pp. 191–292). Elsevier.

Hong, S. S., Gibney, G. T., Esquilin, M., Yu, J., & Xia, Y. (2004). Effect of protein kinases on lactate dehydrogenase activity in cortical neurons during hypoxia. *Brain Res*, *1009*(1-2), 195–202.

Hong, S., Ahn, J. Y., Cho, G. S., Kim, I. H., Cho, J. H., Ahn, J. H., Park, J. H., Won, M. H., Chen, B. H., Shin, B. N., Tae, H. J., Park, S. M., Cho, J. H., Choi, S. Y., & Lee, J. C. (2015). Monocarboxylate transporter 4 plays a significant role in the neuroprotective mechanism of ischemic preconditioning in transient cerebral ischemia. *Neural Regen Res*, *10*(10), 1604–11.

Hoppeler, H., Howald, H., Conley, K., Lindstedt, S. L., Claassen, H., Vock, P., & Weibel, E. R. (1985). Endurance training in humans: Aerobic capacity and structure of skeletal muscle. *J Appl Physiol (1985)*, *59*(2), 320–7.

Horner, P. J., & Gage, F. H. (2000). Regenerating the damaged central nervous system. *Nature*, *407*(6807), 963–70.

Horvat, S., Beyer, C., & Arnold, S. (2006). Effect of hypoxia on the transcription pattern of subunit isoforms and the kinetics of cytochrome c oxidase in cortical astrocytes and cerebellar neurons. *J Neurochem*, *99*(3), 937–51.

Hossmann, K. A. (2006). Pathophysiology and therapy of experimental stroke. *Cell Mol Neurobiol*, *26*(7-8), 1057–83.

Hothorn, T., Bretz, F., & Westfall, P. (2008). Simultaneous inference in general parametric models. *Biometrical Journal*, *50*(3), 346–363.

Hou, W., Pan, Q., Peng, Q., & He, M. (2017). A new method to analyze protein sequence similarity using dynamic time warping. *Genomics*, *109*(2), 123–130.

Howarth, C., Gleeson, P., & Attwell, D. (2012). Updated energy budgets for neural computation in the neocortex and cerebellum. *J Cereb Blood Flow Meta*, *32*, 1222–32.

Hu, S., Xie, Z., Onishi, A., Yu, X., Jiang, L., Lin, J., Rho, H. S., Woodard, C., Wang, H., Jeong, J. S., Long, S., He, X., Wade, H., Blackshaw, S., Qian, J., & Zhu, H. (2009). Profiling the human protein-dna interactome reveals erk2 as a transcriptional repressor of interferon signaling. *Cell*, *139*(3), 610–22.

Hyder, F., Rothman, D. L., & Bennett, M. R. (2013). Cortical energy demands of signaling and nonsignaling components in brain are conserved across mammalian species and activity levels. *Proc Natl Acad Sci U S A*, *110*(9), 3549–54.

Ida, M., Ando, M., Adachi, M., Tanaka, A., Machida, K., Hongo, K., Mizobata, T., Yamakawa, M. Y., Watanabe, Y., Nakashima, K., & Kawata, Y. (2016). Structural basis of cu, zn-superoxide dismutase amyloid fibril formation involves interaction of multiple peptide core regions. *J Biochem*, *159*(2), 247–60.

Ighodaro, O. M., & Akinloye, O. A. (2018). First line defence antioxidants-superoxide dismutase (sod), catalase (cat) and glutathione peroxidase (gpx): Their fundamental role in the entire antioxidant defence grid. *Alexandria Med J*, *54*(4), 287–293.

Italiano, D., Lena, A. M., Melino, G., & Candi, E. (2012). Identification of ncf2/p67phox as a novel p53 target gene. *Cell Cycle*, *11*(24), 4589–96.

Itoh, Y., Esaki, T., Shimoji, K., Cook, M., Law, M. J., Kaufman, E., & Sokoloff, L. (2003). Dichloroacetate effects on glucose and lactate oxidation by neurons and astroglia in vitro and on glucose utilization by brain in vivo. *Proc Natl Acad Sci U S A*, *100*(8), 4879–84.

Jacobs, E., Hissin, P. J., Propper, W., Mayer, L., & Sarkozi, L. (1986). Stability of lactate dehydrogenase at different storage temperatures. *Clin Biochem*, *19*(3), 183–8.

Jensen, K. P., & Ryde, U. (2004). How o2 binds to heme: Reasons for rapid binding and spin inversion. *J Biol Chem*, *279*(15), 14561–9.

Johnson, G. L., & Nakamura, K. (2007). The c-jun kinase/stress-activated pathway: Regulation, function and role in human disease. *Biochim Biophys Acta*, *1773*(8), 1341–8.

Johnson, P., Elsner, R., & Zenteno-Savín, T. (2005). Hypoxia-inducible factor 1 proteomics and diving adaptations in ringed seal. *Free Radic Biol Med*, *39*(2), 205–212.

Jones, P. G., Nawoschik, S. P., Sreekumar, K., Uveges, A. J., Tseng, E., Zhang, L., Johnson, J., He, L., Paulsen, J. E., Bates, B., & Pausch, M. H. (2007). Tissue distribution and functional analyses of the constitutively active orphan g protein coupled receptors, gpr26 and gpr78. *Biochim Biophys Acta*, *1770*(6), 890–901.

Joyce, T. W., Durban, J. W., Claridge, D. E., Dunn, C. A., Fearnbach, H., Parsons, K. M., Andrews, R. D., & Ballance, L. T. (2017). Physiological, morphological, and ecological tradeoffs influence vertical habitat use of deep-diving toothed-whales in the bahamas. *PLoS One*, *12*(10), e0185113.

Kaltschmidt, B., Uherek, M., Volk, B., Baeuerle, P. A., & Kaltschmidt, C. (1997). Transcription factor nf-kappab is activated in primary neurons by amyloid beta peptides and in neurons surrounding early plaques from patients with alzheimer disease. *Proc Natl Acad Sci U S A*, *94*(6), 2642–7.

Kanatous, S. B., DiMichele, L. V., Cowan, D. F., & Davis, R. W. (1999). High aerobic capacities in the skeletal muscles of pinnipeds: Adaptations to diving hypoxia. *J Appl Physiol*, *86*(4), 1247–56.

Kaplan, N. O., Everse, J., & Admiraal, J. (1968). Significance of substrate inhibition of dehydrogenases. *Ann N Y Acad Sci*, *151*(1), 400–12.

Kasischke, K. A., Vishwasrao, H. D., Fisher, P. J., Zipfel, W. R., & Webb, W. W. (2004). Neural activity triggers neuronal oxidative metabolism followed by astrocytic glycolysis. *Science*, *305*(5680), 99–103.

Kenneth, N. S., & Rocha, S. (2008). Regulation of gene expression by hypoxia. *Biochem J*, *414*(1), 19–29.

Kerem, D., & Elsner, R. (1973a). Cerebral tolerance to asphyxial hypoxia in the harbor seal. *Respir Physiol*, *19*(2), 188–200.

Kerem, D., Hammond, D. D., & Elsner, R. (1973b). Tissue glycogen levels in the weddell seal, leptonychotes weddelli: A possible adaptation to asphyxial hypoxia. *Comp Biochem Physiol, Part A Mol Integr Physiol*, *45*, 731–736.

Kilian, A., Yaman, S., von Fersen, L., & Gunturkun, O. (2003). A bottlenose dolphin discriminates visual stimuli differing in numerosity. *Learn Behav*, *31*(2), 133–42.

Kinnula, V. L., Paakko, P., & Soini, Y. (2004). Antioxidant enzymes and redox regulating thiol proteins in malignancies of human lung. *FEBS Lett*, *569*(1-3), 1–6.

Kitazoe, Y., Kishino, H., Waddell, P. J., Nakajima, N., Okabayashi, T., Watabe, T., & Okuhara, Y. (2007). Robust time estimation reconciles views of the antiquity of placental mammals. *PLoS One*, *2*(4), e384.

Kobayashi, M., Sugumaran, G., Liu, J., Shworak, N. W., Silbert, J. E., & Rosenberg, R. D. (1999). Molecular cloning and characterization of a human uronyl 2-sulfotransferase that sulfates iduronyl and glucuronyl residues in dermatan/chondroitin sulfate. *J Biol Chem*, *274*(15), 10474–10480.

Kojima, T. (1951). On the brain of the sperm whale (physeter catodon l.) *Sci Rep Whales Res Inst Tokyo*, *6*, 49–72.

Kokubo, Y., Matson, G. B., Derugin, N., Hill, T., Mancuso, A., Chan, P. H., & Weinstein, P. R. (2002). Transgenic mice expressing human copper-zinc superoxide dismutase exhibit attenuated apparent diffusion coefficient reduction during reperfusion following focal cerebral ischemia. *Brain Res*, *947*(1), 1–8.

Kooyman, G. L., Castellini, M. A., Davis, R. W., & Maue, R. A. (1983). Aerobic diving limits of immature weddell seals. *J Comp Physiol B, Biochem Syst Environ Physiol*, *151*(2), 171–174.

Kooyman, G. L., Hammond, D. D., & Schroeder, J. P. (1970). Bronchograms and tracheograms of seals under pressure. *Science*, *169*(3940), 82–4.

Kooyman, G. L., & Ponganis, P. J. (1998). The physiological basis of diving to depth: Birds and mammals. *Annu Rev Physiol*, *60*, 19–32.

Kooyman, G. L., Wahrenbrock, E. A., Castellini, M. A., Davis, R. W., & Sinnett, E. E. (1980). Aerobic and anaerobic metabolism during voluntary diving in weddell seals: Evidence of preferred pathways from blood chemsitry and behavior. *J Comp Physiol B, Biochem Syst Environ Physiol*, *138*(4), 335–346.

Kopperschläger, G., & Kirchberger, J. (1996). Methods for the separation of lactate dehydrogenases and clinical significance of the enzyme. *J Chromatogr B Biomed Appl*, *684*(1-2), 25–49.

Korshunov, S. S., Krasnikov, B. F., Pereverzev, M. O., & Skulachev, V. P. (1999). The antioxidant functions of cytochrome c. *FEBS Lett*, *462*(1-2), 192–8.

Krieg, A. F., Rosenblum, L. J., & Henry, J. B. (1967). Lactate dehydrogenase isoenzymes a comparison of pyruvate-to-lactate and lactate-to-pyruvate assays. *Clin Chem*, *13*(3), 196–203.

Krüger, A., Fabrizius, A., Mikkelsen, B., Siebert, U., Folkow, L. P., & Burmester, T. (2019). Transcriptome analysis reveals a high aerobic capacity in the whale brain. *Comp Biochem Physiol A Mol Integr Physiol*, *240*, 110593.

Krutzen, M., Mann, J., Heithaus, M. R., Connor, R. C., Bejder, L., & Sherwin, W. B. (2005). Cultural transmission of tool use in bottlenose dolphins. *Proc Natl Acad Sci U S A*, *102*(25), 8939–43.

Kudin, A. P., Augustynek, B., Lehmann, A. K., Kovacs, R., & Kunz, W. S. (2012). The contribution of thioredoxin-2 reductase and glutathione peroxidase to h(2)o(2) detoxification of rat brain mitochondria. *Biochim Biophys Acta*, *1817*(10), 1901–6.

Larson, J., Drew, K. L., Folkow, L. P., Milton, S. L., & Park, T. J. (2014). No oxygen? no problem! intrinsic brain tolerance to hypoxia in vertebrates. *J Exp Biol*, *217*(Pt 7), 1024–39.

Lau, G. Y., Mandic, M., & Richards, J. G. (2017). Evolution of cytochrome c oxidase in hypoxia tolerant sculpins (cottidae, actinopterygii). *Mol Biol Evol*, *34*(9), 2153–2162.

Laughton, J., Charnay, Y., Belloir, B., Pellerin, L., Magistretti, P., & Bouras, C. (2000). Differential messenger rna distribution of lactate dehydrogenase ldh-1 and ldh-5 isoforms in the rat brain. *Neuroscience*, *96*(3), 619–625.

Lee, H. J., Hammond, D. N., Large, T. H., Roback, J. D., Sim, J. A., Brown, D. A., Otten, U. H., & Wainer, B. H. (1990). Neuronal properties and trophic activities of immortalized hippocampal cells from embryonic and young adult mice. *Journal of Neuroscience*, *10*(6), 1779–1787.

Lee, J. M., Grabb, M. C., Zipfel, G. J., & Choi, D. W. (2000). Brain tissue responses to ischemia. *J Clin Invest*, *106*(6), 723–31.

Lee, J.-W., Bae, S.-H., Jeong, J.-W., Kim, S.-H., & Kim, K.-W. (2004). Hypoxia-inducible factor (hif-1) alpha: Its protein stability and biological functions. *Exp Mol Med*, *36*(1), 1.

Lenfant, C., Johansen, K., & Torrance, J. D. (1970). Gas transport and oxygen storage capacity in some pinnipeds and the sea otter. *Respir Physiol*, *9*(2), 277–286.

Lento, G. M., Hickson, R. E., Chambers, G. K., & Penny, D. (1995). Use of spectral analysis to test hypotheses on the origin of pinnipeds. *Mol Biol Evol*, *12*(1), 28–52.

Li, Q., Sun, R., Huang, C., Wang, Z., Liu, X., Hou, J., Liu, J., Cai, L., Li, N., Zhang, S., & Wang, Y. (2001). Cold adaptive thermogenesis in small mammals from different geographical zones of china. *Comp Biochem Physiol A Mol Integr Physiol*, *129*(4), 949–61.

Li, R. C., Guo, S. Z., Lee, S. K., & Gozal, D. (2010). Neuroglobin protects neurons against oxidative stress in global ischemia. *J Cereb Blood Flow Metab*, *30*(11), 1874–82.

Li, Y.-J., & Tsoi, S. C.-M. (2002). Phylogenetic analysis of vertebrate lactate dehydrogenase (ldh) multigene families. *J Mol Evol*, *54*(5), 614–624.

Lien, Y. C., Feinstein, S. I., Dodia, C., & Fisher, A. B. (2012). The roles of peroxidase and phospholipase a2 activities of peroxiredoxin 6 in protecting pulmonary microvascular endothelial cells against peroxidative stress. *Antioxid Redox Signal*, *16*(5), 440–51.

Lipton, P. (1999). Ischemic cell death in brain neurons. *Physiol Rev*, *79*(4), 1431–1568.

Liu, G., Feinstein, S. I., Wang, Y., Dodia, C., Fisher, D., Yu, K., Ho, Y. S., & Fisher, A. B. (2010). Comparison of glutathione peroxidase 1 and peroxiredoxin 6 in protection against oxidative stress in the mouse lung. *Free Radic Biol Med*, *49*(7), 1172–81.

Liu, X., Kim, C. N., Yang, J., Jemmerson, R., & Wang, X. (1996). Induction of apoptotic program in cell-free extracts: Requirement for datp and cytochrome c. *Cell*, *86*(1), 147–57.

Lluis, J. M., Morales, A., Blasco, C., Colell, A., Mari, M., Garcia-Ruiz, C., & Fernandez-Checa, J. C. (2005). Critical role of mitochondrial glutathione in the survival of hepatocytes during hypoxia. *J Biol Chem*, *280*(5), 3224–32.

Lockyer, C., & Waters, T. (1986). Weights and anatomical measurements of northeastern atlantic fin (balaenoptera physalus, linnaeus) and sei (b. borealis, lesson) whales. *Mar Mammal Sci*, *2*(3), 169–185.

Loh, K. P., Qi, J., Tan, B. K., Liu, X. H., Wei, B. G., & Zhu, Y. Z. (2010). Leonurine protects middle cerebral artery occluded rats through antioxidant effect and regulation of mitochondrial function. *Stroke*, *41*(11), 2661–8.

Lopez-Barneo, J., Pardal, R., & Ortega-Saenz, P. (2001). Cellular mechanism of oxygen sensing. *Annu Rev Physiol*, *63*, 259–87.

Ludvigsen, S., & Folkow, L. P. (2009). Differences in in vitro cerebellar neuronal responses to hypoxia in eider ducks, chicken and rats. *J COMP PHYSIOL A*, *195*(11), 1021.

Lutz, P. L., Nilsson, G. E., & Prentice, H. M. (2003). *The brain without oxygen: Causes of failure-physiological and molecular mechanisms for survival*. Springer Science & Business Media.

Magadum, S., Banerjee, U., Murugan, P., Gangapur, D., & Ravikesavan, R. (2013). Gene duplication as a major force in evolution. *J Genet*, *92*(1), 155–161.

Magistretti, P. J., & Allaman, I. (2015). A cellular perspective on brain energy metabolism and functional imaging. *Neuron*, *86*(4), 883–901.

Maine, G. N., & Burstein, E. (2007). Commd proteins: Comming to the scene. *Cell Mol Life Sci*, *64*(15), 1997–2005.

Makar, T. K., Nedergaard, M., Preuss, A., Gelbard, A. S., Perumal, A. S., & Cooper, A. J. (1994). Vitamin e, ascorbate, glutathione, glutathione disulfide, and enzymes of glutathione metabolism in cultures of chick astrocytes and neurons: Evidence that astrocytes play an important role in antioxidative processes in the brain. *J Neurochem*, *62*(1), 45–53.

Makino, T., & McLysaght, A. (2010). Ohnologs in the human genome are dosage balanced and frequently associated with disease. *Proc Natl Acad Sci U S A*, *107*(20), 9270–4.

Malik, A., Domankevich, V., Lijuan, H., Xiaodong, F., Korol, A., Avivi, A., & Shams, I. (2016). Genome maintenance and bioenergetics of the long-lived hypoxia-tolerant and cancer-resistant blind mole rat, spalax: A cross-species analysis of brain transcriptome. *Sci Rep*, *6*, 38624.

Malik, A., Korol, A., Weber, M., Hankeln, T., Avivi, A., & Band, M. (2012). Transcriptome analysis of the spalax hypoxia survival response includes suppression of apoptosis and tight control of angiogenesis. *BMC Genomics*, *13*, 615.

Manevich, Y., Feinstein, S. I., & Fisher, A. B. (2004). Activation of the antioxidant enzyme 1-cys peroxiredoxin requires glutathionylation mediated by heterodimerization with pi gst. *Proc Natl Acad Sci U S A*, *101*(11), 3780–5.

Manevich, Y., & Fisher, A. B. (2005). Peroxiredoxin 6, a 1-cys peroxiredoxin, functions in antioxidant defense and lung phospholipid metabolism. *Free Radic Biol Med*, *38*(11), 1422–32.

Manevich, Y., Sweitzer, T., Pak, J. H., Feinstein, S. I., Muzykantov, V., & Fisher, A. B. (2002). 1-cys peroxiredoxin overexpression protects cells against phospholipid peroxidation-mediated membrane damage. *Proc Natl Acad Sci U S A*, *99*(18), 11599–604.

Mann, G. E., Niehueser-Saran, J., Watson, A., Gao, L., Ishii, T., de Winter, P., & Siow, R. C. (2007a). Nrf2/are regulated antioxidant gene expression in endothelial and smooth muscle cells in oxidative stress: Implications for atherosclerosis and preeclampsia. *Acta Psychol Sin*, *59*(2), 117–27.

Mann, G. E., Rowlands, D. J., Li, F. Y., de Winter, P., & Siow, R. C. (2007b). Activation of endothelial nitric oxide synthase by dietary isoflavones: Role of no in nrf2-mediated antioxidant gene expression. *Cardiovasc Res*, *75*(2), 261–74.

Marina, N., Kasymov, V., Ackland, G. L., Kasparov, S., & Gourine, A. V. (2016). Astrocytes and brain hypoxia. *Adv Exp Med Biol*, *903*, 201–7.

Marino, L. (2004). Cetacean brain evolution: Multiplication generates complexity. *Int J Comp Psychol*, *17*(1).

Marino, L., Sherwood, C. C., Delman, B. N., Tang, C. Y., Naidich, T. P., & Hof, P. R. (2004). Neuroanatomy of the killer whale (orcinus orca) from magnetic resonance images. *Anat Rec A Discov Mol Cell Evol Biol*, *281*(2), 1256–63.

Markert, C. L. (1963). Lactate dehydrogenase isozymes: Dissociation and recombination of subunits. *Science*, *140*(3573), 1329–30.

Markert, C. L., & Ursprung, H. (1962). The ontogeny of isozyme patterns of lactate dehydrogenase in the mouse. *Dev Biol*, *5.3*, 363–381.

Markert, C. L., Shaklee, J. B., & Whitt, G. S. (1975). Evolution of a gene. *Science*, *189*(4197), 102–114.

Mates, J. M., Perez-Gomez, C., & Nunez de Castro, I. (1999). Antioxidant enzymes and human diseases. *Clin Biochem*, *32*(8), 595–603.

Matsunaga, T., Endo, S., Maeda, S., Ishikura, S., Tajima, K., Tanaka, N., Nakamura, K. T., Imamura, Y., & Hara, A. (2008). Characterization of human dhrs4: An inducible short-chain dehydrogenase/reductase enzyme with 3beta-hydroxysteroid dehydrogenase activity. *Arch Biochem Biophys*, *477*(2), 339–347.

McGowen, M. R., Grossman, L. I., & Wildman, D. E. (2012). Dolphin genome provides evidence for adaptive evolution of nervous system genes and a molecular rate slowdown. *Proc Biol Sci*, *279*(1743), 3643–3651.

McGuire, W. (2007). Perinatal asphyxia. *BMJ Clin Evid*, *2007*.

McKernan, R. M., & Whiting, P. J. (1996). Which gabaa-receptor subtypes really occur in the brain? *Trends Neurosci*, *19*(4), 139–43.

Meberg, P. J., Kinney, W. R., Valcourt, E. G., & Routtenberg, A. (1996). Gene expression of the transcription factor nf-kappa b in hippocampus: Regulation by synaptic activity. *Brain Res Mol Brain Res*, *38*(2), 179–90.

Meir, J. U., & Ponganis, P. J. (2009). High-affinity hemoglobin and blood oxygen saturation in diving emperor penguins. *J Exp Biol*, *212*(Pt 20), 3330–8.

Meredith, R. W., Janečka, J. E., Gatesy, J., Ryder, O. A., Fisher, C. A., Teeling, E. C., Goodbla, A., Eizirik, E., Simão, T. L., Stadler, T., Et al. (2011). Impacts of the cretaceous terrestrial revolution and kpg extinction on mammal diversification. *science*, *334*(6055), 521–524.

Messelt, E. B., & Blix, A. S. (1976). The ldh of the frequently asphyxiated beaver (castor fiber). *Comp Biochem Physiol B*, *53*(1), 77–80.

Meyer, M., Schreck, R., & Baeuerle, P. A. (1993). H2o2 and antioxidants have opposite effects on activation of nf-kappa b and ap-1 in intact cells: Ap-1 as secondary antioxidant-responsive factor. *EMBO J*, *12*(5), 2005–15.

Mi, H., Huang, X., Muruganujan, A., Tang, H., Mills, C., Kang, D., & Thomas, P. D. (2017). Panther version 11: Expanded annotation data from gene ontology and reactome pathways, and data analysis tool enhancements. *Nucleic Acids Res*, *45*(D1), D183–D189.

Michiels, C. (2004). Physiological and pathological responses to hypoxia. *Am J Pathol*, *164*(6), 1875–82.

Miller, P. O., Shapiro, A. D., & Deecke, V. B. (2010). The diving behaviour of mammal-eating killer whales (orcinus orca): Variations with ecological not physiological factors. *Can J Zool*, *88*(11), 1103–1112.

Milton, S. L., & Lutz, P. L. (1998). Low extracellular dopamine levels are maintained in the anoxic turtle (trachemys scripta) striatum. *J Cereb Blood Flow Metab*, *18*(7), 803–807.

Milton, S. L., Thompson, J. W., & Lutz, P. L. (2002). Mechanisms for maintaining extracellular glutamate levels in the anoxic turtle striatum. *Am J Physiol Regul Integr Comp Physiol*, *282*(5), R1317–R1323.

Mirceta, S., Signore, A. V., Burns, J. M., Cossins, A. R., Campbell, K. L., & Berenbrink, M. (2013). Evolution of mammalian diving capacity traced by myoglobin net surface charge. *Science*, *340*(6138), 1234192.

Mitz, S. A., Reuss, S., Folkow, L. P., Blix, A. S., Ramirez, J. M., Hankeln, T., & Burmester, T. (2009). When the brain goes diving: Glial oxidative metabolism may confer hypoxia tolerance to the seal brain. *Neuroscience*, *163*(2), 552–560.

Monge, C., & Leon-Velarde, F. (1991). Physiological adaptation to high altitude: Oxygen transport in mammals and birds. *Physiol Rev*, *71*(4), 1135–72.

Moore, M. J., Hammar, T., Arruda, J., Cramer, S., Dennison, S., Montie, E., & Fahlman, A. (2011). Hyperbaric computed tomographic measurement of lung compression in seals and dolphins. *J Exp Biol*, *214*(Pt 14), 2390–7.

Mortensen, H. S., Pakkenberg, B., Dam, M., Dietz, R., Sonne, C., Mikkelsen, B., & Eriksen, N. (2014). Quantitative relationships in delphinid neocortex. *Front Neuroanat*, *8*, 132.

Murphy, B., Zapol, W. M., & Hochachka, P. W. (1980). Metabolic activities of heart, lung, and brain during diving and recovery in the weddell seal. *J Appl Physiol*, *48*(4), 596–605.

Murphy, M. P. (2009). How mitochondria produce reactive oxygen species. *Biochem J*, *417*(1), 1–13.

Meir, J. U., Champagne, C. D., Costa, D. P., Williams, C. L., & Ponganis, P. J. (2009). Extreme hypoxemic tolerance and blood oxygen depletion in diving elephant seals. *Am J Physiol Regul Integr Comp Physiol*, *297*(4), R927–39.

Nabekura, T., Morishima, S., Cover, T. L., Mori, S. I., Kannan, H., Komune, S., & Okada, Y. (2003). Recovery from lactacidosis-induced glial cell swelling with the aid of exogenous anion channels. *Glia*, *41*, 247–259.

Nakanishi, T., Sugawara, M., Huang, W., Martindale, R. G., Leibach, F. H., Ganapathy, M. E., Prasad, P. D., & Ganapathy, V. (2001). Structure, function, and tissue expression pattern of human sn2, a subtype of the amino acid transport system n. *Biochem Biophys Res Commun*, *281*(5), 1343–1348.

Nakayama, M., Nakajima, D., Yoshimura, R., Endo, Y., & Ohara, O. (2002). Megf1/fat2 proteins containing extraordinarily large extracellular domains are localized to thin parallel fibers of cerebellar granule cells. *Mol Cell Neurosci*, *20*(4), 563–578.

Narindrasorasak, S., Kulkarni, P., Deschamps, P., She, Y. M., & Sarkar, B. (2007). Characterization and copper binding properties of human commd1 (murr1). *Biochemistry*, *46*(11), 3116–28.

Nathaniel, T. I., Otukonyong, E. E., Okon, M., Chaves, J., Cochran, T., & Nathaniel, A. I. (2013). Metabolic regulatory clues from the naked mole rat: Toward brain regulatory functions during stroke. *Brain Res Bull*, *98*, 44–52.

Nery, M. F., Arroyo, J. I., & Opazo, J. C. (2013). Genomic organization and differential signature of positive selection in the alpha and beta globin gene clusters in two cetacean species. *Genome Biol Evol*, *5*(12), 2359–67.

Newington, J. T., Harris, R. A., & Cumming, R. C. (2013). Reevaluating metabolism in alzheimer's disease from the perspective of the astrocyte-neuron lactate shuttle model. *J Neurodegener Dis*, *2013*.

Nicholls, P., Fita, I., & Loewen, P. C. (2000). Enzymology and structure of catalases.

Niizuma, K., Endo, H., & Chan, P. H. (2009). Oxidative stress and mitochondrial dysfunction as determinants of ischemic neuronal death and survival. *J Neurochem*, *109 Suppl 1*, 133–8.

Noren, S. R., & Williams, T. M. (2000). Body size and skeletal muscle myoglobin of cetaceans: Adaptations for maximizing dive duration. *Comp Biochem Physiol A Mol Integr Physiol*, *126*(2), 181–91.

Odden, A., Folkow, L. P., Caputa, M., Hotvedt, R., & Blix, A. S. (1999). Brain cooling in diving seals. *Acta Physiology Scand*, *166*, 77–78.

Ogden, K. K., Chen, W., Swanger, S. A., McDaniel, M. J., Fan, L. Z., Hu, C., Tankovic, A., Kusumoto, H., Kosobucki, G. J., Schulien, A. J., Su, Z., Pecha, J., Bhattacharya, S., Petrovski, S., Cohen, A. E., Aizenman, E., Traynelis, S. F., & Yuan, H. (2017). Molecular mechanism of disease-associated mutations in the pre-m1 helix of nmda receptors and potential rescue pharmacology. *PLoS Genet*, *13*(1), e1006536.

Ohno, S. (1970). Evolution by gene duplication springer, new york.

Okada, Y., Sato, K., & Numata, T. (2009). Pathophysiology and puzzles of the volume-sensitive outwardly rectifying anion channel. *J Physiol*, *587*, 2141–2149.

O'Neill, L. A., & Kaltschmidt, C. (1997). Nf-kappa b: A crucial transcription factor for glial and neuronal cell function. *Trends Neurosci*, *20*(6), 252–8.

Ozkosem, B., Feinstein, S. I., Fisher, A. B., & O'Flaherty, C. (2016). Absence of peroxiredoxin 6 amplifies the effect of oxidant stress on mobility and scsa/cma3 defined chromatin quality and impairs fertilizing ability of mouse spermatozoa. *Biol Reprod*, *94*(3), 68.

Padayatty, S. J., Katz, A., Wang, Y., Eck, P., Kwon, O., Lee, J.-H., Chen, S., Corpe, C., Dutta, A., Dutta, S. K., Et al. (2003). Vitamin c as an antioxidant: Evaluation of its role in disease prevention. *J Am Coll Nutr*, *22*(1), 18–35.

Pahl, H. L. (1999). Activators and target genes of rel/nf-kappab transcription factors. *Oncogene*, *18*(49), 6853–66.

Papa, S., Martino, P. L., Capitanio, G., Gaballo, A., De Rasmo, D., Signorile, A., & Petruzzella, V. (2012). The oxidative phosphorylation system in mammalian mitochondria. *Adv Exp Med Biol*, *942*, 3–37.

Pardo, C. A., Xu, Z., Borchelt, D. R., Price, D. L., Sisodia, S. S., & Cleveland, D. W. (1995). Superoxide dismutase is an abundant component in cell bodies, dendrites, and axons of motor neurons and in a subset of other neurons. *Proc Natl Acad Sci U S A*, *92*(4), 954–8.

Park, M. H., Jo, M., Kim, Y. R., Lee, C. K., & Hong, J. T. (2016). Roles of peroxiredoxins in cancer, neurodegenerative diseases and inflammatory diseases. *Pharmacol Ther*, *163*, 1–23.

Park, Y. J., & Luger, K. (2006). Structure and function of nucleosome assembly proteins. *Biochem Cell Biol*, *84*(4), 549–558.

Peers, C., Pearson, H. A., & Boyle, J. P. (2007). Hypoxia and alzheimer's disease. *Essays biochem*, *43*, 153–164.

Pellerin, L. (2005). How astrocytes feed hungry neurons. *Mol Neurobiol*, *32*(1), 59–72.

Pérez, V. I., Lew, C. M., Cortez, L. A., Webb, C. R., Rodriguez, M., Liu, Y., Qi, W., Li, Y., Chaudhuri, A., Van Remmen, H., Richardson, A., & Ikeno, Y. (2008). Thioredoxin 2 haploinsufficiency in mice results in impaired mitochondrial function and increased oxidative stress. *Free Radic Biol Med*, *44*(5), 882–92.

Perry, J. J., Shin, D. S., Getzoff, E. D., & Tainer, J. A. (2010). The structural biochemistry of the superoxide dismutases. *Biochim Biophys Acta*, *1804*(2), 245–62.

Petry, F. (1998). Molecular basis of hereditary c1q deficiency. *Immunobiology*, *199*(2), 286–294.

Pfaffl, M. W. (2001). A new mathematical model for relative quantification in real-time rt-pcr. *Nucleic Acids Res*, *29*(9), e45.

Phelps, C. H. (1972). Barbiturate-induced glycogen accumulation in brain. an electron microscopic study. *Brain Res*, *39*(1), 225–34.

Pilleri, G., & Gihr, M. (1970). The central nervous system of the mysticete and odontocete whales. *Investigations on cetacea*, *2*, 89–127.

Pizzi, M., Goffi, F., Boroni, F., Benarese, M., Perkins, S. E., Liou, H. C., & Spano, P. (2002). Opposing roles for nf-kappa b/rel factors p65 and c-rel in the modulation of neuron survival elicited by glutamate and interleukin-1beta. *J Biol Chem*, *277*(23), 20717–23.

Pizzi, M., Sarnico, I., Boroni, F., Benarese, M., Steimberg, N., Mazzoleni, G., Dietz, G. P., Bahr, M., Liou, H. C., & Spano, P. F. (2005). Nf-kappab factor c-rel mediates neuroprotection elicited by mglu5 receptor agonists against amyloid beta-peptide toxicity. *Cell Death Differ*, *12*(7), 761–72.

Plagemann, P. G., Gregory, K. F., & Wróblewski, F. (1960). The electrophoretically distinct forms of mammalian lactic dehydrogenase i. distribution of lactic dehydrogenases in rabbit and human tissues. *J Biol Chem*, *235*(8), 2282–2287.

Polasek, L. K., & Davis, R. W. (2001). Heterogeneity of myoglobin distribution in the locomotory muscles of five cetacean species. *J Exp Biol*, *204*(Pt 2), 209–215.

Ponganis, P. J. (2011). Diving mammals. *Compr Physiol*, *1*(1), 517–535.

Ponganis, P. J., Kooyman, G. L., & Castellini, M. (1993). Determinants of the aerobic dive limit of weddell seals: Analysis of diving metabolic rates, postdive end tidal po2's, and blood and muscle oxygen stores. *Physiol Zool*, *66*(5), 732–749.

Porollo, A., & Meller, J. (2007). Versatile annotation and publication quality visualization of protein complexes using polyview-3d. *BMC bioinformatics*, *8*(1), 316.

Premack, D., & Hauser, M. D. (2001). A whale of a tale: Calling it culture doesn't help. *Behav Brain Sci*, *24*(2), 350–351.

Prichard, L., Deloulme, J. C., & Storm, D. R. (1999). Interactions between neurogranin and calmodulin in vivo. *J Biol Chem*, *274*(12), 7689–94.

Pucci, S., Mazzarelli, P., Missiroli, F., Regine, F., & Ricci, F. (2008). Neuroprotection: Vegf, il-6, and clusterin: The dark side of the moon. *Prog Brain Res*, *173*, 555–73.

Qiao, H., Dong, L., Zhang, X., Zhu, C., Zhang, X., Wang, L., Liu, Z., Chen, L., Xing, Y., Wang, C., & Li, Y. (2012). Protective effect of luteolin in experimental ischemic stroke: Upregulated sod1, cat, bcl-2 and claudin-5, down-regulated mda and bax expression. *Neurochem Res*, *37*(9), 2014–24.

Quistorff, B., & Grunnet, N. (2011). The isoenzyme pattern of ldh does not play a physiological role; except perhaps during fast transitions in energy metabolism. *Aging (Albany NY)*, *3*(5), 457.

Qvist, J., Hill, R. D., Schneider, R. C., Falke, K. J., Liggins, G. C., Guppy, M., Elliot, R. L., Hochachka, P. W., & Zapol, W. M. (1986). Hemoglobin concentrations and blood gas tensions of free-diving weddell seals. *J Appl Physiol*, *61*(4), 1560–1569.

Ramanathan, L., Gozal, D., & Siegel, J. M. (2005). Antioxidant responses to chronic hypoxia in the rat cerebellum and pons. *J Neurochem*, *93*(1), 47–52.

Ramirez, J. M., Folkow, L. P., & Blix, A. S. (2007). Hypoxia tolerance in mammals and birds: From the wilderness to the clinic. *Annu Rev Physiol*, *69*, 113–43.

Ramirez, J. M., Folkow, L. P., Ludvigsen, S., Ramirez, P. N., & Blix, A. S. (2011). Slow intrinsic oscillations in thick neocortical slices of hypoxia tolerant deep diving seals. *Neuroscience*, *177*, 35–42.

Rasbach, K. A., & Schnellmann, R. G. (2007). Signaling of mitochondrial biogenesis following oxidant injury. *J Biol Chem*, *282*(4), 2355–62.

Read, J., Winter, V., Eszes, C., Sessions, R., & Brady, R. (2001). Structural basis for altered activity of m-and h-isozyme forms of human lactate dehydrogenase. *Proteins*, *43*(2), 175–185.

Reidarson, T. H., McBain, J., & Dalton, L. M. (1999). Lactate dehydrogenase isoenzyme patterns in cetaceans. *J Zoo Wildl Med*, *30*(2), 228–34.

Reisinger, R. R., Keith, M., Andrews, M. D., & de Bruyn, P. J. N. (2015). Movement and diving of killer whales (orcinus orca) at a southern ocean archipelago. *J Exp Mar Biol Ecol*, *473*, 90–102.

Reiss, D., & McCowan, B. (1993). Spontaneous vocal mimicry and production by bottlenose dolphins (tursiops truncatus): Evidence for vocal learning. *J Comp Psychol*, *107*(3), 301–12.

Rendell, L., & Whitehead, H. (2001). Culture in whales and dolphins. *Behav Brain Sci*, *24*(2), 309–324.

Ridgway, S. H., & Brownson, R. H. (1984). Relative brain sizes and cortical surface areas in odontocetes. *Acta Zool Fenn*, *172*, 149–152.

Ridgway, S. H., Scronce, B. L., & Kanwisher, J. (1969). Respiration and deep diving in the bottlenose porpoise. *Science*, *166*(3913), 1651–1654.

Robinson, M. D., & Smyth, G. K. (2007). Small-sample estimation of negative binomial dispersion, with applications to sage data. *Biostatistics*, *9*(2), 321–332.

Rolfe, D. F., & Brown, G. C. (1997). Cellular energy utilization and molecular origin of standard metabolic rate in mammals. *Physiol Rev*, *77*, 731–58.

Rosafio, K., & Pellerin, L. (2014). Oxygen tension controls the expression of the monocarboxylate transporter mct4 in cultured mouse cortical astrocytes via a hypoxia-inducible factor-1alpha-mediated transcriptional regulation. *Glia*, *62*(3), 477–90.

Santos, M. B., Monteiro, S. S., Vingada, J. V., Ferreira, M., López, A., Martínez Cedeira, J. A., Reid, R. J., Brownlow, A., & Pierce, G. J. (2014). Patterns and trends in the diet of long-finned pilot whales (globicephala melas) in the northeast atlantic. *Mar Mammal Sci*, *30*(1), 1–19.

Sarnico, I., Lanzillotta, A., Boroni, F., Benarese, M., Alghisi, M., Schwaninger, M., Inta, I., Battistin, L., Spano, P., & Pizzi, M. (2009). Nf-kappab p50/rela and c-rel-containing dimers: Opposite regulators of neuron vulnerability to ischaemia. *J Neurochem*, *108*(2), 475–85.

Schenkman, K. A., Marble, D. R., Burns, D. H., & Feigl, E. O. (1997). Myoglobin oxygen dissociation by multiwavelength spectroscopy. *J Appl Physiol*, *82*(1), 86–92.

Schieber, M., & Chandel, N. S. (2014). Ros function in redox signaling and oxidative stress. *Curr Biol*, *24*(10), R453–62.

Schmidt, M., Giessl, A., Laufs, T., Hankeln, T., Wolfrum, U., & Burmester, T. (2003). How does the eye breathe? evidence for neuroglobin-mediated oxygen supply in the mammalian retina. *J Biol Chem*, *278*(3), 1932–5.

Schmidt-Kastner, R., Zhang, B., Belayev, L., Khoutorova, L., Amin, R., Busto, R., & Ginsberg, M. D. (2002). Dna microarray analysis of cortical gene expression during early recirculation after focal brain ischemia in rat. *Brain Res Mol Brain Res*, *108*(1-2), 81–93.

Schmutz, S., Dapp, C., Wittwer, M., Durieux, A. C., Mueller, M., Weinstein, F., Vogt, M., Hoppeler, H., & Fluck, M. (2010). A hypoxia complement differentiates the muscle response to endurance exercise. *Exp Physiol*, *95*(6), 723–35.

Schneider, A., Martin-Villalba, A., Weih, F., Vogel, J., Wirth, T., & Schwaninger, M. (1999). Nf-kappab is activated and promotes cell death in focal cerebral ischemia. *Nat Med*, *5*(5), 554–9.

Schneuer, M., Flachsbarth, S., Czech-Damal, N. U., Folkow, L. P., Siebert, U., & Burmester, T. (2012). Neuroglobin of seals and whales: Evidence for a divergent role in the diving brain. *Neuroscience*, *223*, 35–44.

Scholander, P. F. (1940). Experimantal investigations on the respiratory function in diving mammals and birds. *Hvalradets Skr*, *22*, 1–131.

Schorr, G. S., Falcone, E. A., Moretti, D. J., & Andrews, R. D. (2014). First long-term behavioral records from cuvier's beaked whales (ziphius cavirostris) reveal record-breaking dives. *PLoS One*, *9*(3), e92633.

Schreck, R., Rieber, P., & Baeuerle, P. A. (1991). Reactive oxygen intermediates as apparently widely used messengers in the activation of the nf-kappa b transcription factor and hiv-1. *EMBO J*, *10*(8), 2247–58.

Schülke, S., Dreidax, D., Malik, A., Burmester, T., Nevo, E., Band, M., Avivi, A., & Hankeln, T. (2012). Living with stress: Regulation of antioxidant defense genes in the subterranean, hypoxia-tolerant mole rat, spalax. *Gene*, *500*(2), 199–206.

Schurr, A. (2002). Energy metabolism, stress hormones and neural recovery from cerebral ischemia/hypoxia. *Neurochem. Int.*, *41*(1), 1–8.

Schuster-Böckler, B., Conrad, D., & Bateman, A. (2010). Dosage sensitivity shapes the evolution of copy-number varied regions. *PloS one*, *5*(3), e9474.

Scott, G. R. (2011). Elevated performance: The unique physiology of birds that fly at high altitudes. *J Exp Biol*, *214*(Pt 15), 2455–62.

Scott, G. R., Egginton, S., Richards, J. G., & Milsom, W. K. (2009). Evolution of muscle phenotype for extreme high altitude flight in the bar-headed goose. *Proc Biol Sci*, *276*(1673), 3645–53.

Sea, K., Sohn, S. H., Durazo, A., Sheng, Y., Shaw, B. F., Cao, X., Taylor, A. B., Whitson, L. J., Holloway, S. P., Hart, P. J., Cabelli, D. E., Gralla, E. B., & Valentine, J. S. (2015). Insights into the role of the unusual disulfide bond in copper-zinc superoxide dismutase. *J Biol Chem*, *290*(4), 2405–18.

Seeger, R. C., Brodeur, G. M., Sather, H., Dalton, A., Siegel, S. E., Wong, K. Y., & Hammond, D. (1985). Association of multiple copies of the n-myc oncogene with rapid progression of neuroblastomas. *N Engl J Med*, *313*(18), 1111–6.

Semenza, G. L. (2001). Hif-1 and mechanisms of hypoxia sensing. *Curr Opin Cell Biol*, *13*(2), 167–71.

Shaffer, S. A., Costa, D. P., Williams, T. M., & Ridgway, S. H. (1997). Diving and swimming performance of white whales, delphinapterus leucas: An assessment of plasma lactate and blood gas levels and respiratory rates. *J Exp Biol*, *200*(Pt 24), 3091–9.

Shams, I., Avivi, A., & Nevo, E. (2005). Oxygen and carbon dioxide fluctuations in burrows of subterranean blind mole rats indicate tolerance to hypoxic-hypercapnic stresses. *Comp Biochem Physiol A Mol Integr Physiol*, *142*(3), 376–82.

Sheafor, B. A. (2003). Metabolic enzyme activities across an altitudinal gradient: An examination of pikas (genus ochotona). *J Exp Biol*, *206*(Pt 7), 1241–9.

Sheng, Y., Chattopadhyay, M., Whitelegge, J., & Valentine, J. S. (2012). Sod1 aggregation and als: Role of metallation states and disulfide status. *Curr Top Med Chem*, *12*(22), 2560–72.

Shoubridge, E. A., Carscadden, J. E., & Leggett, W. C. (1976). Ldh isozyme patterns in cetaceans: Evidence for a biochemical adaptation to diving. *Comp Biochem Physiol B*, *53*(3), 357–9.

Siebenlist, U., Franzoso, G., & Brown, K. (1994). Structure, regulation and function of nf-kappa b. *Annu Rev Cell Biol*, *10*, 405–55.

Siesjo, B. K., Katsura, K., & Kristian, T. (1996). Acidosis-related damage. *Adv Neurol*, *71*, 209–33, discussion 234–6.

Silver, I. A., Deas, J., & Erecinska, M. (1997). Ion homeostasis in brain cells: Differences in intracellular ion responses to energy limitation between cultured neurons and glial cells. *Neuroscience*, *78*(2), 589–601.

Singh, S. P., Chhunchha, B., Fatma, N., Kubo, E., Singh, S. P., & Singh, D. P. (2016). Delivery of a protein transduction domain-mediated prdx6 protein ameliorates oxidative stress-induced injury in human and mouse neuronal cells. *Am J Physiol Cell Physiol*, *310*(1), C1–16.

Singleton, A. B., Farrer, M., Johnson, J., Singleton, A., Hague, S., Kachergus, J., Hulihan, M., Peuralinna, T., Dutra, A., Nussbaum, R., Lincoln, S., Crawley, A., Hanson, M., Maraganore, D., Adler, C., Cookson, M. R., Muenter, M., Baptista, M., Miller, D., ... Gwinn-Hardy, K. (2003). Alpha-synuclein locus triplication causes parkinson's disease. *Science*, *302*(5646), 841.

Skulachev, V. P. (1998). Cytochrome c in the apoptotic and antioxidant cascades. *FEBS Lett*, *423*(3), 275–80.

Snyder, G. K. (1983). Respiratory adaptations in diving mammals. *Respir Physiol*, *54*(3), 269–294.

Soares, P., Abrantes, D., Rito, T., Thomson, N., Radivojac, P., Li, B., Macaulay, V., Samuels, D. C., & Pereira, L. (2013). Evaluating purifying selection in the mitochondrial dna of various mammalian species. *PLoS One*, *8*(3), e58993.

Soegaard, L. B., Hansen, M. N., van Elk, C., Brahm, J., & Jensen, F. B. (2012). Respiratory properties of blood in the harbor porpoise, phocoena phocoena. *J Exp Biol*, *215*(Pt 11), 1938–43.

Somero, G. N., & Childress, J. J. (1990). Scaling of atp-supplying enzymes, myofibrillar proteins and buffering capacity in fish muscle: Relationship to locomotory habit. *J Exp Biol*, *149*, 319–333.

Stadtman, E. R., & Levine, R. L. (2000). Protein oxidation. *Ann N Y Acad Sci*, *899*, 191–208.

Steiner, J. L., Murphy, E. A., McClellan, J. L., Carmichael, M. D., & Davis, J. M. (2011). Exercise training increases mitochondrial biogenesis in the brain. *J Appl Physiol*, *111*(4), 1066–71.

Stenzel-Poore, M. P., Stevens, S. L., King, J. S., & Simon, R. P. (2007). Preconditioning reprograms the response to ischemic injury and primes the emergence of unique endogenous neuroprotective phenotypes: A speculative synthesis. *Stroke*, *38*(2 Suppl), 680–5.

Stephenson, D., Yin, T., Smalstig, E. B., Hsu, M. A., Panetta, J., Little, S., & Clemens, J. (2000). Transcription factor nuclear factor-kappa b is activated in neurons after focal cerebral ischemia. *J Cereb Blood Flow Metab*, *20*(3), 592–603.

Stockard, T. K., Levenson, D. H., Berg, L., Fransioli, J. R., Baranov, E. A., & Ponganis, P. J. (2007). Blood oxygen depletion during rest-associated apneas of northern elephant seals (mirounga angustirostris). *J Exp Biol*, *210*(Pt 15), 2607–17.

Stranger, B. E., Forrest, M. S., Dunning, M., Ingle, C. E., Beazley, C., Thorne, N., Redon, R., Bird, C. P., De Grassi, A., Lee, C., Et al. (2007). Relative impact of nucleotide and copy number variation on gene expression phenotypes. *Science*, *315*(5813), 848–853.

Sugano, E., Murayama, N., Takahashi, M., Tabata, K., Tamai, M., & Tomita, H. (2013). Essential role of thioredoxin 2 in mitigating oxidative stress in retinal epithelial cells. *J Ophthalmol*, *2013*, 185825.

Sugawara, T., Lewen, A., Gasche, Y., Yu, F., & Chan, P. H. (2002a). Overexpression of sod1 protects vulnerable motor neurons after spinal cord injury by attenuating mitochondrial cytochrome c release. *FASEB J*, *16*(14), 1997–9.

Sugawara, T., Noshita, N., Lewen, A., Gasche, Y., Ferrand-Drake, M., Fujimura, M., Morita-Fujimura, Y., & Chan, P. H. (2002b). Overexpression of copper/zinc superoxide dismutase in transgenic rats protects vulnerable neurons against ischemic damage by blocking the mitochondrial pathway of caspase activation. *J Neurosci*, *22*(1), 209–17.

Suh, S. W., Aoyama, K., Matsumori, Y., Liu, J., & Swanson, R. A. (2005). Pyruvate administered after severe hypoglycemia reduces neuronal death and cognitive impairment. *Diabetes*, *54*(5), 1452–8.

Sukhanova, I. A., Sebentsova, E. A., Khukhareva, D. D., Vysokikh, M. Y., Bezuglov, V. V., Bobrov, M. Y., & Levitskaya, N. G. (2019). Early-life n-arachidonoyl-dopamine exposure increases antioxidant capacity of the brain tissues and reduces functional deficits after neonatal hypoxia in rats. *Int J Dev Neurosci*, *78*, 7–18.

Suliman, H. B., Carraway, M. S., Welty-Wolf, K. E., Whorton, A. R., & Piantadosi, C. A. (2003). Lipopolysaccharide stimulates mitochondrial biogenesis via activation of nuclear respiratory factor-1. *J Biol Chem*, *278*(42), 41510–8.

Suzuki, T., & Imai, K. (1998). Evolution of myoglobin. *Cell Mol Life Sci*, *54*(9), 979–1004.

Swan, L. W. (1970). Goose of the himalayas. *Nat Hist*, *70*(68-75), 213.

Swanson, R. A., & Choi, D. W. (1993). Glial glycogen stores affect neuronal survival during glucose deprivation in vitro. *J Cereb Blood Flow Metab*, *13*(1), 162–9.

Tang, Y., Pacary, E., Freret, T., Divoux, D., Petit, E., Schumann-Bard, P., & Bernaudin, M. (2006). Effect of hypoxic preconditioning on brain genomic response before and following ischemia in the adult mouse: Identification of potential neuroprotective candidates for stroke. *Neurobiol Dis*, *21*(1), 18–28.

Team, R. C. (2013). R: A language and environment for statistical computing.

Tew, K. D. (2007). Redox in redux: Emergent roles for glutathione s-transferase p (gstp) in regulation of cell signaling and s-glutathionylation. *Biochem Pharmacol*, *73*(9), 1257–69.

Therade-Matharan, S., Laemmel, E., Carpentier, S., Obata, Y., Levade, T., Duranteau, J., & Vicaut, E. (2005). Reactive oxygen species production by mitochondria in endothelial cells exposed to reoxygenation after hypoxia and glucose depletion is mediated by ceramide. *Am J Physiol Regul Integr Comp Physiol*, *289*(6), R1756–62.

Thewissen, J. G., Cooper, L. N., Clementz, M. T., Bajpai, S., & Tiwari, B. N. (2007). Whales originated from aquatic artiodactyls in the eocene epoch of india. *Nature*, *450*(7173), 1190–4.

Tholey, G., Roth-Schechter, B., & Mandel, P. (1981). Activity and isoenzyme pattern of lactate dehydrogenase in neurons and astroblasts cultured from brains of chick embryos. *J Neurochem*, *36*(1), 77–81.

Thompson, J. W., Prentice, H. M., & Lutz, P. L. (2007). Regulation of extracellular glutamate levels in the long-term anoxic turtle striatum: Coordinated activity of glutamate transporters, adenosine, k (atp) (+) channels and gaba. *J Biomed Sci*, *14*(6), 809–817.

Tian, R., Seim, I., Ren, W., Xu, S., & Yang, G. (2018). Comparative genomics reveals contraction in cytosolic glutathione transferase genes in cetaceans: Implications for oxidative stress adaptation. *bioRxiv*, 485615.

Tian, R., Wang, Z., Niu, X., Zhou, K., Xu, S., & Yang, G. (2016). Evolutionary genetics of hypoxia tolerance in cetaceans during diving. *Genome Biol Evol*, *8*(3), 827–839.

Tian, R., Yin, D., Liu, Y., Seim, I., Xu, S., & Yang, G. (2017). Adaptive evolution of energy metabolism-related genes in hypoxia-tolerant mammals. *Front Genet*, *8*, 205.

Timon-Gomez, A., Nyvltova, E., Abriata, L. A., Vila, A. J., Hosler, J., & Barrientos, A. (2018). Mitochondrial cytochrome c oxidase biogenesis: Recent developments. *Semin Cell Dev Biol*, *76*, 163–178.

Towers, J. R., Tixier, P., Ross, K. A., Bennett, J., Arnould, J. P. Y., Pitman, R. L., & Durban, J. W. (2018). Movements and dive behaviour of a toothfish-depredating killer and sperm whale. *ICES J Mar Sci*, *76*(1), 298–311.

Tsagkogeorga, G., McGowen, M. R., Davies, K. T., Jarman, S., Polanowski, A., Bertelsen, M. F., & Rossiter, S. J. (2015). A phylogenomic analysis of the role and timing of molecular adaptation in the aquatic transition of cetartiodactyl mammals. *R Soc Open Sci*, *2*(9), 150156.

Tsang, C. K., Liu, Y., Thomas, J., Zhang, Y., & Zheng, X. F. (2014). Superoxide dismutase 1 acts as a nuclear transcription factor to regulate oxidative stress resistance. *Nat Commun*, *5*, 3446.

Tyack, P. L., Johnson, M., Soto, N. A., Sturlese, A., & Madsen, P. T. (2006). Extreme diving of beaked whales. *J Exp Biol*, *209*(Pt 21), 4238–53.

Valerio, A., Dossena, M., Bertolotti, P., Boroni, F., Sarnico, I., Faraco, G., Chiarugi, A., Frontini, A., Giordano, A., Liou, H. C., De Simoni, M. G., Spano, P., Carruba, M. O., Pizzi, M., & Nisoli, E. (2009). Leptin is induced in the ischemic cerebral cortex and exerts neuroprotection through nf-kappab/c-rel-dependent transcription. *Stroke*, *40*(2), 610–7.

van de Sluis, B., Muller, P., Duran, K., Chen, A., Groot, A. J., Klomp, L. W., Liu, P. P., & Wijmenga, C. (2007). Increased activity of hypoxia-inducible factor 1 is associated with early embryonic lethality in commd1 null mice. *Mol Cell Biol*, *27*(11), 4142–56.

van Hall, G., Stromstad, M., Rasmussen, P., Jans, O., Zaar, M., Gam, C., Quistorff, B., Secher, N. H., & Nielsen, H. B. (2009). Blood lactate is an important energy source for the human brain. *J Cereb Blood Flow Metab*, *29*(6), 1121–9.

Vangeison, G., Carr, D., Federoff, H. J., & Rempe, D. A. (2008). The good, the bad, and the cell type-specific roles of hypoxia inducible factor-1 alpha in neurons and astrocytes. *J Neurosci*, *28*(8), 1988–93.

Vangeison, G., & Rempe, D. A. (2009). The janus-faced effects of hypoxia on astrocyte function. *Neuroscientist*, *15*(6), 579–88.

Vazquez-Medina, J. P., Dodia, C., Weng, L., Mesaros, C., Blair, I. A., Feinstein, S. I., Chatterjee, S., & Fisher, A. B. (2016). The phospholipase a2 activity of peroxiredoxin 6 modulates nadph oxidase 2 activation via lysophosphatidic acid receptor signaling in the pulmonary endothelium and alveolar macrophages. *FASEB J*, *30*(8), 2885–98.

Vazquez-Medina, J. P., Zenteno-Savin, T., & Elsner, R. (2006). Antioxidant enzymes in ringed seal tissues: Potential protection against dive-associated ischemia/reperfusion. *Comp Biochem Physiol C Toxicol Pharmacol*, *142*(3-4), 198–204.

Vazquez-Medina, J. P., Zenteno-Savin, T., Elsner, R., & Ortiz, R. M. (2012). Coping with physiological oxidative stress: A review of antioxidant strategies in seals. *J Comp Physiol B*, *182*(6), 741–50.

Vázquez-Medina, J. P., Zenteno-Savín, T., & Elsner, R. (2007). Glutathione protection against dive-associated ischemia/reperfusion in ringed seal tissues. *J Exp Mar Biol Ecol*, *345*(2), 110–118.

Vijayasarathy, C., Damle, S., Prabu, S. K., Otto, C. M., & Avadhani, N. G. (2003). Adaptive changes in the expression of nuclear and mitochondrial encoded subunits of cytochrome c oxidase and the catalytic activity during hypoxia. *Eur J Biochem*, *270*(5), 871–9.

Vislobokova, I. A. (2013). On the origin of cetartiodactyla: Comparison of data on evolutionary morphology and molecular biology. *Paleontol J*, *47*(3), 321–334.

Visser, F., Kok, A. C. M., Oudejans, M. G., Scott-Hayward, L. A. S., DeRuiter, S. L., Alves, A. C., Antunes, R. N., Isojunno, S., Pierce, G. J., Slabbekoorn, H., Huisman, J., & Miller, P. J. O. (2017). Vocal foragers and silent crowds: Context-dependent vocal variation in northeast atlantic long-finned pilot whales. *Behav Ecol Sociobiol*, *71*(12), 170.

Walsh, B., Pearl, A., Suchy, S., Tartaglio, J., Visco, K., & Phelan, S. A. (2009). Overexpression of prdx6 and resistance to peroxide-induced death in hepa1-6 cells: Prdx suppression increases apoptosis. *Redox Rep*, *14*(6), 275–84.

Walton, M., Connor, B., Lawlor, P., Young, D., Sirimanne, E., Gluckman, P., Cole, G., & Dragunow, M. (1999). Neuronal death and survival in two models of hypoxic-ischemic brain damage. *Brain Res Rev*, *29*(2-3), 137–168.

Wang, G. L., Jiang, B.-H., Rue, E. A., & Semenza, G. L. (1995). Hypoxia-inducible factor 1 is a basic-helix-loop-helix-pas heterodimer regulated by cellular o2 tension. *Proc Natl Acad Sci U S A*, *92*(12), 5510–5514.

Wang, H., & Joseph, J. A. (1999). Quantifying cellular oxidative stress by dichlorofluorescein assay using microplate reader. *Free Radic Biol Med*, *27*(5-6), 612–6.

Wang, X., Phelan, S. A., Forsman-Semb, K., Taylor, E. F., Petros, C., Brown, A., Lerner, C. P., & Paigen, B. (2003). Mice with targeted mutation of peroxiredoxin 6 develop normally but are susceptible to oxidative stress. *J Biol Chem*, *278*(27), 25179–90.

Wang, Y., Feinstein, S. I., Manevich, Y., Ho, Y. S., & Fisher, A. B. (2004). Lung injury and mortality with hyperoxia are increased in peroxiredoxin 6 gene-targeted mice. *Free Radic Biol Med*, *37*(11), 1736–43.

Wang, Y., Feinstein, S. I., Manevich, Y., Ho, Y. S., & Fisher, A. B. (2006). Peroxiredoxin 6 gene-targeted mice show increased lung injury with paraquat-induced oxidative stress. *Antioxid Redox Signal*, *8*(1-2), 229–37.

Wang, Y., Manevich, Y., Feinstein, S. I., & Fisher, A. B. (2004b). Adenovirus-mediated transfer of the 1-cys peroxiredoxin gene to mouse lung protects against hyperoxic injury. *Am J Physiol Lung Cell Mol Physiol*, *286*(6), L1188–93.

Watkins, W. A. (1985). Investigations of sperm whale acoustic behaviors in the southeast caribbean. *Cetology*, *49*, 1–15.

Watkins, W. A., Daher, M. A., Fristrup, K. M., Howald, T. J., & Di Sciara, G. N. (1993). Sperm whales tagged with transponders and tracked underwater by sonar. *Mar Mammal Sci*, *9*(1), 55–67.

White, B. C., Sullivan, J. M., DeGracia, D. J., O'Neil, B. J., Neumar, R. W., Grossman, L. I., Rafols, J. A., & Krause, G. S. (2000). Brain ischemia and reperfusion: Molecular mechanisms of neuronal injury. *J Neurol Sci*, *179*(S 1-2), 1–33.

Widmer, H. R., Hoppeler, H., Nevo, E., Taylor, C. R., & Weibel, E. R. (1997). Working underground: Respiratory adaptations in the blind mole rat. *Proc Natl Acad Sci U S A*, *94*(5), 2062–7.

Wilhelm Filho, D., Sell, F., Ribeiro, L., Ghislandi, M., Carrasquedo, F., Fraga, C. G., Wallauer, J. P., Simoes-Lopes, P. C., & Uhart, M. M. (2002). Comparison between the antioxidant status of terrestrial and diving mammals. *Comp Biochem Physiol A Mol Integr Physiol*, *133*(3), 885–92.

Wilks, H. M., Hart, K. W., Feeney, R., Dunn, C. R., Muirhead, H., Chia, W. N., Barstow, D. A., Atkinson, T., Clarke, A. R., & Holbrook, J. J. (1988). A specific, highly active malate dehydrogenase by redesign of a lactate dehydrogenase framework. *Science*, *242*(4885), 1541–1544.

Willford, D. C., Gray, A. T., Hempleman, S. C., Davis, R. W., & Hill, E. P. (1990). Temperature and the oxygen-hemoglobin dissociation curve of the harbor seal, phoca vitulina. *Respir Physiol*, *79*(2), 137–44.

Williams, T. M., Haun, J. E., & Friedl, W. A. (1999). The diving physiology of bottlenose dolphins (tursiops truncatus). i. balancing the demands of exercise for energy conservation at depth. *J Exp Biol*, *202*(Pt 20), 2739–2748.

Williams, T. M., Zavanelli, M., Miller, M., Goldbeck, R., Morledge, M., Casper, D., Pabst, D. A., McLellan, W., Cantin, L. P., & Kliger, D. S. (2008). Running, swimming and diving modifies neuroprotecting globins in the mammalian brain. *Proc Royal Soc Lond*, *275*, 751–8.

Wingrove, P., Hadingham, K., Wafford, K., Kemp, J. A., Ragan, C. I., & Whiting, P. (1992). Cloning and expression of a cdna encoding the human gaba-a receptor alpha 5 subunit. *Biochem Soc Trans*, *20*(1), 18S.

Wright, B. M., Ford, J. K. B., Ellis, G. M., Deecke, V. B., Shapiro, A. D., Battaile, B. C., & Trites, A. W. (2017). Fine-scale foraging movements by fish-eating killer whales (orcinus orca) relate to the vertical distributions and escape responses of salmonid prey (oncorhynchus spp.) *Mov Ecol*, *5*, 3.

Xu, L., Sapolsky, R. M., & Giffard, R. G. (2001). Differential sensitivity of murine astrocytes and neurons from different brain regions to injury. *Exp Neurol*, *169*(2), 416–24.

Xu, M., & Zhang, H. L. (2011). Death and survival of neuronal and astrocytic cells in ischemic brain injury: A role of autophagy. *Acta Pharmacol Sin*, *32*(9), 1089–99.

Yan, W., & Chen, X. (2006). Gpx2, a direct target of p63, inhibits oxidative stress-induced apoptosis in a p53-dependent manner. *J Biol Chem*, *281*(12), 7856–62.

Yim, H. S., Cho, Y. S., Guang, X., Kang, S. G., Jeong, J. Y., Cha, S. S., Oh, H. M., Lee, J. H., Yang, E. C., Kwon, K. K., Kim, Y. J., Kim, T. W., Kim, W., Jeon, J. H., Kim, S. J., Choi, D. H., Jho, S., Kim, H. M., Ko, J., ... Lee, J. H. (2014). Minke whale genome and aquatic adaptation in cetaceans. *Nat Genet*, *46*(1), 88–92.

Yuan, G., Bin, J. C., McKay, D. J., & Snyder, F. F. (1999). Cloning and characterization of human guanine deaminase. purification and partial amino acid sequence of the mouse protein. *J Biol Chem*, *274*(12), 8175–8180.

Zapol, W. M., Liggins, G. C., Schneider, R. C., Qvist, J., Snider, M. T., Creasy, R. K., & Hochachka, P. W. (1979). Regional blood flow during simulated diving in the conscious weddell seal. *J Appl Physiol Respir Environ Exerc Physiol*, *47*(5), 968–73.

Zenteno-Savin, T., Clayton-Hernandez, E., & Elsner, R. (2002). Diving seals: Are they a model for coping with oxidative stress? *Comp Biochem Physiol C Toxicol Pharmacol*, *133*(4), 527–36.

Zhang, J., Ye, Z. W., Singh, S., Townsend, D. M., & Tew, K. D. (2018). An evolving understanding of the s-glutathionylation cycle in pathways of redox regulation. *Free Radic Biol Med*, *120*, 204–216.

Zhang, W., Potrovita, I., Tarabin, V., Herrmann, O., Beer, V., Weih, F., Schneider, A., & Schwaninger, M. (2005). Neuronal activation of nf-kappab contributes to cell death in cerebral ischemia. *J Cereb Blood Flow Metab*, *25*(1), 30–40.

Zhou, J., Lemos, B., Dopman, E. B., & Hartl, D. L. (2011). Copy-number variation: The balance between gene dosage and expression in drosophila melanogaster. *Genome Biol Evol*, *3*, 1014–1024.

Zhu, K., Ge, D., Wen, Z., Xia, L., & Yang, Q. (2018). Evolutionary genetics of hypoxia and cold tolerance in mammals. *J Mol Evol*, *86*(9), 618–634.

Zielke, H. R., Zielke, C. L., & Baab, P. J. (2009). Direct measurement of oxidative metabolism in the living brain by microdialysis: A review. *J Neurochem*, *109 Suppl 1*, 24–9.

12 Danksagung

Zuerst möchte ich Prof. Dr. Thorsten Burmester einen herzlichen Dank aussprechen für die Bereitstellung dieses großartigen Forschungsthemas und die Möglichkeit, diese Doktorarbeit in seiner Arbeitsgruppe anzufertigen. Ich danke dir für die Unterstützung bei der Geldbeschaffung und die Betreuung während meiner Promotion und wünsche dir alles Gute für die Zukunft!

Mein besonderer Dank gilt Dr. Andrej Fabrizius für eine wundervolle Betreuung. Nicht erst seit du die AG Burmester adoptiert hast, hast du einen großen Teil zum Gelingen dieser Arbeit beigetragen. Danke, dass du stets ein offenes Ohr für alle fachlichen und persönlichen Probleme hattest, dass du mich mit deinem Vertrauen zu Höchstleistungen angetrieben und mich mit deiner Begeisterung für die Wissenschaft angesteckt hast.

Vielen Dank an Prof. Dr. Susanne Dobler für die spontane Zusage, als Erstgutachter für diese Arbeit zu fungieren und für die Unterstützung in der Endphase meiner Promotion.

Bei der Studienstiftung des deutschen Volkes bedanke ich mich für die finanzielle und ideelle Förderung, die ich für drei Jahre erhalten habe. Ohne diese Unterstützung wäre meine Promotion nicht möglich gewesen.

Prof. Dr. Lars P. Folkow, Dr. Ursula Siebert und Bjarni Mikkelsen möchte ich dafür danken, dass sie das Probenmaterial für diese Arbeit zur Verfügung gestellt haben und stets bereit waren, Manuskripte zu korrigieren und kommentieren.

Ein herzliches Dankeschön geht an Michelle Wisniewsky, Maria Machola, Katja Reimann und Marilou Kloock. Vielen Dank für eure unermüdliche Hilfestellung im Labor und für den seelischen Beistand den ihr geleistet habt.

Eda Dönmez, Dustin Krüger und Christopher Schnoor möchte ich für ihren Beitrag zu den experimentellen Arbeiten danken und dafür, dass ich an ihnen das Betreuen üben durfte. Ich hoffe ihr habt von mir genauso viel gelernt wie ich von und durch euch.

Danke an meine Mitstreiter Annette Schlosser, Elsa Ziegler, Gerrit Martens, Julia Orth, Kathrin Helfenrath und Paressa Papadopoulou-Wörner, die mich während meiner Promotion begleitet haben. Ich danke euch für das interessante Fachsimpeln beim Mittagessen, die moralische Unterstützung, schöne und lustige Erinnerungen auf Konferenzen und für unvergessliche Partys. Ich hoffe ihr findet einen würdigen Nachfolger in der Rolle des Partybeauftragten :) Ein großes Dankeschön möchte ich außerdem Dr. Cornelia Geßner widmen, die mit mir die Leiden der tauchenden Säuger geteilt hat. Danke für die schönen Gespräche und die grandiosen Experimente mit Heliumballons.

Meinen Eltern verdanke ich es, dass ich bin, wer und wo ich bin. Danke Mama und Papa, dass ihr immer alles möglich gemacht habt, was ich mir in den Kopf gesetzt habe und mich bei jeder unsinnigen und sinnigen Idee unterstützt habt. Danke Cornelius und Matteo, dass ihr die besten Brüder seid, die ich je hatte. Auch geht ein riesiges Dankeschön an den neueren Teil

meiner Familie. Danke Rüdiger, Denys, Nele und Fine für schöne Wochenenden mit aufregenden Unternehmungen, lustigen Gesprächen und gemütlichen Filmabenden und danke für eure Unterstützung in allen Lebenslagen.

Das Beste kommt zum Schluss: Paul Adler, du bist mein Zuhause geworden, egal wo auf der Welt ich bin. Mit niemandem ist Eichhörnchen füttern und Meisen beobachten schöner! Und auch wenn du immer noch meine Fähigkeiten als Captain Botaniker anzweifelst, hätte ich mir keine bessere Unterstützung wünschen können. Danke dass du meine PCRs mit mir auswertest, mich zum Lachen bringst, auch wenn mir nicht danach ist und immer für mich da bist. Ohne dich hätte ich das alles nicht geschafft und ich möchte nie wieder ohne dich sein.

13 Declaration on oath (Eidesstattliche Versicherung)

I hereby declare, on oath, that I have written the present dissertation by my own and have not used other than the acknowledged resources and aids.

Hiermit erkläre ich an Eides statt, dass ich die vorliegende Dissertationsschrift selbst verfasst und keine anderen als die angegebenen Quellen und Hilfsmittel benutzt habe.

Hamburg, December 2019

.....
Alena Krüger